S9T

DOE/NASA/0115-80-1
NASA CR-159841
BALES-McCOIN 80-BMT-002

DESIGN STUDY OF CONTINUOUSLY VARIABLE ROLLER CONE TRACTION CVT FOR ELECTRIC VEHICLES

(NASA-CR-159841) DESIGN STUDY OF A CONTINUOUSLY VARIABLE ROLLER CONE TRACTION CVT FOR ELECTRIC VEHICLES Final Report (Bales-McCoin Tractionmatic, Inc.) 197 p HC A09/MF A01 CSCL 13I G3/37 N82-12445 Unclas 08424

D.K. McCoin and R.D. Walker
Bales-McCoin Tractionmatic, Inc.
El Paso, Texas

September 1980

Prepared for
NATIONAL AERONAUTICS AND SPACE ADMINISTRATION
Lewis Research Center
Cleveland, Ohio 44135
Under Contract DEN 3-115

for
U.S. DEPARTMENT OF ENERGY
Electric and Hybrid Vehicle Division
Office of Transportation Programs

DOE/NASA/0115-80/1
NASA CR-159841
80-BMT-002

DESIGN STUDY OF A CONTINUOUSLY VARIABLE CONE - ROLLER TRACTION TRANSMISSION FOR ELECTRIC VEHICLES

Dan K. McCoin and Richard D. Walker, Authors

Bales-McCoin, Inc.
9032 Roseway
El Paso, Texas

September 1980

Prepared for:

National Aeronautics and Space Administration
Lewis Research Center
Cleveland, Ohio 44135

Under Contract DEN 3-115

For:

US DEPARTMENT OF ENERGY
Electric and Hybrid Vehicle Division
Office of Transportation Programs
Washington, D.C. 20545

1. Report No.	2. Government Accession No.	3. Recipient's Catalog No.
NASA CR-159841		
4. Title and Subtitle Design Study of a Continuously Variable Cone/Roller Traction Transmission for Electric Vehicles		5. Report Date September 1980
		6. Performing Organization Code
7. Author(s) Dan K. McCoin, Richard D. Walker		8. Performing Organization Report No. 80-BMT-002
		10. Work Unit No.
9. Performing Organization Name and Address Bales-McCoin Tractionmatic, Inc. 9032 Roseway El Paso, Texas 79907		11. Contract or Grant No. DEN 3-115
		13. Type of Report and Period Covered Contractor Report
12. Sponsoring Agency Name and Address U.S. Department of Energy Office of Transportation Programs Washington, D.C. 20645		14. Sponsoring Agency Code DOE/NASA/0115-80/1

15. Supplementary Notes

Final Report Prepared Under Interagency Agreement EC-77-A-31-1044. Project Manager, S. Loewenthal, Bearing, Gearing, and Transmission. Section, NASA Lweis Research Center, Cleveland, Ohio 44135

16. Abstract

This report presents the results of design studies of continuously variable ratio transmissions (CVT) featuring cone and roller traction elements and computerized controls.

Based on the design and analysis results obtained, the CVT as presented herein meets or exceeds all requirements set forth in the design criteria. Further, a scalability analysis indicates the basic concept to be applicable to lower and higher power units, with upward scaling for increased power being more readily accomplished.

17. Key Words (Suggested by Author(s))	18. Distribution Statement
Electric Vehicle, Continuously Variable Transmission (CVT)-Roller-Cone Traction Drives	Unclassified - unlimited STAR category 37 DOE category UC-96

19. Security Classif. (of this report)	20. Security Classif. (of this page)	21. No. of Pages	22. Price*
Unclassified	Unclassified	189	

* For sale by the National Technical Information Service, Springfield, Virginia 22161

NASA-C-168 (Rev. 10-75)

TABLE OF CONTENTS

TABLE OF CONTENTS (CONTINUED)

LIST OF FIGURES

LIST OF TABLES

Table No.	Table Title	Page
21.	Cone Normal Loan (LB).	141
22.	Cone Bearing Loss (4 Cones).	143
23.	Spin Velocity (RAD/SEC).	145
24.	J_6, Dimensionless Spin Torque.	146
25.	Traction Power Loss (4 Contacts)	149
26.	Contact Ellipse Dimensions	151
27.	"g".	153
28.	J_7/J_4 Loss Factor.	162
29.	J_1, Dimensionless Slip Factor.	163
30.	J_3, Dimensionless Spin Factor.	164
31.	$g^3/(W_n)^{1/3}$	166
32.	Flywheel to RPM_s	168

EXECUTIVE SUMMARY

This report presents the results of design studies of continuously variable ratio transmissions (CVT) featuring cone and roller traction elements and computerized controls.

This work was part of the Electric and Hybrid Vehicle Program of the U.S. Department of Energy. It was performed under contract DEN 3-115 and managed by the Bearing, Gearing, and Transmission Section of the NASA Lewis Research Center.

A computer controlled traction drive CVT embodying traction cones and rollers in a regenerative path epicyclic gear differential was designed and analyzed.

Detailed assessment of cone-roller Traction CVT suitability to the electrical vehicle application was made. Vehicle configurations included: 1) flywheel energy storage system driving through the CVT to an electric motor into the vehicle differential; 2) electric motor driving through the CVT into the differential; and 3) hybrid I.C. engine driving through the CVT with CVT and electric motor input into the differential. (See Figures 1 through 3, pages 5 through 7).

The computer controlled regenerative traction unit controls the speed of the ring gear in the epicyclic gear differential. The traction unit consists of a crowned roller and four cones. The roller, driven by the center shaft through a recirculating ball spline, drives the traction cones. The center shaft also drives the sun gear of the epicyclic gear differential (Figure 4, 5 and 6, pages 16, 17 and 18.)

Speed variation of the output shaft is accomplished by moving the traction roller axially along the cones, thus varying the cone rotational speed and, in turn, varying the ring gear speed relative to the sun gear speed.

Power from a flywheel is transmitted through an input epicyclic reduction stage to the center shaft. The ring gear of the input reduction unit is controlled by a modulating clutch. The clutch allows de-coupling of the flywheel at flywheel speeds below minimum (less than 14000 RPM), to de-couple the flywheel at output shaft speeds below 850 RPM and reverse output speeds.

The computer control system maintains optimum traction, speed, and power for all operating conditions via traction slip monitoring and slip control feedback. Continuous sampling of system parameters (cone and roller speed, zero slip ratio setting, cone piston pressure, input speed, accelerator pedal position, brake pedal pressure, provides continuous control system updating. Optimum traction control provides maximum component life, minimum power drain from the batteries, and maximum vehicle range and performance.

Study results indicate an overall operating efficiency of the regenerative CVT as 91.5% for the mean power condition, 16KW (22HP) and 3,000 Rpm output. Calculated efficiency ranged from 92.1% at 15KW (20HP), 14,000 Rpm in, 3,000 Rpm out, to 76.64% at wheel slip "Torque Limit" of 39.8KW (53.4 HP) with 28,000 Rpm input and 850 Rpm output. (See Appendix B, page 79).

Based on the design and analysis results obtained, the computer controlled traction CVT's as presented herein meets or exceeds all requirements set forth in the design criteria. Further, a scalability analysis indicates the basic concept to be applicable to lower and higher power units, with upward scaling for increased power designs being more readily accomplished.

The present study specifically addresses:

- Efficiency
- Size and weight
- Reliability
- Noise
- Controls
- Maintainability
- Cost

of a traction regenerative configuration. The objective of this study is to design a traction CVT which meets or exceeds all the design specifications and operating requirements established in the contract. Analytical substantiation of traction elements, bearings, and gear stresses and life will also be investigated for the design. Structural alternatives are presented for prospective problem areas and trade-off considerations made.

- Weight: Approximately 34 Kg (75 lbs) for 75 KW (100 HP)
- Production Cost: Estimated at $330.00

INTRODUCTION

As a fuel efficient alternative to the reciprocating engine driven vehicle, the electric vehicle (E.V.) has been recognized and is being developed. Considerable E.V. investigations have been performed through analysis, subsystem development testing, and vehicle service evaluation. Combinations of hybrid power plant, energy storage flywheel, variable ratio transmission, and vehicle/motor control systems are being investigated for the purpose of devising a viable electric vehicle.

The purpose of the present study is to contribute to the mechanical transmission subsystem technology for the electric vehicle. The study covers analysis and design of a continuously variable traction transmission (CVT) which accepts input from an energy storage flywheel and provides variable speed drive continuity to the electric motor. Two alternative approaches which utilize the CVT are pure electric and hybrid reciprocating/electric drives.

It has long been recognized that the E.V. could most effectively utilize the CVT to achieve maximum performance. The innate ability of the CVT to allow the drive motor to operate at optimum speed and minimize battery drain strongly suggests justification for intensive study and development of the CVT. A government sponsored study concluded that the CVT with flywheel was necessary to make the electric postal jeep meet minimum satisfactory performance. Without the CVT the vehicle could not perform satisfactorily for most terrains.

PROGRAM SCOPE

The scope of the program encompasses the design of CVT of reasonable size, weight, and cost to provide an effective and reliable means of controlling and utilizing power augmentation of an energy storage flywheel in an electric vehicle. The CVT must accept power output from the flywheel at any speed between 14,000 RPM and 28,000 RPM and provide output shaft power at any speed between 850 RPM and 5,000 RPM. De-coupling must be accomplished for output shaft speeds below 850 RPM, and reverse. An alternative to de-coupling is a CVT design which provides neutral and reverse (effectively an IVT, infinitely variable transmission), Figure 1, page 5.

Alternative applications are the pure electric and hybrid electric vehicles as depicted in Figures 2 and 3, pages 6 and 7, respectively.

SCHEMATIC OF CVT DRIVETRAIN, UTILIZING FLYWHEEL AND ELECTRIC MOTOR

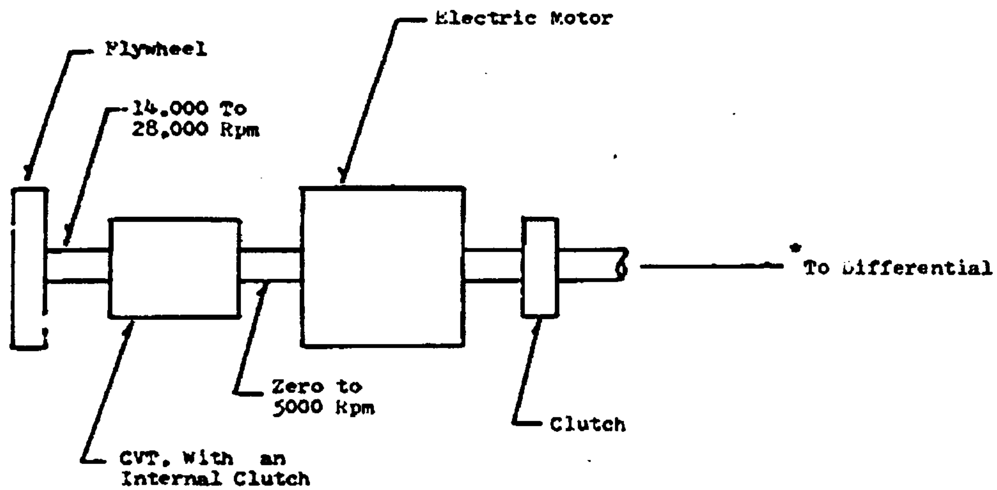

*Torsional dampening as required

Figure 1:

SCHEMATIC OF ELECTRICALLY DRIVEN CVT DRIVETRAIN

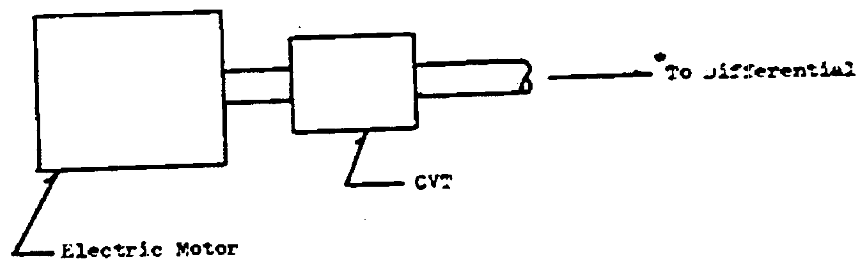

*Torsional dampening as required

Figure 2:

SCHEMATIC OF I.C. ENGINE/ELECTRIC MOTOR DRIVEN (HYBRID) CVT DRIVETRAIN

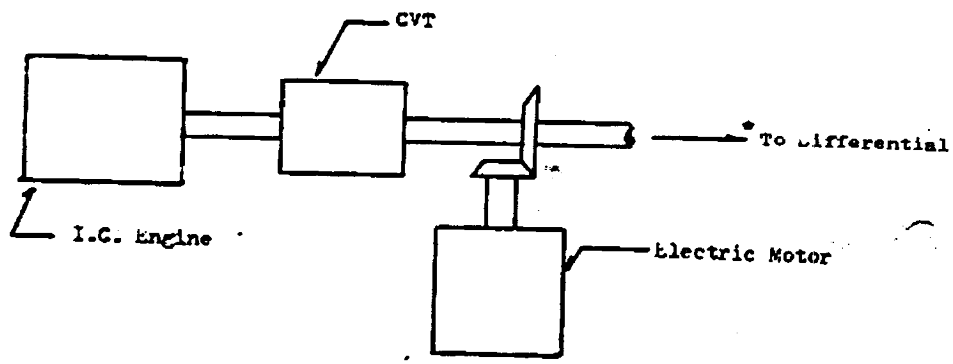

Figure 3.

*Torsional dampening as required

APPROACH

The approach taken herein was to perform the design study through iterative layouts concurrent with an assessment of possible technology advancements required to support the design. The study was implemented through the following statement of work.

A. Task 1 - Design Study of a CVT for Flywheel Application

A. Conduct an engineering design study and perform the necessary analysis to determine the optimum arrangement of a continuously variable speed transmission (CVT) to couple the high speed output shaft of an energy storage flywheel to the drive train of an electric vehicle as shown in Figure 1, page 5. The CVT shall be comprised of the variable speed element together with any ancillary mechanical components, such as couplings, clutches or gear sets, which are required to satisfy the requirements specified below.

DESIGN REQUIREMENTS

The following design requirements, based on a representative vehicle having a curb weight of 1700 Kilograms (3750 pounds), shall apply:

1. The speed ratio of the CVT shall be continuously controllable over the following range of input and output speeds:

High speed (flywheel output shaft), 14,000 to 28,000 RPM.

Low speed (differential input shaft), zero to 5000 RPM.

If it is impractical to design the proposed CVT to be continuously controllable down to zero output speed, then the CVT shall be designed to be continuously controllable down to a minimum speed not to exceed 850 RPM and a variable speed clutch element shall be incorporated to regulate differential input speed to zero.

2. The CVT shall provide forward vehicle speed only, since reverse may be accomplished by reversing electric motor rotation, unless reverse can be accomplished within the CVT without additional complexity.

3. Disengagement of the flywheel from the drive train shall be accomplished with the CVT or with a clutch, if required.

4. The CVT shall be capable of withstanding all sudden shock loads and sudden torque conditions that may be expected in typical automotive applications.

5. The CVT shall be capable of bi-directional power flow at the above power ratings for regenerative braking and for charging of the flywheel with the electric motor.

The operating power and life requirements for the transmission as stipulated are:

1. Mean output power = 16 KW (22 HP)
2. Mean output speed = 3,000 RPM
3. Mean input speed = 21,000 RPM
4. Life at mean conditions = 2,600 hours at 90% surviviability.
5. Maximum output speed - 5,000 RPM
6. Maximum input speed = 28,000 RPM
7. Minimum output speed = 850 RPM (clutched to zero)
8. Minimum input speed = 14,000 RPM

In addition, the following operating parameters are considered:

1. Maximum useable energy from flywheel = 1.8 MJ (1.5 KWH)
2. Maximum CVT transient power output = 75 KW (100 HP) for 5 sec.
3. Maximum CVT torque output at wheel slip = 450 N-m (330 ft. lb.)
4. Maximum time from maximum to minimum reduction ratio, or vice versa, 2 seconds.

DESIGN CRITERIA

The design of the CVT and associated drive system components, shall be on the basis of the following criteria in order of overall importance:

1. Efficiency - The transmission shall have high efficiency over its entire operating spectrum. Special attention shall

be given to maximizing transmission efficiency under those operating conditions in which the transmission spends most of its operating time.

2. Cost - The future production cost of the transmission, on a large scale basis (100,000 units per year), shall be an early consideration. The use of special manufacturing processes and materials shall be avoided. Design techniques, as well as drive system components such as bearings, gears, and seals, shall be typical of, and consistent with, automotive practice.

3. Size and Weight - The overall size and weight of the CVT, including suitable controls and all ancillary mechanical components, shall not be significantly greater than present automotive transmission of equal horsepower capacity.

4. Reliability - The transmission, including all support systems (i.e., cooling and controls), shall be designed to operate a minimum of 2600 hours at the conditions specified in the design requirements.

5. Noise - An important consideration in the early stages of design shall be to eliminate potential noise generating sources and to contain (within the transmission housing) that noise which is unavoidably generated.

6. Controls - The control system used to operate the transmission drive system shall be stable, reliable and responsive. The system shall provide driver "feel" response similar to that of a standard passenger vehicle, equipped with an internal combustion engine and standard automatic transmission. The control system selected shall closely simulate the full-scale system required for actual vehicle application.

7. Maintainability - The transmission shall be designed with maintainability equal to, or better than, the maintainability of present-day automotive automatic transmission. All internal components which require normal maintenance and/or occasional replacement shall be made readily accessible.

B. <u>Task II - Identification of Required Technology Advancements</u>

Identify all technology advancements required to develop the selected CVT to the point of satisfying the design requirements and criteria of Task I.

Define the nature of the required advancements, define the difficulty of the problems, and estimate the means and effort required to solve the problems. Areas of technology considered shall include, but shall not be limited to, materials, lubricants, bearings, seals, gears, controls, and other subsystems or modules required.

C. <u>Task III - Determination of CVT Concept Suitability for Alternate Electric and Hybrid Vehicle Applications</u>

Determine the suitability of the concept of the CVT designed in Task I for the alternate electric and hybrid vehicle applications specified below. This task shall be limited to the identification of: (1) the differences in arrangement, size, ratio, or other design variables, and (2) any additional new technology required to apply the CVT concept to each alternate application. Perform only the preliminary design analysis necessary to identify in a broad, general sense, the above differences and not perform specific design analyses or prepare layout drawings for these alternate applications.

<u>Electric Vehicle Powered by Electric Motor Only</u>

Determine the suitability of the CVT concept of Task I to match an electric motor to the drive train of an electric vehicle (without flywheel energy storage) as shown in Figure 2, page 6.

Design Requirements

1. The speed ratio of the CVT shall be continuously controllable over the following range of input and output speeds:

High speed (motor output shaft), zero to 6000 RPM

Low speed (differential input shaft), zero to 3000 RPM

2. All other requirements shall apply except for those specifically referring to the flywheel storage device which are deleted for this application.

Design Criteria

All criteria stated in Task I shall apply to this alternate application.

<u>Hybrid Electric Vehicle With An Internal Combustion Engine</u>

Determine the suitability of the CVT concept of Task I to match an internal combustion engine to the drive train of a hybrid electric vehicle as shown in Figure 3, page 7.

Design Requirements

1. The speed ratio of the CVT shall be continuously controllable such that the output speed shall range from zero to 3000 RPM with the input speed and power requirements according to the specified engine operating schedule.

2. The CVT shall provide forward, reverse, neutral, and at-rest vehicle operation with single lever operation.

3. All other requirements, as stated in Task I, shall apply, except those specifically referring to the flywheel storage device which are deleted from this application.

Scalability of Selected CVT With Flywheel Energy Storage for Alternate Maximum Output Torques

Determine the suitability of the CVT concept of Task I with flywheel energy storage for scaling to alternate maximum output torques. The design requirements and criteria shall be the same as specified in Task I except that the following alternate maximum output torques at wheel slip shall be considered. Low speed (differential input) shall be zero to 5000 RPM and the CVT input speeds shall be 14,000 to 28,000 RPM in all cases.

CASE	VEHICLE WEIGHT	MAXIMUM CVT OUTPUT (DIFFERENTIAL INPUT) TORQUE
1	790 kg (1750 lbs.)	210 N-m (155 lb-ft)
2	10,000 (22,000 lbs.)	2,600 N-m (1900 lb-ft)

D. Task IV - Design and Technology Assessment Report

Submit a design report of the CVT concept together with supporting data and analysis. Sufficient detail and analysis shall be provided to verify that the design is credible and capable of meeting the required design specifications and criteria.

An estimation of the steady state efficiencies at 7.5, 15, 30, 52, and 75 KW, output speed range of zero to 5000 RPM for input speeds of 14,000, 21,000, and 28,000 RPM.

DISCUSSION

Transmission Description

The transmission is a continuously variable (CVT) regenerative traction drive gearbox (Figure 5, page 17). Power flows through the input planetary assembly to the splined throughshaft. The power is transmitted to the traction cone by the roller together with part of the power which is transmitted regeneratively from the sun gear of the output planetary assembly back to the roller shaft. The cones drive the ring gear of the output planetary assembly through a spiral bevel-helical gear. The purpose of the regenerative power loop is to expand the basic cone speed ratio.

It may be seen in Figure 6, page 18, that if the output carrier shaft is restrained; rotating the input roller shaft turns the planetary sun gear. With the carrier stationary, the sun causes counter rotation of the planet idlers and couples that rotation to the ring gear. The ring gear motion then turns the cones via the idler, so as to cause it to counter rotate against the roller. It may be seen therefore that roller and cone diameters may be selected so that the system simply rotates without driving the carrier. This point occurs when the ring and sun gear have velocities that are equal in magnitude but opposite in their direction and is equivalent to neutral or an infinite (input/output) Rpm ratio. Moving the roller from this neutral position upsets the peripheral velocity balances in the system and causes carrier output motion or traction in the contact to occur.

Moving the roller toward the minor diameter of the cone would cause the cone Rpm to increase to maintain the same peripheral velocity as the roller. The increased cone Rpm is transmitted to the ring gear and thereby causes the carrier to be driven in a reverse direction in respect to the input. The transmission studied, as shown in Figure 5, page 17, is of this type by has gear and traction component diameters selected to preclude the output from reaching neutral at the largest cone diameter.

If a restraint, such as an external load, is applied to the carrier output shaft, it will tend to decrease in Rpm. The ring gear and hence the cone Rpm would also tend to decrease. The cone Rpm decrease produces shear (slip) in the fluid film between the traction conjunction and the resulting shear force creates a torque load. The amount of torque load varies with the amount of shear (slip), temperature, contract geometry and peripherial velocity but in the design studied the maximum power transfer (optimum slip) ranged from 0.8% to 2.0% over the range of design variables. Due to the output planetary expansion of cone ratio, the effect of slip is also expanded and appears as speed droop in the output shaft. Speed droop for the design ranged from 1.75% to 3.25% for 0.8% to 2.0% slip respectively.

It is clear from Figure 6, page 18, that a transmission with any desired input to output ratio range can be designed using any given cone geometry, by selecting the appropriate roller-cone diameters. This feature is used in the current design to expand the approxiamte traction cone-roller ratio range of 3.5/1 to produce the required overall transmission ratio range of about 12/1.

Transmissions which go to zero (neutral) as described are called "Infinitely Variable Transmissions (IVT)." Even though the design presented is not an IVT, it employs the same regenerative principles to expand the basic cone ratio and therefore must be evaluated as a limited range IVT. Specifically, regenerative gearing used in IVT's or in this case a high reduction ratio "Continuously Variable Transmission (CVT)", produces magnification of power internally and this must be considered in the design. This is reflected in the data and may be seen by noting that for 75 KW (100 HP) output the total cone-roller traction power varies from 95 KW (127 HP) to 316 KW (424 HP) in this design. (A magnification "m" value of 1.27 to 4.24).

The overall efficiency of the transmission is impacted by any change in internal power. When internal power rises above output power, efficiency is decreased because the internal percentage power loss of components are applied against larger amounts of horsepower.

Also any increase in internal horsepower increases the heat load that must be dissapated by the oil cooler. So there is a compound effect to efficiency loss by using regeneration to expand basic cone ratio.

[redacted]

Regeneration may be viewed as "recycling" and therefore power must make multiple passes through the same contacts or components, which logically holds that net efficiency must also be decreased in direct relation to the amount of regeneration in the system for any given operating point. So this effect varies as the system operating ratio is varied. [redacted]

These features, inherent in any regenerative design, make it imperative that a judgement be made between the losses generated in the traction contact by the basic cone design, chosen to produce a variable speed component, versus the amount of regeneration used to expand the cone ratio; and must further be weighed against other means of expanding overall transmission ratio (See Appendix B, page 79). [redacted]

Torque capacity of an IVT or high reduction CVT that employs regeneration, is a function of the gearing used and the traction coefficient. The traction coefficient is a function of the fluid selected, temperature, Rpm, surface finish and component geometry used. The normal load applied (pressure) between the traction components, in conjunction with the traction coefficient, results in the production of the specific torque generated. [redacted]

The design takes advantage of a thin fluid film which separates the traction elements and the fact that the fluid viscosity and resistance to shear (slip) rises rapidly under high pressure (contact Hertz stress in the conjunction). The transmittal of power through a fluid film requires that some shearing action (strain) in the fluid occur. [redacted]

Figure 7, page 19, is a plot of torque multiplication and speed ratio of an IVT without the input planetary reduction (Figure 6, page 18) versus output speed and for the operating range of the current design, percent speed is carrier Rpm/Sun gear Rpm. The graph reflects that the current design is well above the point where torque capacity is lost. Torque capacity to input/output ratio in a CVT, unlike gears, is limited by the tractive force produced at specific shear velocities in the fluid film separating the variable speed components. High Overall reduction ratios are produced in regenerative CVT's by decreasing differential velocities across planetary components. When the percentage differential velocity in the planetary gears becomes smaller than the "optimum" percent shear (slip) velocity for peak torque transfer by the fluid film then the capacity to transmit torque decreases. This feature allows the traction conjunction to effectively become a variable taut-band fluid coupling which in the normal operating ranges varies from fractions of a percent slip to around 2% but rapidly goes to 100% at neutral. In comparison a fluid torque converter will typically vary from 10% to 50% in the operating range with variation in load and still applies some minimum torque load when the output shaft is stopped with low Rpm to the input.

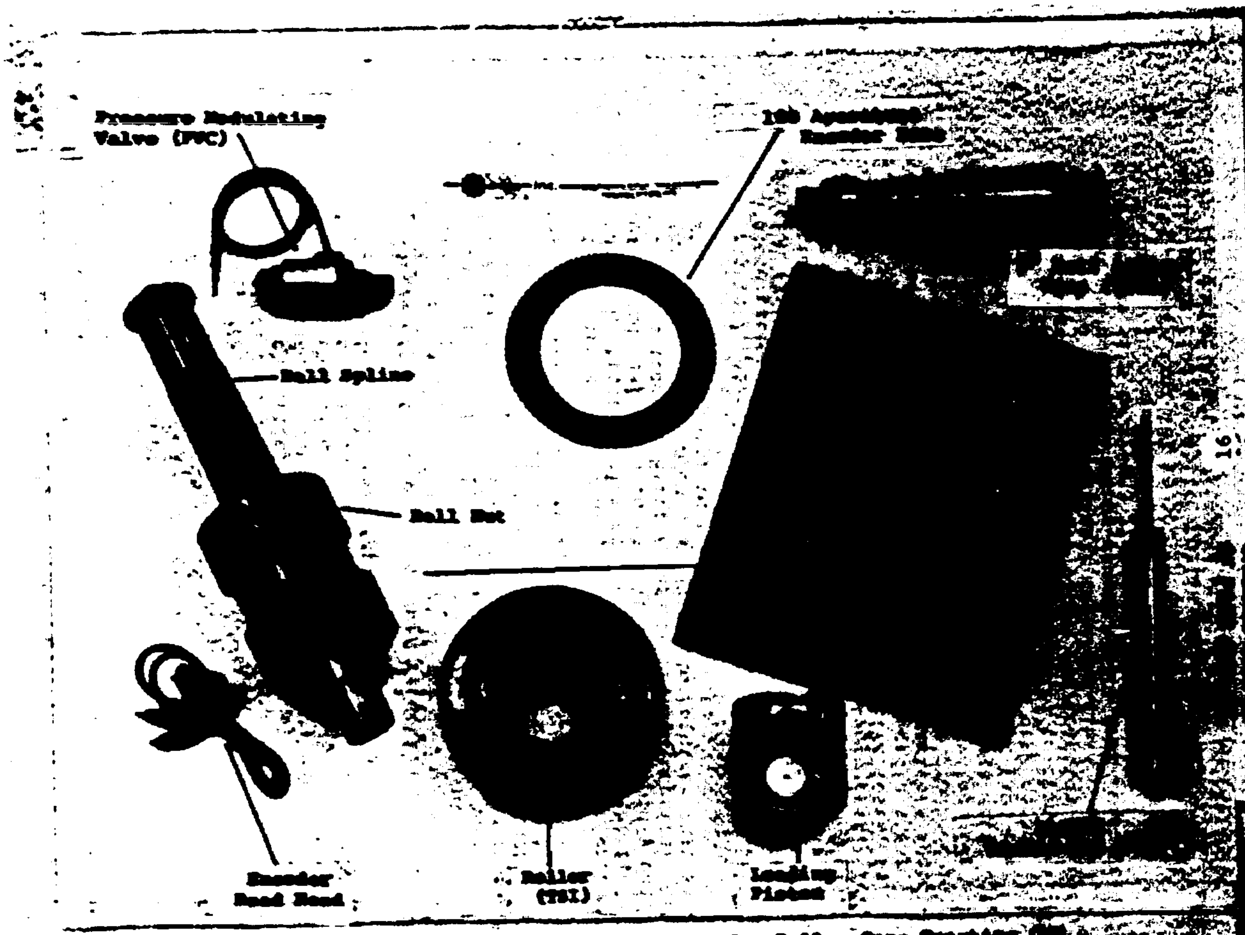

Figure 4 Photograph of Key Components of a Roller-Gear Traction [illegible]

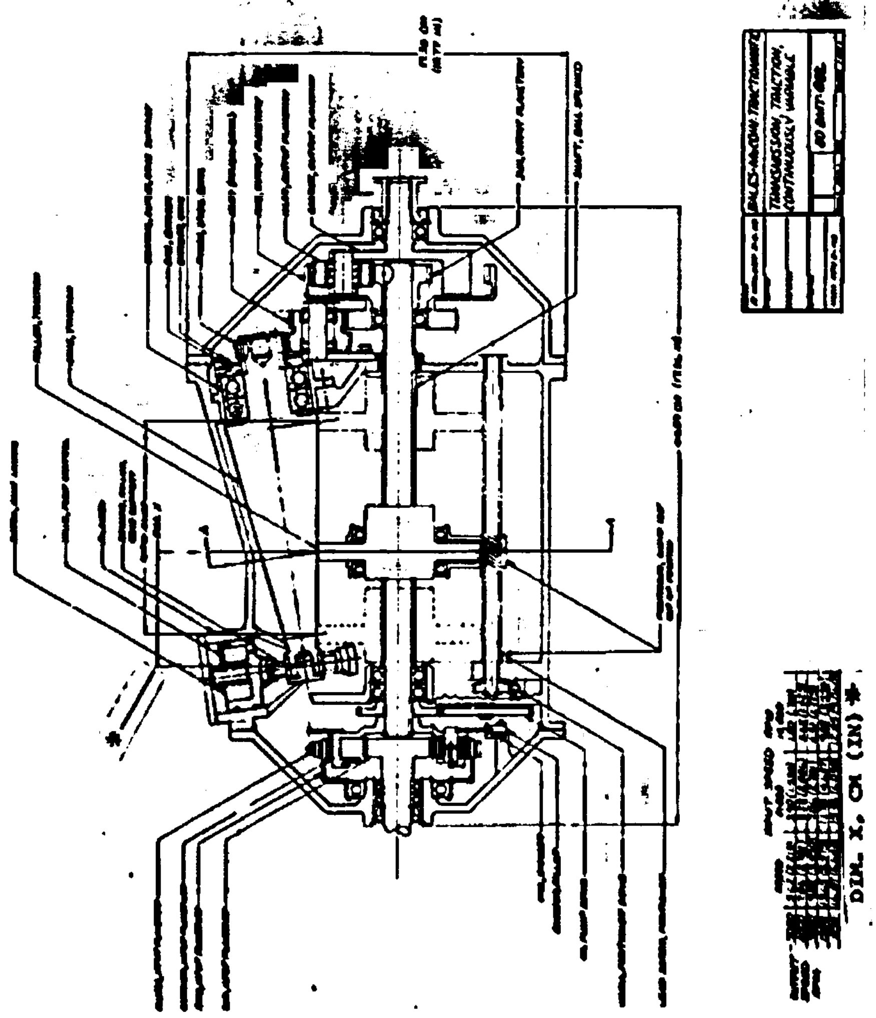

Figure 5:

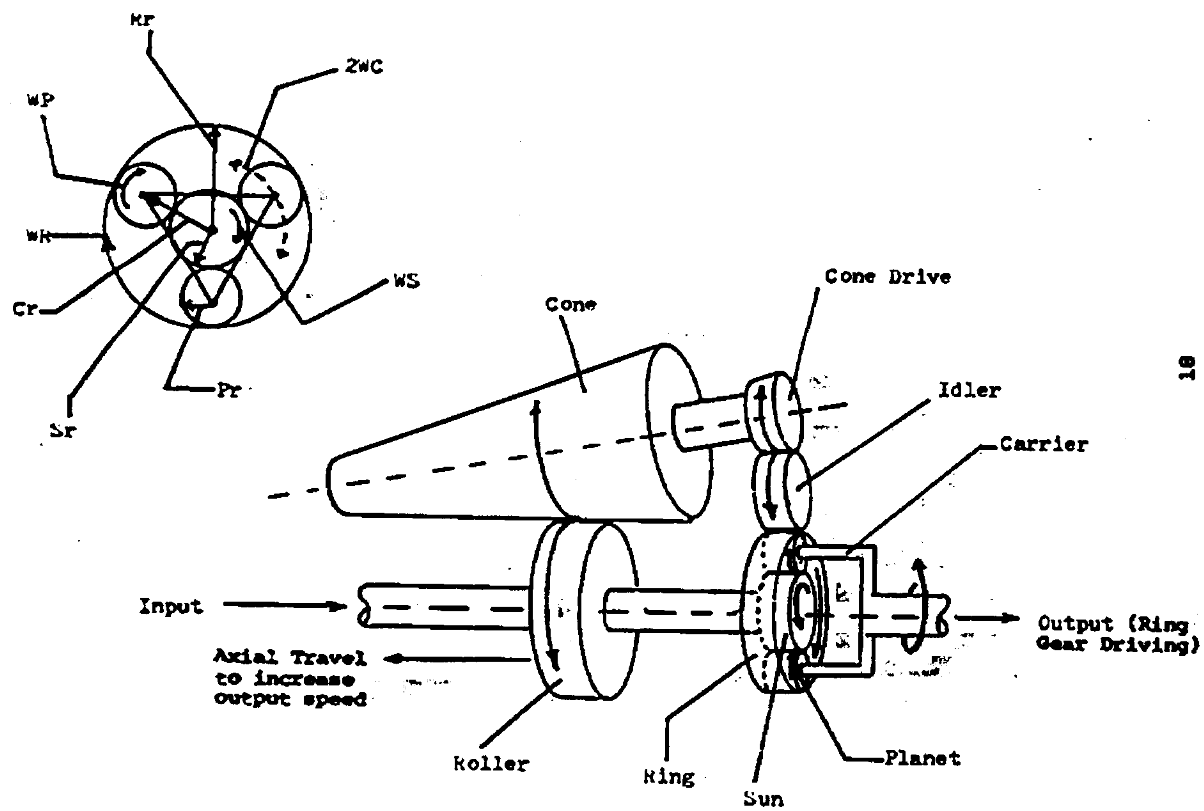

Figure 6. Regenerative CVT
(Less Input Reduction)

X Ratio (Rpm In/Rpm Out) = Normal Torque Multiplication of gears.

• Torque Multiplication Computed, Traction IVT.

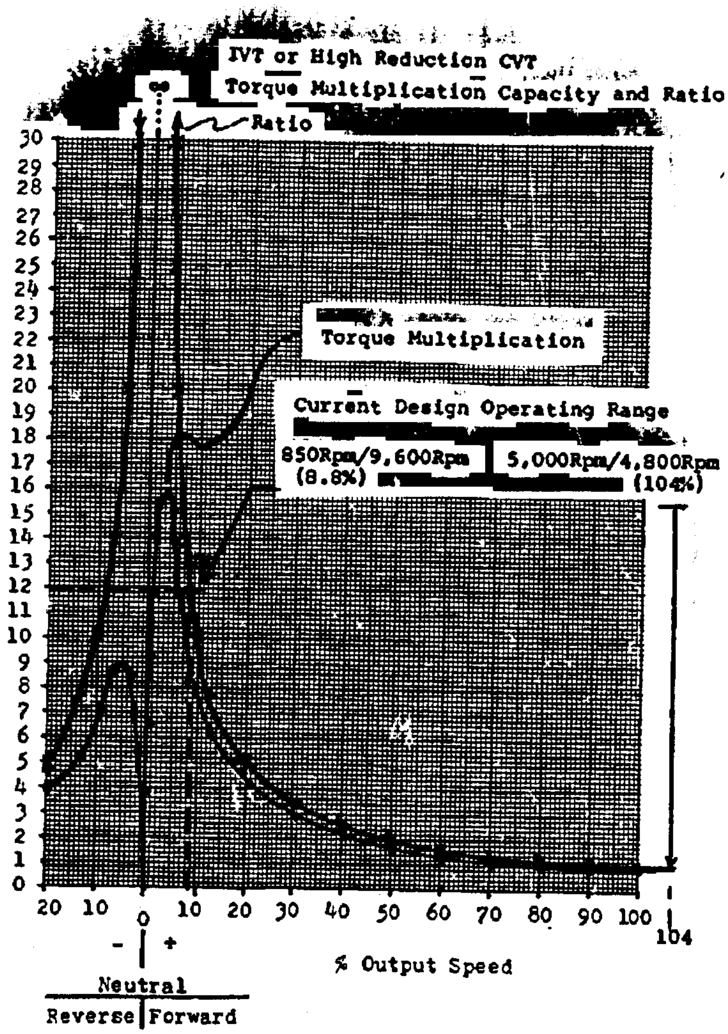

Figure 7:

The transmission ratio variation is accomplished by moving the traction roller along, and parallel to, the traction cones, thereby varying the rolling radius of the cones. The speed of the output ring gear is therefore varied, which, in turn, proportionally varies the output shaft.

Traction forces are generated between the roller and cones through a normal force applied at the small end of the cone. The force is supplied by a hydraulic piston which houses a cone support bearing. The magnitude of the normal force is determined by the transmission output torque requirement, traction coefficient (μ), ratio expansion and operating slip.

Pressure modulation to the hydraulic cylinder (which furnishes the cone force) is provided by a signal from the computer control system. (See control system description, page 25).

Referring to Figure 5, page 17, output from the flywheel powers the sun gear of the input planetary assembly. The ring gear is clutched by a band brake to engage or disengage the flywheel. The input planetary carrier is attached to the splined through-shaft, as is the oil pump drive gear.

The through-shaft is the inner race of a recirculating ball spline which drives the traction roller, while allowing relatively free axial motion of the roller to accomplish ratio change. The through-shaft also supports, and is driven by, the output sun gear. Four traction cones, driven at high speed by the roller, transmit power to the spiral bevel-helical cluster gears which, in turn, drive the output ring gear.

Spiral bevel gears on the idler are necessary to turn the 9.24° shaft angle of the cones to the centerline of the gearbox. The helical gear teeth have a helix angle which produces an opposite and equal axial force to the spiral bevel gear axial load. This enables the use of cylindrical roller bearings since no thrust exists. The use of helical gears also reduces noise generation. The action of helical and spiral bevel gears with adequate spiral or helix angles is much smoother than straight spur gears; hence, the operating noise levels are relatively much lower.

The output planetary carrier is the transmission output member. With the inputs of the through-shaft to the sun gear and the cones to the ring gear a variable ratio is accomplished to the carrier (output shaft). For normal input speed range of 14,000 to 28,000 RPM of the flywheel, the output speed range is from 850 RPM to 5,000 RPM.

The output shaft is de-clutched from the flywheel by the input planetary band clutch when zero output speed is required. De-clutching is necessary to enable the drive motor to reverse direction and drive the vehicle in reverse. The clutch also allows the electric motor to propel the vehicle when the flywheel is not charged.

A toothed disc is mounted on the cone (or to reduce its speed and provide greater circumference it may be located on the ring gear) to provide cone speed information to the controller via a photoelectric or magnetic read head. Pulses or square waves are generated by the encoder read head as the aperatures rotate past the device. Spatial timing or frequency to voltage I/O processing converts the encoder signals into speed data. The system is insensitive to absolute accuracy of speed measurement because the technique employs speed ratios. See Figure 8, page 22.

It is the ratio in speed indicated that is important to the system, not the absolute representation of "true" RPM, or "true" ratio. This dramatically reduces the controller design requirements.

Similarly the disc mounted on the input planetary carrier provides roller speed information. From the "relative" cone-roller speed information, cone/roller speed ratio is derived by division producing MSR (Measured Speed Ratio). And as above, the absolute accuracy of the MSR is unimportant. What becomes important is the ability of the controller to predict an equivalent Theoretical Speed Ratio (TSR) with no slip, which is based upon the selected component geometry and the traction conjunction location axially. This is accomplished by attaching a linear transducer between the case and the roller carrier assembly.

TSR positional accuracy in absolute terms is not needed. However, correlation between TSR and the MSR (with no-slip) is most important because deviation between MSR and TSR signals represents "slip" in the traction junction.

Traction component speeds are divided to produce Measured Speed Ratio (MSR), which is then divided by Theoretical Speed Ratio (TSR) to produce a % speed result. 1 - % speed becomes % slip and is subtracted from a varying slip reference to produce % slip error. The error is integrated and the driver amplifier modulates the pressure control valve to regulate normal force in a direction to correct for slip error. For a more detailed discussion on the system, and specifically regarding components of producing the variable slip reference, see control system details in the appendix starting on page 84.

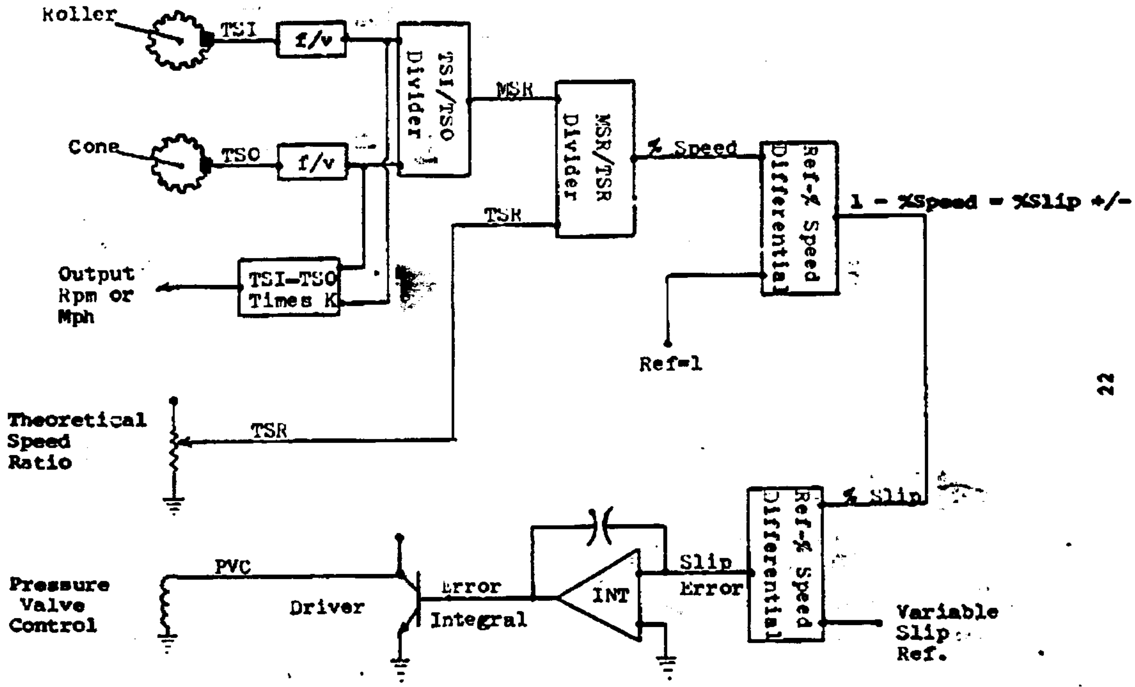

Slip Control Block Diagram

Figure 8:

Transmission output speed is provided by Traction Speed In (TSI) and Traction Speed Out (TSP), in accordance with the planetary power flow formulation and may likewise be converted to road speed by mathematical treatment including rear axle ratio and tire size.

$$Rpm_o = WC = \frac{WSSr - WRRr}{2\ Cr} = \frac{TSI(Sr) - TSO(Rr)K}{2\ Cr} \qquad (1.$$

Where K is the reduction ratio between the cone and ring.

Output speed and road speed are not required for traction control but may be used in the vehicle control system (VCS).

Materials

The materials which comprise the rolling elements are chosen for particular stresses and/or associated failure modes. The prevalent failure mode is rolling-element fatique for virtually all dynamically loaded roller and gear elements.

All gears in the transmission will be fabricated from surface hardenable steel (eg., SAE 93100, SAE 4620) and finished to automotive tolerances and surface conditions. Operating bending and surface compressive stresses are kept relatively low in order to avoid the traction losses associated with the traction fluid under high compressive contacts (high pressure with sliding). The gears will be relatively fine pitch helical spur designs except for the spiral bevel gears on the cones.

The bearings in the transmission are commercially available, fabricated from vacuum degassed 52100 steel, heat treated to Rc 58-61.

The roller in the transmission is fabricated from vacuum-degassed 52100 steel heat treated to Rc 60-63. The roller outside diameter is finish ground with a 12.7 cm (5 inch) crown radius. Normal bearing steel heat treatment practice is observed in producing the roller.

The cones are fabricated from premium vacuum-processed SAE 9210 steel. They are carburized all over to produce a .10 cm (.040 inch) deep case of Rc 60 hardness. The roller journals, cone surfaces, and spiral bevel gear cone journal diameters are finish ground to a surface finish of approximately 6 RMS.

The housings are cast aluminum. Their simplicity suggests the use of the die casting technique in their production.

Lubrication System

The lubrication system consists of an oil pump, oil filter, pressure modulation valve, pressure reducing valve, and relief valve. The distribution of oil to the pertinent dynamic elements is accomplished by oil transfer tubes, cast passages, and an oil manifold/jet system on the roller positioner.

Oil is pumped from the sump through the filter to the pressure modulator valve. The oil flow is then divided; part flowing to the cone loading cylinders, and part to the lubrication system of the gearbox.

Oil that is directed to the cone loading cylinders is pressure modulated to provide a closely controlled piston load on the cones. The modulating signal is produced through the computer to maintain the required amount of normal force between the rollers and cones to provide optimum slip. A flow control valve in each cylinder allows pressure relief during load relaxation periods.

Oil that flows to the pressure reducing valve is directed to the lubricating jets and passages at 34×10^4 to 48 to 10^4 N/m^2 (50 to 70 psi). Surplus oil then flows through a relief valve to the sump.

The jet system on the roller positioner consists of a manifold which supplies oil to four jets. These jets, in turn, spray oil into the traction conjunction. A telescoping transfer piston attached at one end to the forward bearing support provides oil to the positioner.

Traction Control System

The instantaneous torque capacity of the traction contact depends on the normal load between the roller and cone, the lubrication traction coefficient, peripheral velocity, surface finish, temperature and component geometry. Figure 9, page 27 depicts the relationship existing between roller and cone traction force (proportional to torque) versus slip at constant normal force (proportional to control pressure). At sufficient rolling velocity (Vr), to form and maintain an elastohydrodynamic (EHD) film thickness great enough to separate the contacting elements, the transmitted torque increases rapidly as slip (Vr-Vc) increases from zero until a peak is reached. This is the optimum operating slip value for the traction to exhibit maximum torque at the particular normal force. As can be seen the amount of torque that may be generated diminishes for values of slip greater or lesser than the optimum value. Conversely, in order to generate a predetermined or definite amount of torque, it is necessary to apply the depicted normal force (for fixed rotational speed, temperature, etc.). The depicted normal force is then the minimum necessary to give required transmitted torque. The relationship between traction and various normal forces is shown in Figure 10, page 28. It can be seen from the figures that traction torque capacity dimishes when slip is too high or too low or when normal force is changed while operating at optimum slip conditions. Therefore, if slip can be maintained at the optimum value for any normal force then maximum traction torque will be generated. Extending this rationale to cover a variable torque requirement, if optimum slip can be obtained by varying the normal force then maximum traction may be generated with minimum normal force for all values of required traction torque. Minus (-) slip is defined as insufficient slip (less than optimum) and positive (+) slip as excessive slip for control logic purposes. Referring to Figure 11, it can be seen that 1,112 N (250 lbf) traction may be generated by normal forces of 21,240 N (4,775 lbf) at -2.8% and +6.4% slip. Also by 18,896 N (4,248 lbf) at -3.5% slip and +5.2% slip, or 17,940 N (4,033 lbf) at +/- 4.2% slip. Obviously, any normal force greater than 17,940 N (4,033 lbf) is excessive and if more is actually supplied to the traction components then an insufficient (-) slip condition exists for the 1,112 N (250 lbf) traction requirement. With less normal force, slip becomes excessive. Component life and horsepower capacity suffer for any slip/pressure conditions except optimum.

The computer analyzes the information and outputs control information to the pressure control valve modulating the cone loading hydraulic system. System pressure to the cone loading piston is increased if sensed slip is too high, so that a greater normal force is imposed which will reduce slip to the required value. Conversely, the pressure is decreased, if slip is too low, until slip increases to the required value. The control system assures optimum pressure between roller and cones for all traction loop torque requirements.

Control System Component Description

Components comprising the control system are an analog or micro-processor computer (MPU), two encoder read heads, two toothed discs, two linear transducers, a pressure modulating value, two pressure transducers, and a positioner drive motor. (One linear transducer is used on the accelerator, one pressure transducer is used on the brakes, and the remainder of components are used for Optimized Traction Control (OTC)). See Figures 32 and 37, pages 85 and 97 in the appendix.

The positioner drive motor reversibly actuates the lead screw on the roller carrier. The vehicle control system (VCS) delivers the required polarity and motor speed information to an amplifier, and then to the drive motor. The positioner is moved at the rate and in the direction dictated by the computer. The motion of the drive motor ceases when the ratio is correct, as determined by the linear actuator attached to the accelerator or pressure on the brake, in comparison to true vehicle speed.

Functionally, when the accelerator is depressed the ratio changes and causes the flywheel to deliver increased power through the CVT and hence to the rear wheels. The actual ratio is determined by instantaneous flywheel speed and output speed requirement. As power is delivered to the CVT the slip condition in the traction cones and roller will change. This change will be manifest as an acceleration between the roller and cones, and electronically is an MSR change without comensurate TSR change.

Typical Traction Force VS Slip Curve

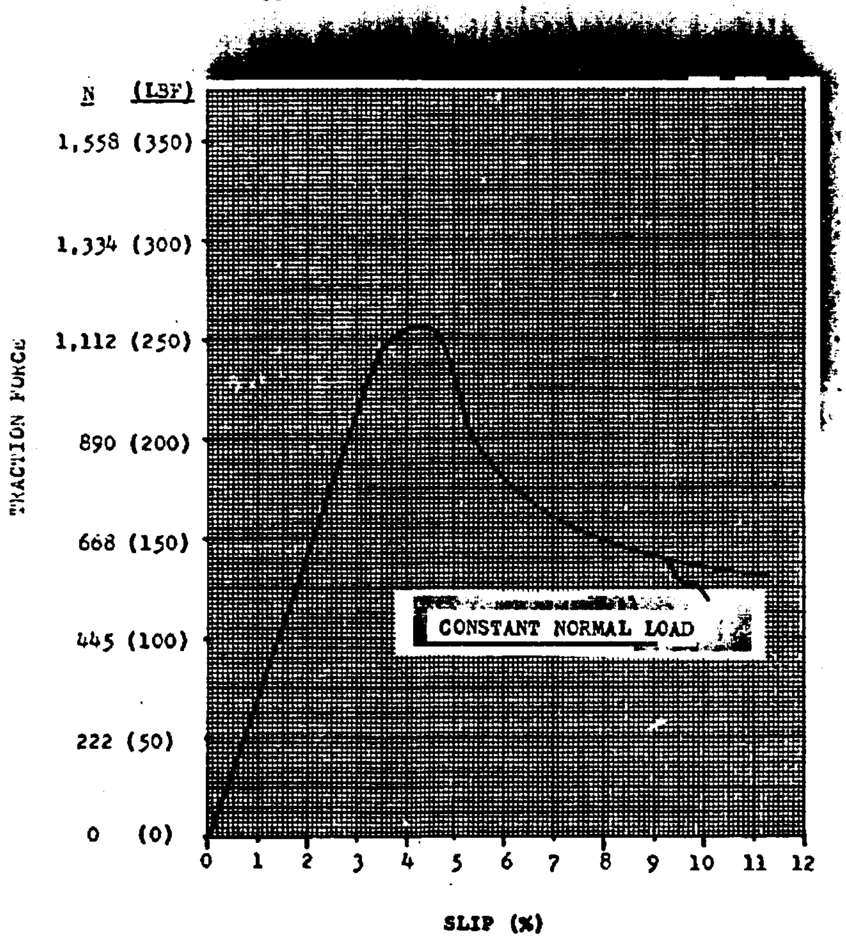

Figure 9:

Typical Traction VS Slip Curve Family

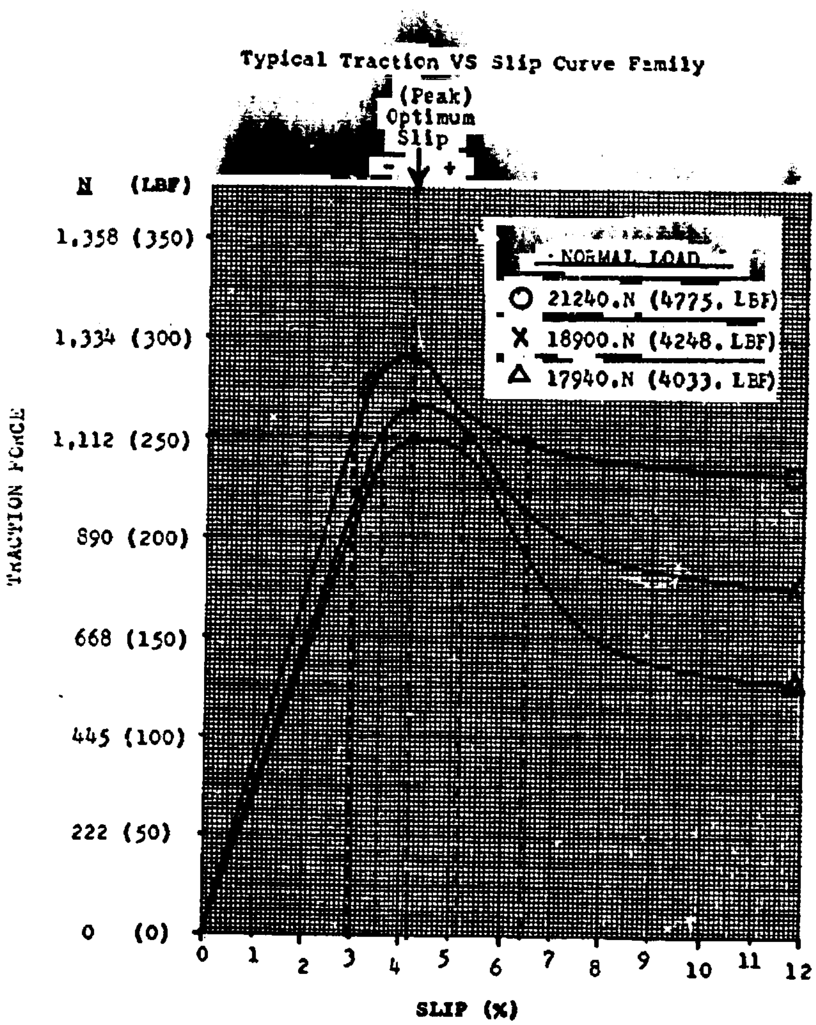

Figure 10 :

ANALYTICAL RESULTS

Efficiency

The overall efficiency of the Transmission is determined by summing the individual component power losses. Each gear and bearing is analyzed and the power losses multiplied by the number of like gears or bearings, then added together. The traction component losses are likewise added to produce the cumulative effect of the four cone/roller contacts. Total power loss for varied input and output speeds the power is shown in Table 1, page 30. Corresponding efficiencies are shown in Table 2, page 32, and Figure 11 through 15, page 34 through 38, respectively.

Figure 16, page 39, graphically expresses the linear relationship between the ratio of recirculating horsepower (m) to total output horsepower, and the total CVT ratio. Figure 17 through 21, page 40 through 44, are plots of total efficiency versus the total CVT ratio and the ratio of recirculating horsepower to total output horsepower.

The bearings are analyzed by a high speed digital computer which calculates bearing lives, operating stresses, and internal loads, kinematics, and friction losses. Bearing friction losses are predicated on a constant coefficient of friction of .075. This value is reasonably close at very high bearing loads, but the actual friction coefficient at moderate to low loads is much lower. The power loss attributed to the bearings is therefore much lower than is calculated by the computer program. A corresponding increase in efficiency would be reflected through lower power loss if a variable friction coefficient were used.

Gear losses are determined from the gear geometry, ratio, and friction coefficients as presented in Reference 1. Each different gear mesh is analyzed to determine the power loss factor then multiplied by the number of like meshes. Total power loss attributed to the gears is then determined for each power condition by multiplying the gear loss factor by the operating power (Hp_o X m). The component power loss factors

were assumed to be constant, for a conservative appraisal, and were used as such throughout the analysis. (Table 3, page 45).

REGENERATIVE CVT
TOTAL POWER LOSS
(INCLUDES GEARS, BEARINGS AND TRACTION ELEMENTS)

Rpm_o ↓ \ Rpm_n →	28,000	21,000	14,000
	KW Loss		
7.5 KW (10 HP)			
5000	1.00	.93	.91
4000	.92	.95	.83
3000	1.01	.99	.80
1500	1.39	1.24	.95
850	1.97	1.59	1.21
15 KW (20 HP)			
5000	1.89	1.75	1.61
4000	1.73	1.64	1.58
3000	1.92	1.75	1.62
1500	2.86	2.45	1.93
850	4.06	3.31	2.47
30 KW (40 HP)			
5000	3.53	3.62	3.64
4000	3.45	3.43	3.56
3000	3.98	3.70	3.58
1500	6.28	5.35	4.28
850	8.91	7.30	5.31
52 KW (70 HP)			
5000	6.63	7.05	7.88
4000	6.73	6.61	7.40
3000	7.68	7.23	7.46
1500	12.00	10.43	8.69
*(39.8KW) 850 *(53.4 HP)	17.79 (10.3)*	14.62 (7.86)*	10.65 (5.55)*

Table 1: *() Wheel Slip Limit

TOTAL POWER LOSS (REGENERATIVE CVT), continued

	75 KW (100 HP)	KW Loss		
	5000	9.66	10.52	12.54
	4000	9.98	9.98	11.09
	3000	11.11	10.54	11.32
*(70.3KW)	1500 *(94.3 HP)	16.73 (16.09)*	14.73 (12.86)*	13.70 (9.76)*
*(39.8KW)	850 *(53.4 HP)	26.46 (12.8)*	21.62 (9.59)*	16.92 (6.85)*

Table 1: *() Wheel Slip Limit
Continued

REGENERATIVE CVT EFFICIENCY

Rpm$_o$ ↓ \ Rpm$_n$ →	28,000	21,000	14,000
	Percent		
7.5 KW (10 HP)			
5000	90.0	90.7	90.9
4000	90.8	90.5	91.7
3000	89.9	90.1	92.0
1500	86.1	87.6	90.5
850	80.3	84.1	87.9
15 KW (20 HP)			
5000	90.6	91.3	92.0
4000	91.4	91.8	92.1
3000	90.4	91.3	91.9
1500	85.7	87.8	90.4
850	79.7	83.5	87.7
30 KW (40 HP)			
5000	91.2	91.0	90.9
4000	91.4	91.4	91.1
3000	90.1	90.8	91.1
1500	84.3	86.6	89.3
850	77.7	81.8	86.7
52 KW (70 HP)			
5000	90.5	89.9	88.7
4000	90.4	90.6	89.4
3000	89.0	89.7	89.3
1500	82.9	85.1	87.6
*(39.8KW) 850 *(53.4 HP)	74.6 (80.72)*	79.1 (85.30)*	84.8 (89.61)*

Table 2: *() Wheel Slip Limit

REGENERATIVE CVT EFFICIENCY (continued)

75 KW (100 HP)	Percent		
5000	90.3	89.5	87.5
4000	90.0	90.0	88.9
3000	88.9	89.5	88.7
*(70.3KW) 1500 *(94.3 HP)	83.3 (86.14)*	85.3 (86.36)*	86.3 (89.65)*
*(39.8KW) 850 *(53.4 HP)	73.5 (76.64)*	78.4 (82.04)*	83.1 (87.17)*

Table 2: *() Wheel Slip Limit

REGENERATIVE CVT

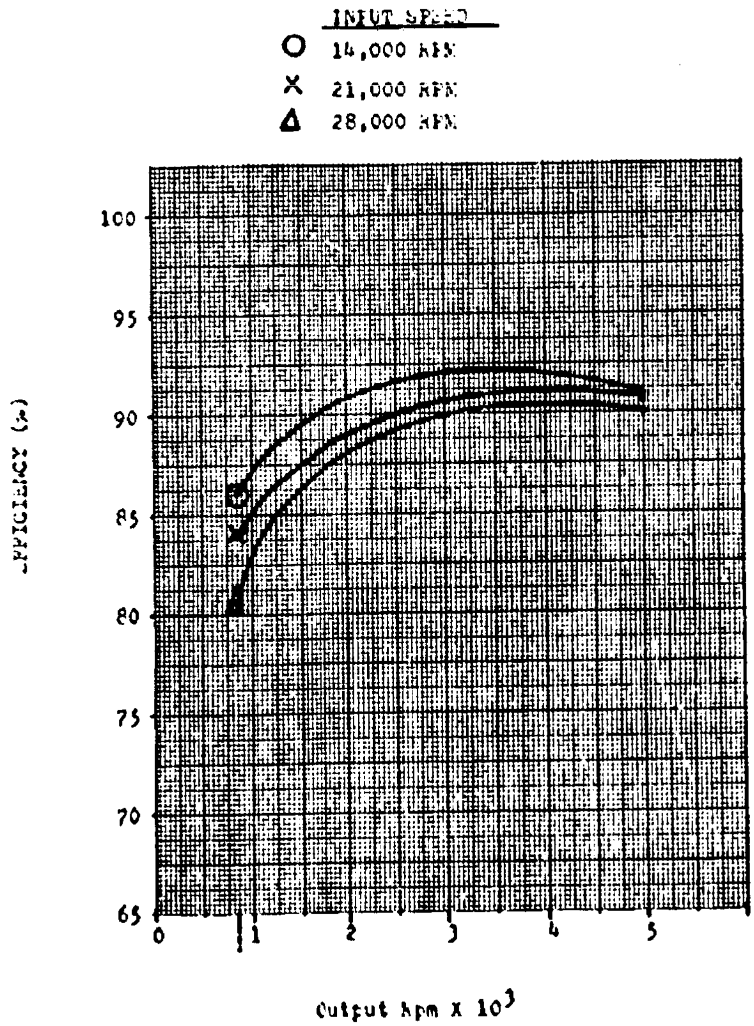

Figure 11: CVT Efficiency At 7.5 kW (10 Hp).

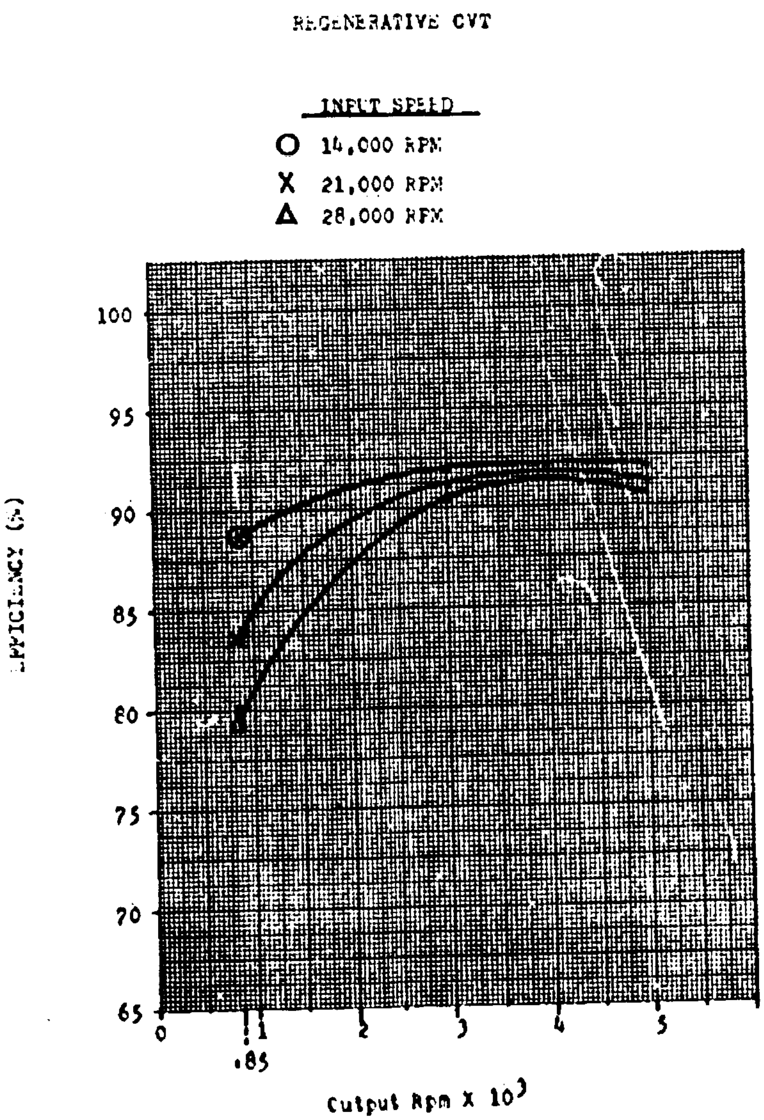

Figure 12: CVT Efficiency At 15 Kw (20 Hp).

REGENERATIVE CVT

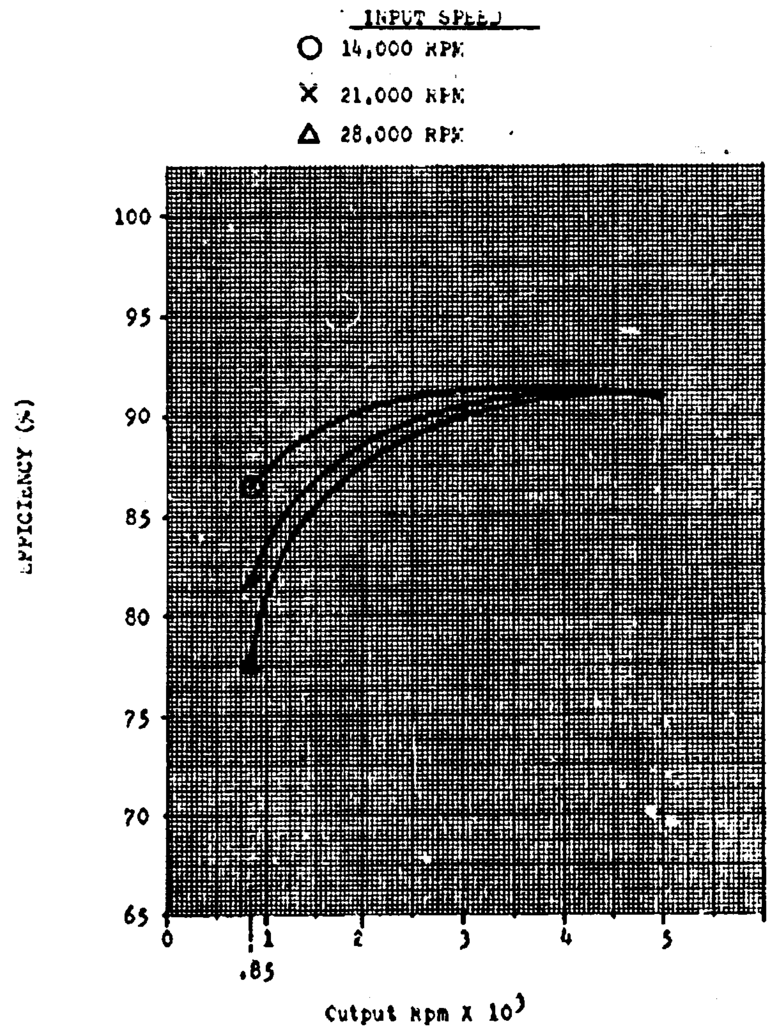

Figure 13 : CVT Efficiency At 30 Kw (40 Hp)

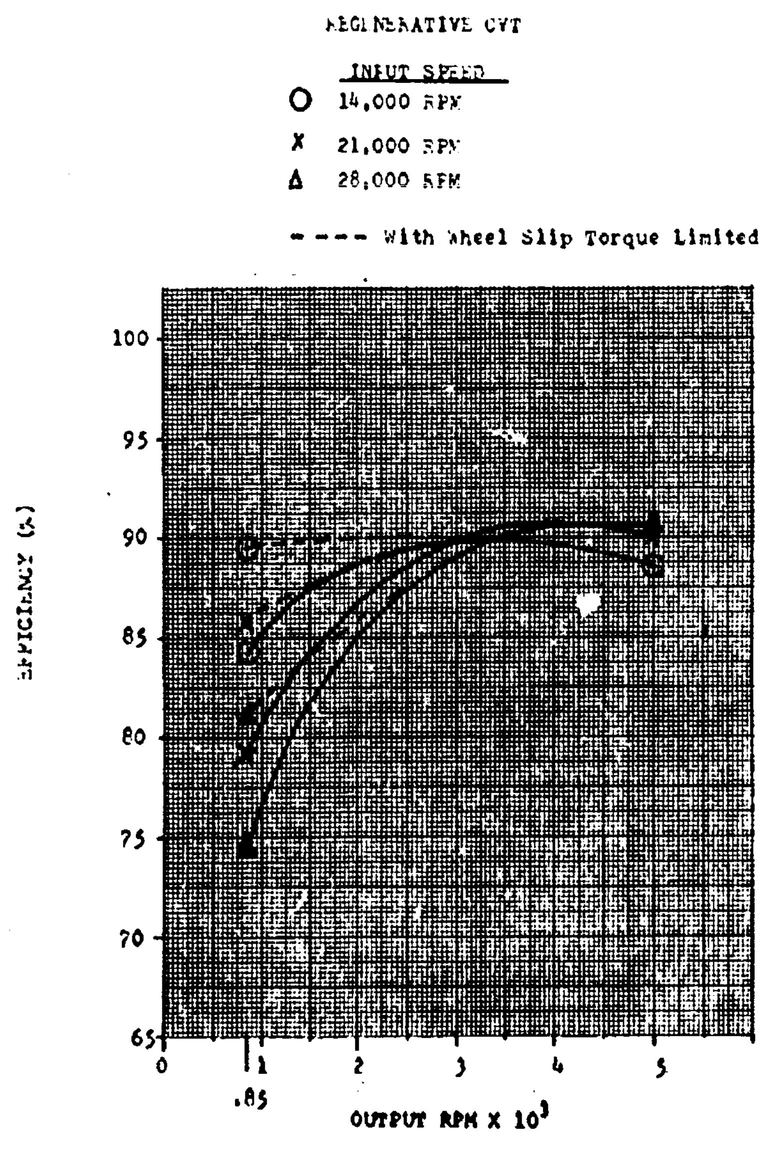

Figure 14: CVT Efficiency at 52 Kw (70 Hp).

REGENERATIVE CVT

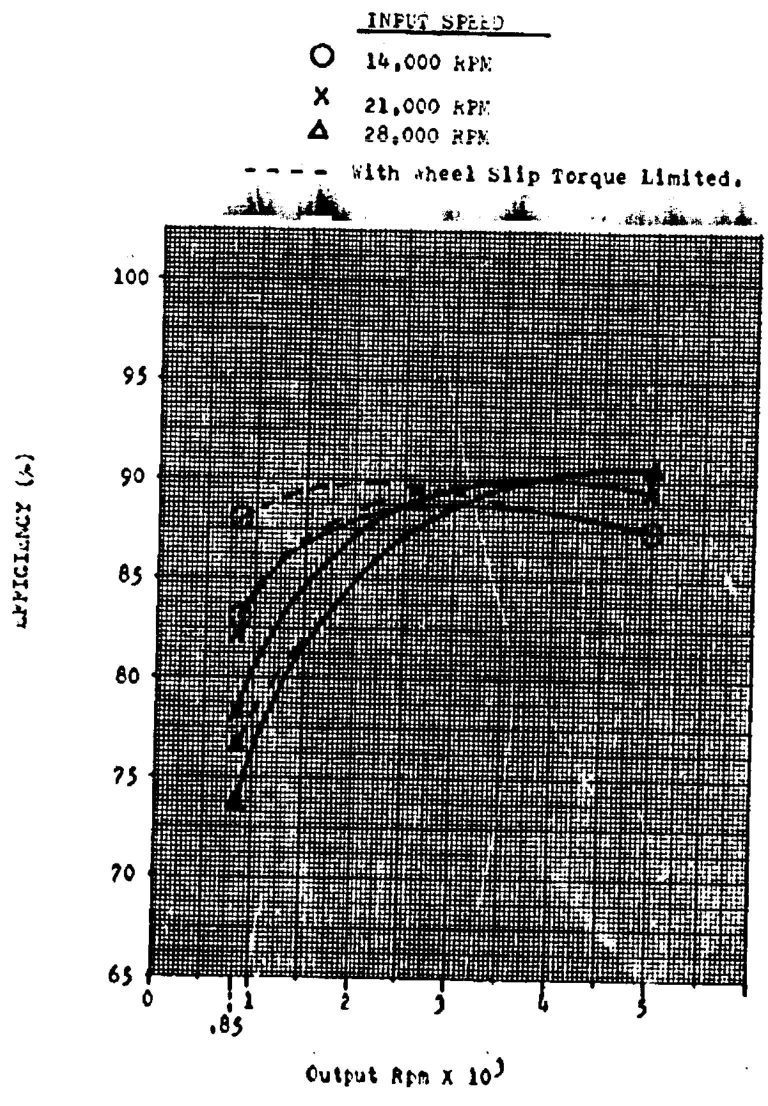

Figure 14 CVT Efficiency At 75 KW (100 Hp).

REGENERATIVE CVT

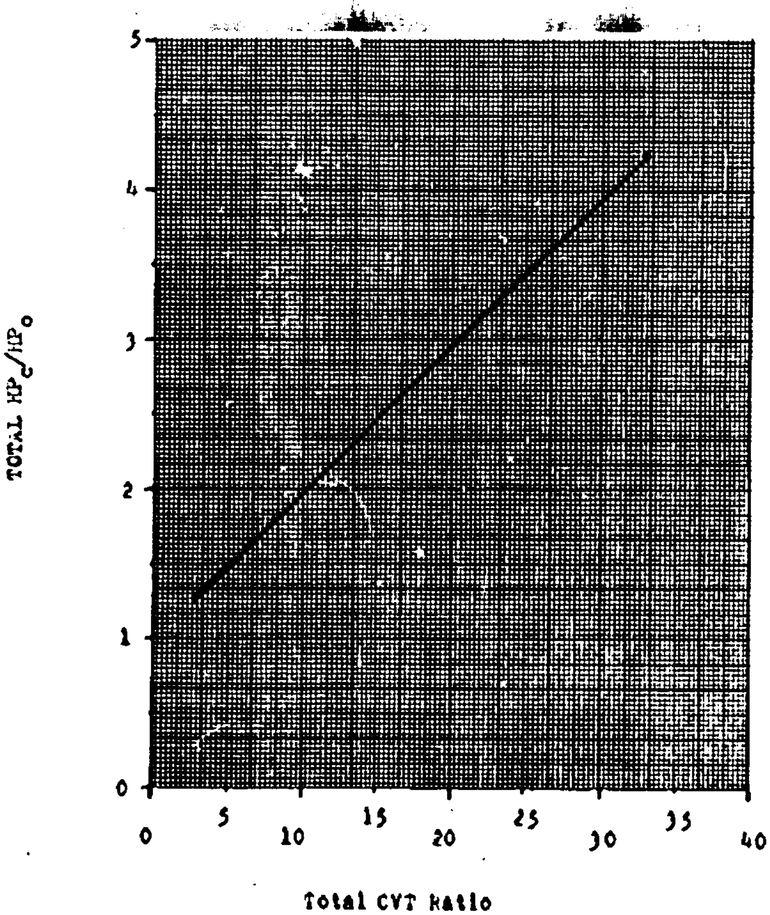

Figure 16: Ratio of Recirculating Hp To Output Hp VS Total CVT Ratio

Efficiency VS Ratio of Recirculating Hp To Output Hp and Total CVT Ratio At 7.5 Kw (10 Hp).

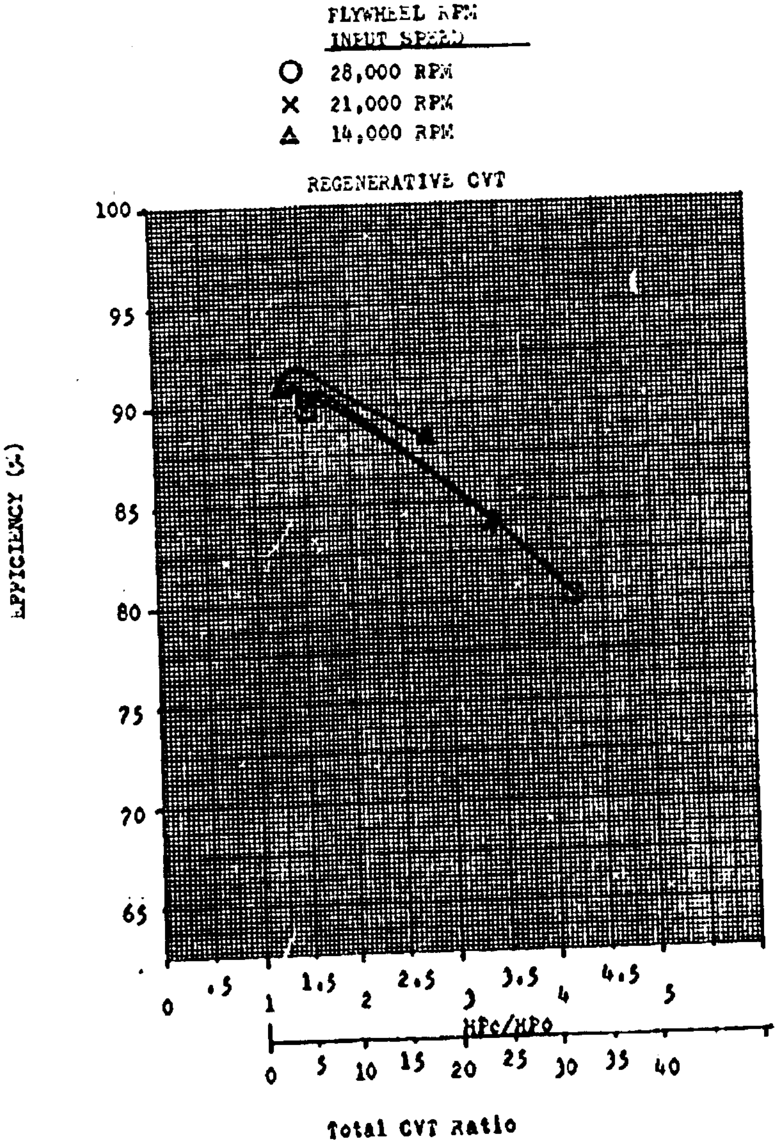

Figure 17.

Efficiency Vs Ratio of Recirculating Hp to Output Hp and Total CVT Ratio At 15 KW (20 Hp).

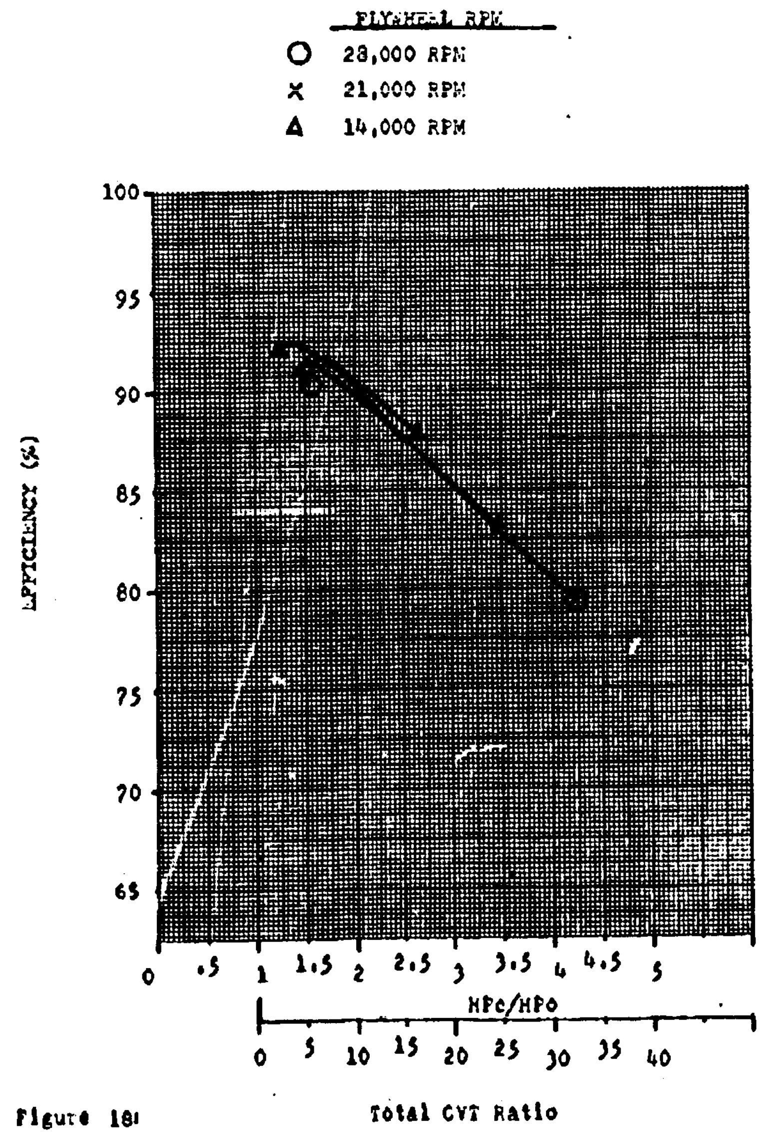

Figure 18

Efficiency VS Ratio of Recirculating Hp to Output Hp and Total CVT Ratio At 30 KW (40 Hp).

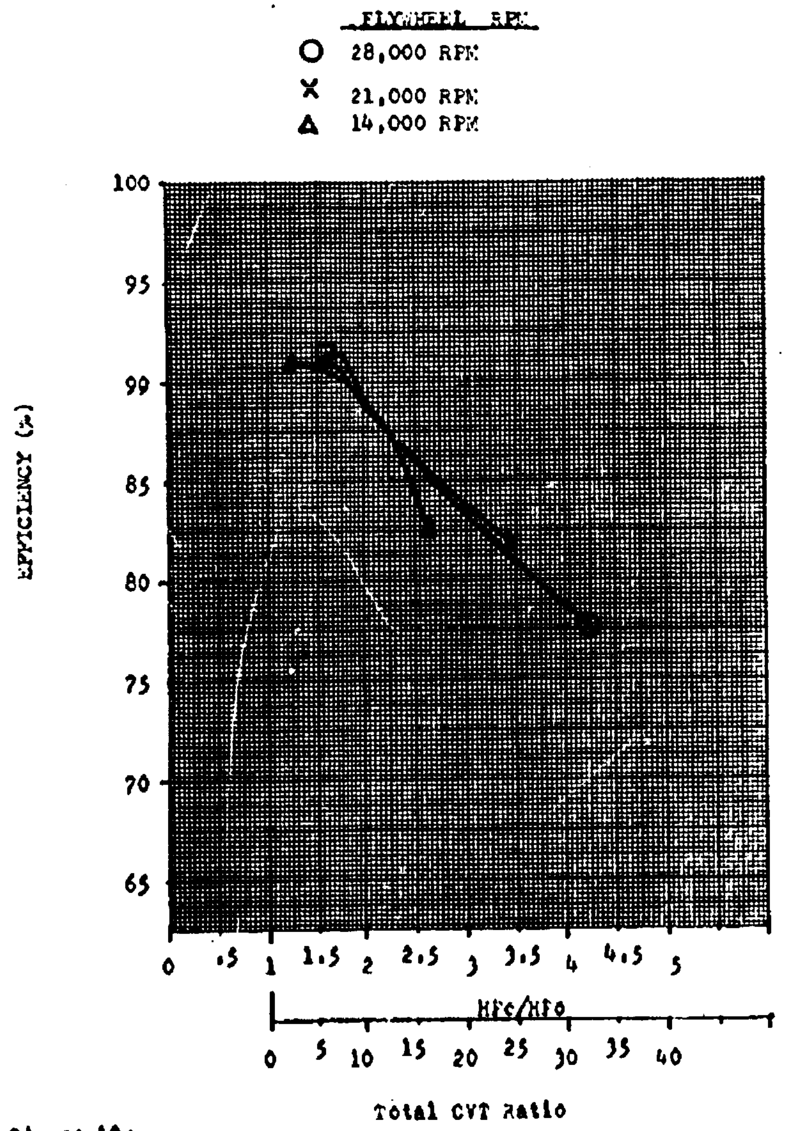

Figure 19:

Efficiency VS Ratio of Recirculating Hp to Output Hp and Total CVT Ratio At 52 KW (70 Hp).

FLYWHEEL RPM

O 28,000 RPM

X 21,000 RPM

Δ 14,000 RPM

---- Whith Wheel Slip Torque Limited.

REGENERATIVE CVT

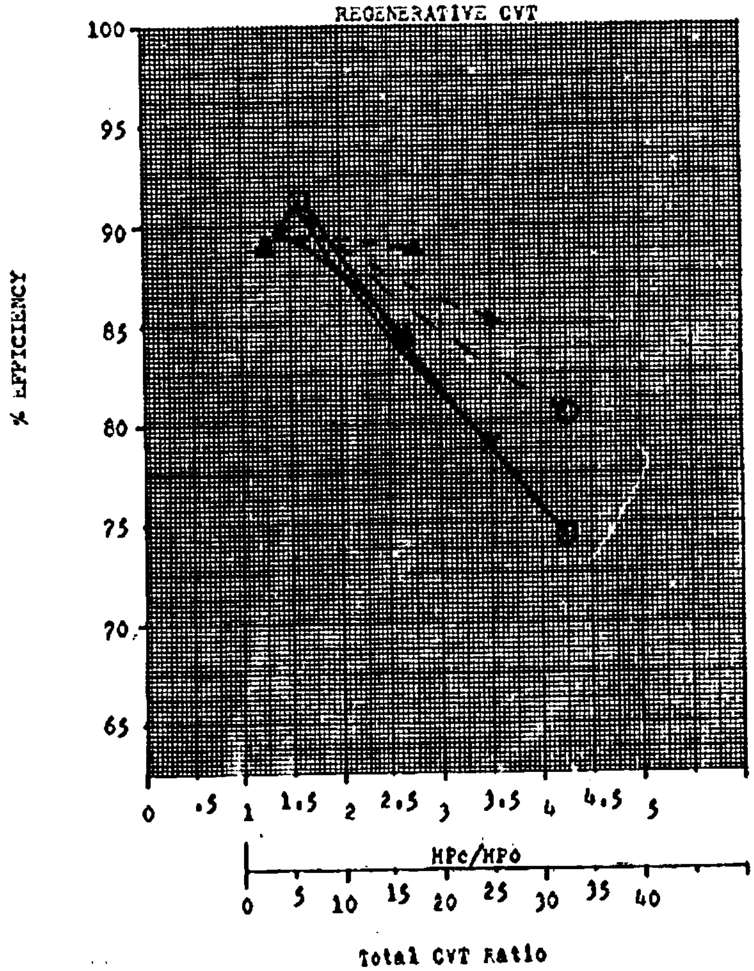

Figure 20 :

Efficiency VS Ratio of Recirculating Hp to Output Hp and Total CVT Ratio At 75 KW (100 Hp).

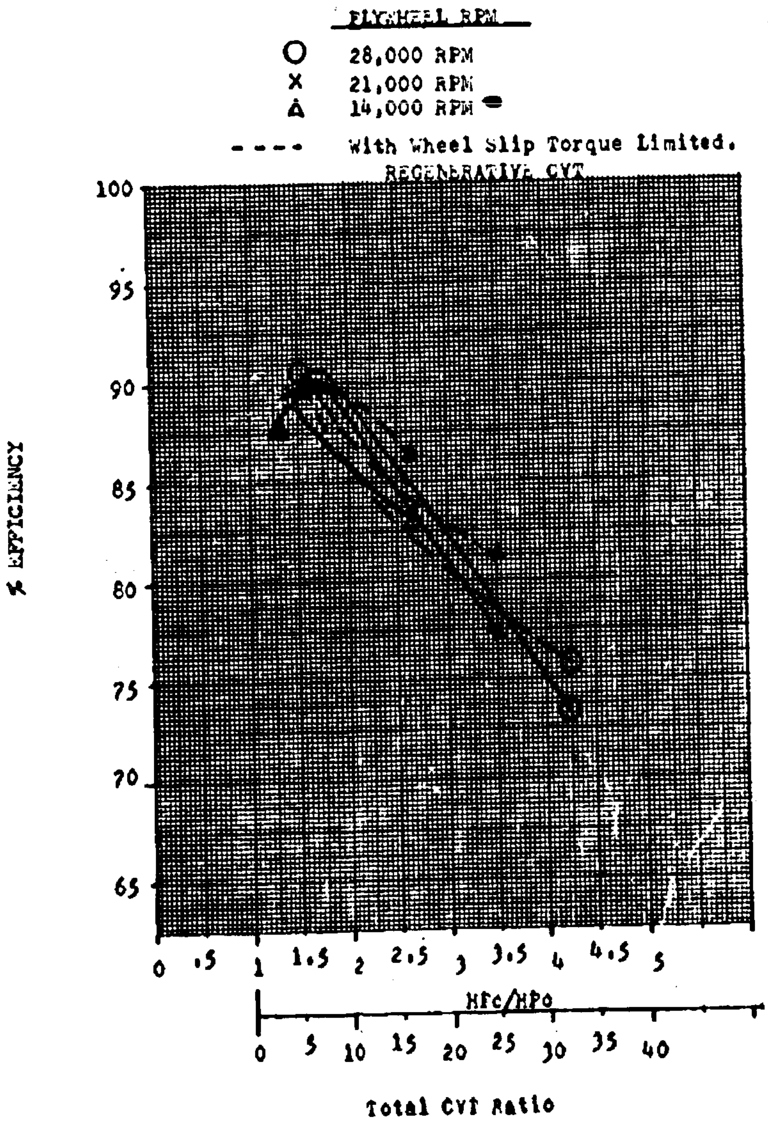

Figure 21:

Regenerative CVT Loss Source

	% Loss Each
Input Planetary	0.65
Spiral Bevel - Idler	0.81
Helical - Idler	0.44
Output Planetary	0.49
9.24° Cone/Roller Junction	1.60
Cone Bearings (3 sets/cone) wide variance with RPM and roller position (radial load distribution).	2.3/8.1
Loss Totals	6.29/12.09
Baseline Efficiency	93.7 to 87.91

The % loss totals are of internal horsepower. "m", and wheel slip limit values producing net output efficiency over the operating spectrum of 76.64% to 92.1%.

Table 3:

The traction unit losses are determined by using the method shown in Reference 1 as a guide. An example calculation is shown in the Appendix on page 159. Incremental positions of the roller along the cone (Table 4, page 47) for fixed flywheel Rpm (Rpm_n) to fix output Rpm (Rpm_o) is used to identify cone diameters at specific transmission ratio points (Table 5, page 48), and from which Traction Ratio and Cone Speed may be equated. These relationships are carried throughout calculations to determine Cone Torque (Table 18, page 135), Cone Normal Load (Table 21, page 141), Single Cone Horsepower (Table 19, page 137), Total Cone Horsepower (Table 20, page 159), and Traction Power Loss (Table 25, page 149) at specific output horsepower levels to quantify efficiency over the operating spectrum under given conditions. Sample calculations of these values are given in the Appendix as listed on page 70.

The contact geometry is calculated (Appendix page 151), then the spin velocity in the contact area is determined (Appendix page 145). Finally, the power loss through the traction unit (J7/J4), reference 1) is determined from tabulated values of slip and spin parameters (Appendix page 163 and 164). The power loss factor is then used to establish power loss in the traction unit for each power spectrum transmitted.

The coefficient of traction was taken to be a constant 0.07 for all calculations. Figure 22, page 49, is a volumetric plot of computer calculated peak traction coefficients over the operating spectrum for the regenerative CVT geometry.

Power loss due to windage of the gears was shown to be negligible. (See Appendix D, page 112). An overall loss factor of 0.037 KW (0.05 HP) was added to account for lightly loaded roller bearing conditions.

Study results indicate an overall operating efficiency of the regenerative CVT as 91.5% for the mean power condition, 16KW (22HP) and 3,000 Rpm output. Calculated efficiency ranged from 92.1% at 15KW (20 HP), 14,000 Rpm in, 3,000 Rpm out, to 76.64% at wheel slip "Torque Limit" of 39.8KW (53.4 HP) with 28,000 Rpm input and 650 Rpm output. Cone speed at the mean condition is approximately 23,480 Rpm; roller speed is 7,200 Rpm. The Roller Rpm equates to the output planetary sun gear (Rpm_s) and is used in certain calculations.

$$Rpm_s = \text{Flywheel Rpm } (Rpm_n) \;/\; 2.91666$$

(See Table 32, page 168).

ROLLER
AXIAL LOCATION

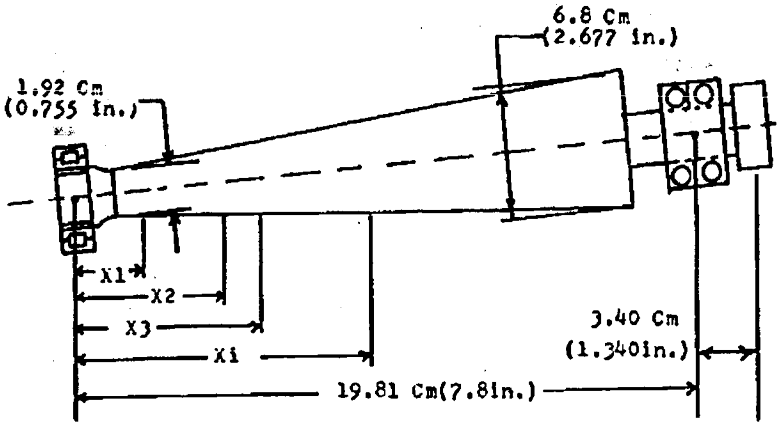

Xi, Cm (in.)
AXIAL LOCATION

RPM_o ↓ \ RPM_n →	28,000	21,000	14,000
5000	5.62(2.213)	3.90(1.534)	1.80(0.710)
4000	7.06(2.781)	5.22(2.056)	3.62(1.142)
3000	9.02(3.550)	7.06(2.781)	4.51(1.775)
1500	13.65(5.375)	11.78(4.637)	9.02(3.550)
850	16.87(6.643)	15.34(6.038)	12.85(5.060)

Table 4:

CONE DIAMETER, Cm (in.)

D_c = 11.53 cm/R_c (4.65 in./R_c)   RPMs = RPMn/2.91666

RPMo ↓ \ RPMs →	9600	7200	4800
5000	3.15(1.242)	2.60(1.022)	1.92(0.755)
4000	3.62(1.426)	3.03(1.191)	2.27(0.895)
3000	4.25(1.675)	3.62(1.426)	2.79(1.100)
1500	5.76(2.266)	5.15(2.027)	4.25(1.675)
850	6.80(2.677)	6.30(2.481)	5.50(2.164)

TRACTION RATIO

RPMo = (.2154 R_c - .2857) RPMs   RPMs = RPMn/2.91666

$$R_c = \frac{\frac{(RPMo)}{(RPMs)} + .2857}{.2154}$$

RPMo ↓ \ RPMs →	9600	7200	4800
5000	3.744	4.550	6.162
4000	3.261	3.906	5.195
3000	2.777	3.261	4.228
1500	2.052	2.294	2.777
850	1.737	1.874	2.149

CONE SPEED (RPM)

$RPM_c = (R_c)\ (RPM_s)$ $RPM_s = RPM_n$ / 2.9166

RPM_o ↓ \ RPM_s →	9600	7200	4800
5000	35942	32760	29578
4000	31306	28123	24936
3000	26659	23479	20294
1500	19699	16516	13329
850	16675	13493	10315

Table 5:

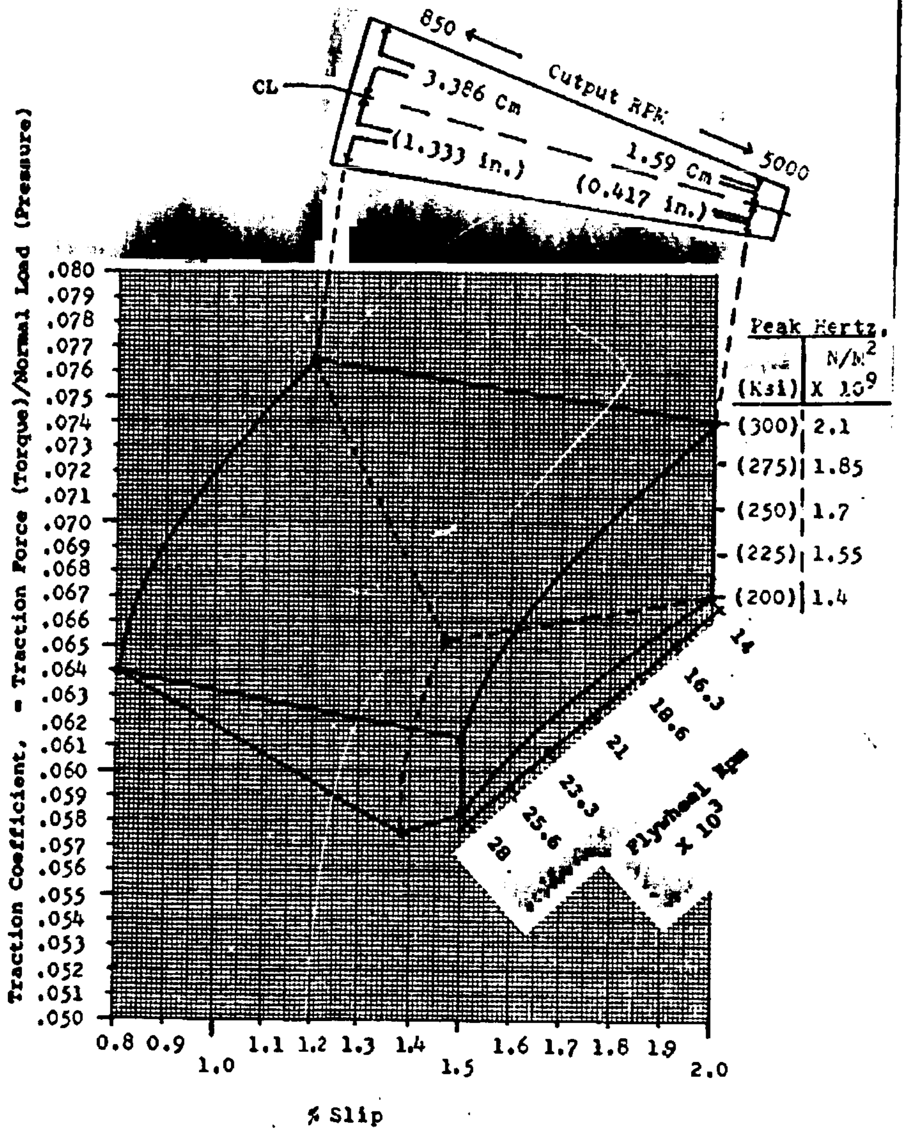

Volume-graph of Optimum Slip for Santotrac 50 at 70°F over normal operating range. (Current Geometery)

Figure 22:

Cost

A detailed review of all the elements comprising the transmission based on operating parameters and quantity per gearbox and a comparison to standard automotive parts was made. A weight and cost analysis was conducted for 5 makes of passenger car automatic transmissions in use for the past 10 years. Common elements in the CVT uses conventional automotive gears and bearings, planetary assemblies, and housings. The weight and cost analysis (Table 6, page 51) indicates a cost/pound of \$3.20 to \$7.40 for existing automatic transmissions with torque converters. Elements that differ are torque converter, control valve body, disc clutches, and control system in the standard automatic, and in the traction components and control system in the CVT.

The automatic transmission is considerably more complex than the CVT in the areas of number of detail parts, machining requirements, and assembly time, based on 100,000 units of each. The CVT has stringent tolerance and balance requirements on the cones and the finish requirements are on the order of antifriction bearing values.

However, all machining and processing variables necessary to manufacture the cones and rollers are well established. Tooling requirements would be no more restrictive or costly than for bearings or other precision components. Although no actual cost analysis has been possible (as by a bearing manufacturer) the processing techniques (grinding, heat treat, inspection) are well developed. A qualitative statement based on relative similarities between detail parts and processes in the automatic transmission and the CVT then would indicate a close similarity in cost per pound for each on a like production level basis. Based on this premise, it is believed that the CVT cost would be \$330.00, based on a dry weight of 34 KG (75 lbs.).

Weight

A detailed weight analysis of the CVT produced a total weight of 39 KG (85 lbs), Table 7, page 52. The housings are cast aluminum and the planetary carriers as shown are forged aluminum. However, in a value analysis program for the gearbox, the carriers would probably be made from steel stampings with selective welded construction. The weight and cost would be reduced for a high volume production run.

REGENERATIVE CVT

TRANSMISSION COSTS

(RETAIL, AUTOMOTIVE)

TYPE	COST*	WEIGHT*	$/KG	$/LB
FORD C-4	$ 532.85	60.8(134)	$ 8.76	$3.98
FORD C-6	$ 562.85	79.9(176)	$ 7.04	$3.20
GM 200	$ 829.00	50.8(112)	$16.32	$7.40
GM 300	$ 862.00	53.1(117)	$16.23	$7.37
GM 350	$1008.00	65.8(145)	$15.32	$6.95
CHRYLSER (TORQUEFLITE)	$ 650.00	72.2(159)	$ 9.00	$4.09

*WITH TORQUE CONVERTER

AVERAGE COST = $12.11/KG ($5.50/LB)

RETAIL MARK-UP (ASSUMED) = 20%

MANUFACTURING COST = (.8) ($12.11) = $9.69/KG ($4.40/LB)

QUANTITY PRODUCTION COST OF CVT = $9.69/KG

FOR 34 KG (75 LB) (MAX), COST = $330.00

Table 6:

REGENERATIVE CVT
TRANSMISSION WEIGHT

ITEM	WEIGHT (LB) KG	QUANTITY	TOTAL WEIGHT (LB) KG
INPUT HOUSING	(2.14)0.97	1	(2.14)0.97
MAIN HOUSING	(11.86)5.39	1	(11.86)5.39
OUTPUT HOUSING	(3.39)1.54	1	(3.39)1.54
INPUT SUN GEAR	(.71)0.32	1	(.71)0.32
INPUT RING GEAR	(.89)0.40	1	(.89)0.40
INPUT PLANET	(.07)0.03	3	(.21)0.10
INPUT CARRIER	(.44)0.20	1	(.44)0.20
INPUT PLANET SHAFT	(.03)0.01	3	(.09)0.04
BRAKE	(.28)0.13	1	(.28)0.13
ENCODER DISC	(.21)0.10	1	(.21)0.10
OIL PUMP PINION	(.25)0.11	1	(.25)0.11
OIL PUMP GEAR	(.30)0.14	1	(.30)0.14
PLANETARY KEY	(.004)0.0018	1	(.004)0.0018
LEAD SCREW	(1.72)0.78	1	(1.72)0.78
WORM GEAR	(.05)0.02	1	(.05)0.02
WORM	(.06)0.03	1	(.06)0.03
ROLLER POSITIONER	(.97)0.44	1	(.97)0.44
ROLLER	(3.40)1.55	1	(3.40)1.55
BALL SPINE	(1.96)0.89	1	(1.96)0.89
PISTON	(.17)0.08	4	(.68)0.31
SPRING	(.03)0.01	4	(.12)0.05
SPHERICAL SLEEVE	(.25)0.11	4	(1.00)0.45

Table 7

ITEM	WEIGHT (LB) KG	QUAN-TITY	TOTAL WEIGHT (LB) KG
CONE	(5.05)2.3	4	(20.20)9.18
CONE NUT (ROLLER BRG END)	(.05)0.02	4	(.20)0.09
CONE NUT (DUPLEX BRG END)	(.05)0.02	4	(.20)0.09
DUPLEX LINER	(.60)0.27	4	(2.40)0.11
DUPLEX CLAMP PLATE	(.58)0.26	4	(2.32)1.05
CONE ENCODER	(.09)0.04	1	(.09)0.04
SPIRAL BEVEL PINION	(.12)0.05	4	(.48)0.22
PINION KEY	(.01)0.0045	4	(.04)0.02
IDLER	(.43)0.20	4	(1.72)0.78
IDLER SHAFT	(.09).041	4	(.36) .16
IDLER PLATE (LEFT)	(1.29)0.58	1	(1.29) .58
IDLER PLATE (RIGHT)	(.71)0.32	1	(.71) .32
SPACER, BALL SPLINE SHAFT	(.05)0.22	1	(.05) .22
OUTPUT RING GEAR	(2.04)0.93	1	(2.04) .93
OUTPUT PLANET GEAR	(.29)0.13	4	(1.16) .53
OUTPUT PLANET SHAFT	(.07)0.03	4	(.28) .13
OUTPUT CARRIER	(.70)0.32	1	(.70) .32
OUTPUT SUN GEAR	(.34)0.15	1	(.34)0.15
OUTPUT FLANGE	(.18)0.08	1	(.18)0.08
BEARING, INPUT SUN DUPLEX (6904)	(.16)0.07	1	(.16)0.07
BEARING, INPUT RING BALL (6910)	(.28)0.13	1	(.28)0.13
BEARING, BALL SPLINE DUPLEX (6004)	(.32)0.15	1	(.32)0.15

Table 7 (continued)

ITEM	WEIGHT (LB) KG	QUANTITY	TOTAL WEIGHT (LB) KG
BEARING, ROLLER POSITIONER BALL (SPECIAL)	(.24)0.11	2	(.48)0.22
BEARING, OUTPUT RING BALL (6004)	(.16)0.07	1	(.16)0.07
BEARING, OUTPUT BALL (6004)	(.16)0.07	1	(.16)0.07
BEARING, CONE ROLLER (304)	(.38)0.17	4	(1.52)0.69
BEARING, CONE DUPLEX (7206)	(.90)0.41	4	(3.60)1.64
BEARING, INPUT PLANET ROLLER (B-78)	(.02)0.009	3	(.06)0.03
BEARING, BALL SPLINE ROLLER (B-167, IR-128)	(.08)0.04	1	(.08)0.04
BEARING, IDLER ROLLER (MR-100)	(.02)0.009	8	(.16)0.07
BEARING, OUTPUT PLANET ROLLER (MR-100)	(.02)0.009	8	(.16)0.07
OIL PUMP	*(.50)0.23	1	(.50)0.23
OIL	(9.38)4.26	1	(9.38)4.26
MISC. (NUTS, BOLTS, SNAP RINGS, SEALS, ETC.)	*(2.00)0.91	1	(2.00)0.91

*Estimated

TOTAL TRANSMISSION WEIGHT = 38.37KG (84.51LB)
DRY WEIGHT = 34.11KG (75.13LB)

(DOES NOT INCLUDE CONTROLS, ELECTRONICS, OR FILTER)

Table 7 (Continued)

Noise

Noise generating components in the CVT are gears, hydraulics and windage loss components (wind noise).

The gear teeth in the CVT are helical spur designs and spiral bevel designs which are sized to have a sufficiently large helix (spiral) angle to yield a high (> 2.0) total contact ratio. Helical action at the beginning and end of action of the conjugate teeth is much quieter than for straight spur gears. Gear tooth modifications of lead and profile also are used to assure smooth action. The gear teeth are lightly loaded so modifications will be small. By virtue of the light loads and helical and spiral gear designs the noise generated by the operating gears will be well below the audible range in the vehicle. The windage losses within the CVT are also quite low, hence the noise level will be below the audible level.

The noise effect of bearings and traction components will be much lower than for the gears. Therefore it is expected that the CVT will run quieter than the comparable automatic transmission.

Reliability

The CVT is designed for 2600 hours minimum life at the mean condition of 16 KW (22 HP) out at 3000 RPM output and 21,000 RPM input. The gear stresses at mean and maximum torque are all less than 82.7×10^6 N/m^2 (12,000 psi) and 413.7×10^6 N/m^2 (60,000 psi), respectively, which results in a virtual infinite life for the maximum stressed component. Similarly, the lowest life bearing is the input planetary pinion roller bearing with a life of 22,960 hours at the mean condition (Table 8, page 57). ASME life modification factors for the bearings are shown.

The minimum traction element life is 2920 hours (Appendix, page 134), as determined by the analytical method defined in Reference 3. The life of the traction elements, again, are determined at mean condition: 16 KW (22 HP) out 21,000 RPM in, 3,000 RPM out. Stress calculations are based on an 11.8 cm (4.65 inch) diameter roller, at 7200 RPM, with a 12.7 cm (5 inch) crown radius and 3,6 cm (1.426 inch) diameter cone, with a normal load of 2,217 n (498.5 lbs). Figure 23, page 58, illustrates the dramatic decrease in contact life as the power to the CVT is increased. Hertz stress at the traction contact point at the mean and maximum torque conditions was 1.58×10^9 N/m^2 (230,480 psi) and 2.97×10^9 N/m^2 (432,060 psi), respectively (Appendix LL, page 157).

The respective cone bending stresses were 38.3×10^6 N/m^2 (5560 psi) and 259.0×10^6 N/m^2 (37,530 psi) (Appendix U, page 130). Figure 24, page 59, is single cone HP vs output RPM.

While fatigue life of the dynamic elements is the general criterion for determining gearbox longevity, it is equally necessary to consider wear. The elements which are subjected to relative sliding may produce wear and wear particles which further accelerate the tendency to wear. Gear teeth, bearings, and traction elements are subject to wear, depending on the lubrication regime in which they operate. In all instances the dynamic elements are operating at such a relative velocity as to preclude gross metal to metal contact. Each set of gears in mesh are separated by a film of oil sufficiently thick to virtually eliminate any metallic contact. The same is true of the traction elements where the film thickness is 10.1×10^{-4} mm (39.6 in.) at the mean power condition (Appendix KK, page 155). The worst condition of power loading, 75 KW (100 HP) at 450 N-m (330 ft-lbs) output results in a film thickness of 7.1×10^{-4} mm (27.8 in.).

The ratio of film thickness to composite roughness in the traction cone and roller is h/ = 4.66 (mean). There will be relatively insignificant wear associated with this condition. Table 9, page 60, reflects gear stresses at maximum and mean power conditions.

Maintainability

Maintenance requirements for the CVT will be minimal. Due to the lack of wear exhibited by the dynamic components in conjunction with the variable load mechanism for the cones against the roller, it is anticipated that the only service required after initial run-in will consist of no more than an oil filter change.

Seal leakage, the major cause of transmission removal, will be minimized. The input seal is a carbon face magnetic seal, operating in a well aligned state, which adequately accepts the speed of the input shaft (up to 28,000 RPM). The output seal is a standard double lip elastomeric seal operating at low rubbing speed also in a well aligned condition. The only other seal is a double lip seal on the positioner motor. This seal is well above the static oil level in the CVT so no leakage is anticipated. This seal will be splash lubricated.

BEARING LIVES AT MEAN CONDITION

BEARING (LOCATION)	ASME LIFE FACTOR (D) (E) (F) (REF. 5)	L_{10} (HOURS)
BALL, DUPLEX (INPUT)	--	$> 10^6$
BALL, INPUT (RING SUPPORT)	--	$> 10^6$
ROLLER (INPUT PLANETARY)	6	22,960
BALL, DUPLEX (ROLLER SHAFT)	--	$> 10^6$
ROLLER (CONE SUPPORT)	6	23,480
BALL, DUPLEX (CONE SUPPORT)	6	34,590
BALL, OUTPUT (RING SUPPORT)	--	$> 10^6$
ROLLER (ROLLER SHAFT)	--	$> 10^6$
ROLLER (OUTPUT PLANETARY)	--	31,120
BALL (OUTPUT SHAFT)	--	$> 10^6$

Table 8

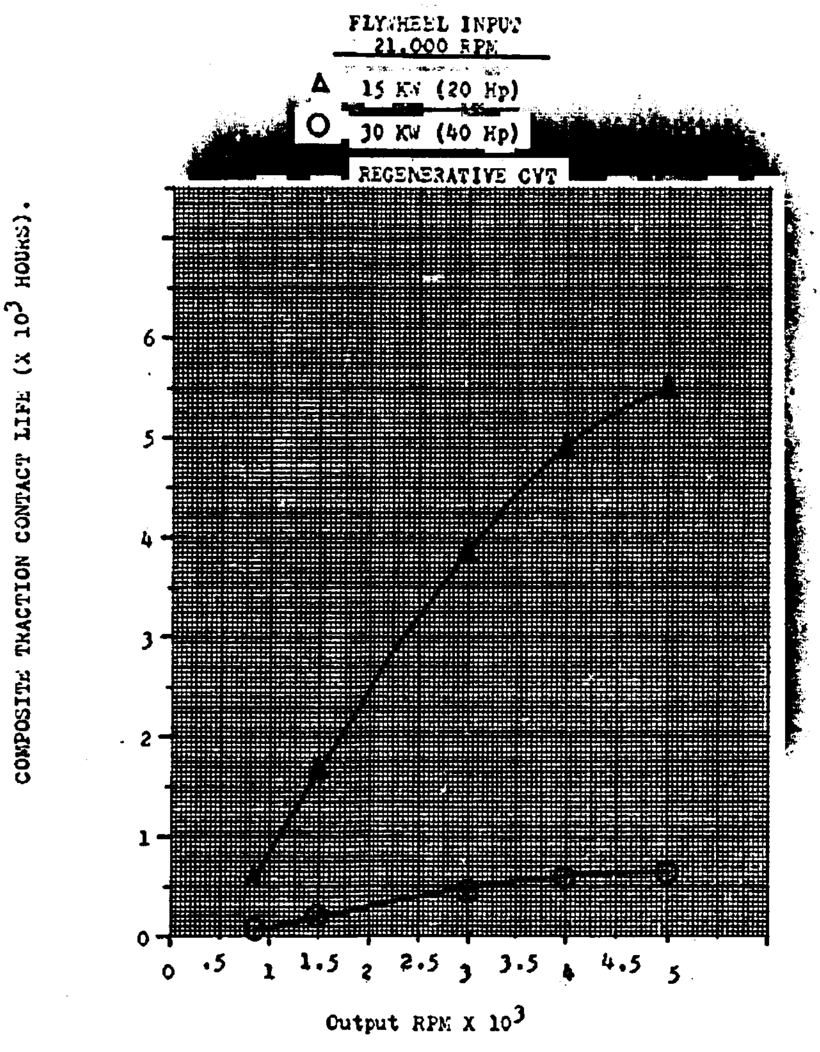

Composite Traction Contact Life VS Output Speed.

Figure 23:

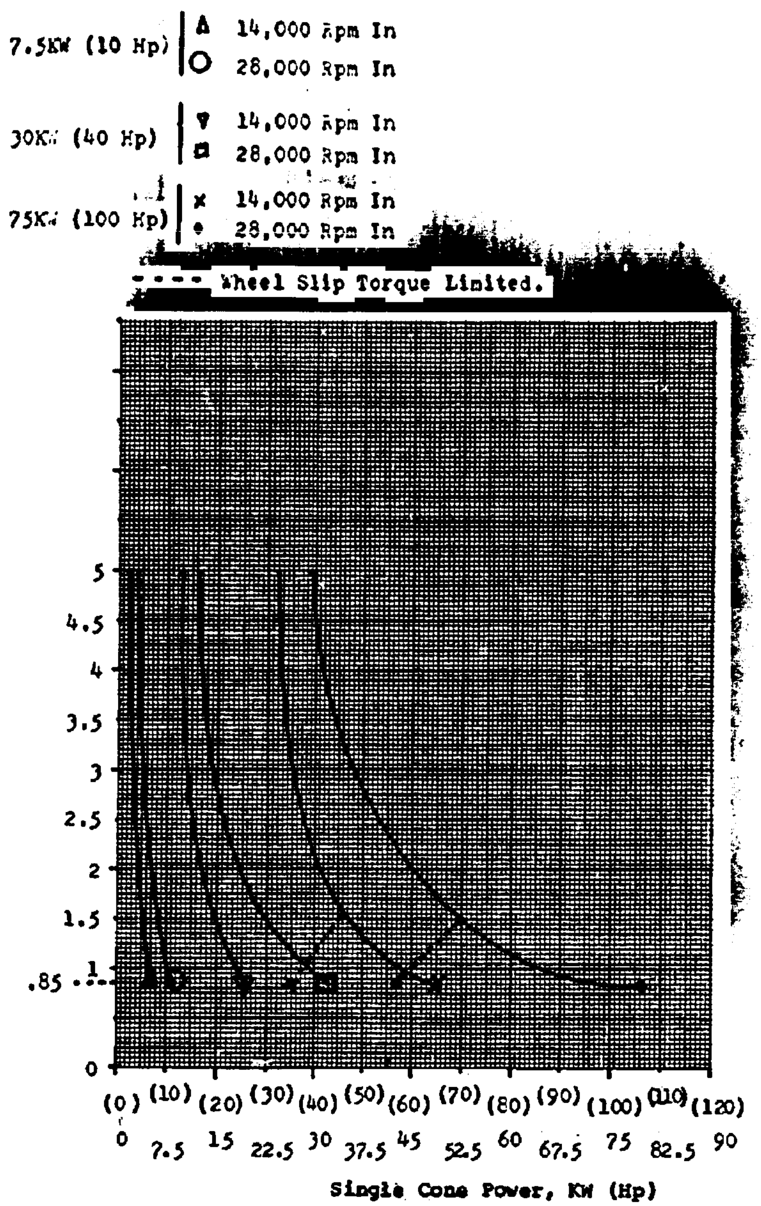

Figure 24 : Cone Power VS Output Speed

GEAR STRESSES

	BENDING 10^8 N/m^2 (10^3 PSI)		COMPRESSIVE 10^8 N/m^2 (10^3 PSI)	
	MEAN	MAX	MEAN	MAX
INPUT PLANETARY SUN PLANET	.630(9.15) .483(7.01)	3.267(47.42) 2.502(36.32)	6.231(90.44)	14.18(205.79)
SPIRAL BEVEL PINION GEAR	.0096(1.400) .0096(1.400)	.4992(7.240) .4992(7.240)	4.859(70.47)	11.06(160.42)
IDLER HELICAL SUN PLANET	.234(3.400) .194(2.810)	1.213(17.60) 1.005(14.58)	3.191(46.29)	7.264(105.36)
OUTPUT PLANETARY SUN PLANET	.143(2.080) .101(1.460)	.073(10.77) .5198(7.54)	2.490(36.12)	5.669(82.22)

Table 9

Scalability

The design requirement and criteria for scalability are the same as specified previously, with the exception of maximum output torque at wheel slip. The wheel slip torques to be considered are 210 N-m (155 lb ft) and 2690 N-m (1900 lb ft).

In reference 3 it is shown that the life of a traction conjunction varies in proportion to the size to the 8.4 power. That is, the life increases at a very rapid rate with any increases in size. While no actual calculations were performed to verify a similar trend of capacity with size, one set of calculations using a 22.9cm (9.0 in.) diameter roller and a 7.6 cm (3.0 in.) diameter cone was used to determine the capacity of the traction elements. With the surface velocity maintained the same as the baseline unit, 44.5 m/s, and using six cones, the capacity of the traction unit was 810 KW(1086 HP) based on 13.2×10^8 N/m^2 (192,300 psi) Hertz stress in the conjunction. The rotational speed of roller and cones was reduced to maintain the same surface velocity. The weight of such a unit would vary at a slightly higher rate than the square of the diameters. That is, the weight of an 810 KW gearbox would vary slightly more than $(9/4.65)^2 = 3.76$ times the 75 KW (100 HP) unit, which was designed for this study.

Downward scalability is more difficult to attain except by reducing the number of traction cones. In the case of the lower horsepower unit the rating was attained by simply reducing the number of cones from 4 to 2. Although for other practical reasons it would be advantageous to redesign the unit and maintain a minimum of 3 cones to maximize inherent component stability and equal distribution of forces and stresses within the system. An attempt to reduce the size resulted in very little actual reduction when faced with maintaining the life based on surface stresses in the traction conjunction.

Alternate Electric Drive

The electric motor input differs very little from the flywheel input in actual function. The use of the CVT, being directly driven by the electric motor and directly driving the differential, will provide the required performance. The only modification to the basic CVT shown in Figure 1 will be ratio changes in the planetary and cluster gear assemblies to produce the required output speed.

This will allow the traction portion of the transmission to remain virtually unchanged for the change in prime mover and operating speeds. The motor is allowed to operate at its optimum speed for the required vehicle drive power. The motor current would be monitored by the computer, with the control effect being to either speed up or slow down the motor, in conjunction with a CVT ratio change, to seek the minimum power drain for all conditions. Parameteric sampling by the computer would be exactly as with the flywheel input. The CVT would furnish the optimum performance for the electric motor only when compared to the use of stepping devices or other speed control means to control the motor. In all alternate schemes to provide an adequate vehicle speed for all terrains (i.e., uphill), the motor lugs down or absorbs too high a current drain to function efficiently. The use of the CVT, coupled with the constant monitoring by the computer, eliminates the adverse effects of excess power drain and assures optimum performance, to the extent that a smaller motor could be used in the same vehicle and exceed the operating characteristics of the vehicle without the CVT.

Alternate Hybrid-Electric Drive

A similar situation exists with the internal combustion (I.C.) engine driving into the CVT. I.C. input speed would be required to go through a speed-up planetary assembly to provide proper traction component speeds. The CVT will perform the function of allowing the I.C. engine to operate at its optimum BSFC for all output power requirements. The addition of the electric motor to the output shaft would have no effect on the actual CVT operation. The electric motor, when augmenting I.C. engine power at high power operating regimes, would simply transfer power to the vehicle drive wheels.

As previously described, the output planetary ratio and cone drive idler ratio would necessarily change in order to accomplish the output operating speed range. The ratio could be changed to accomplish the reverse and neutral conditions, as required. However, the efficiency at or near the neutral position suffers due to the regenerated power in the traction loop. As an alternative, the addition of an output planetary with reversing clutches could accomplish the range change without diminishing the efficiency beyond accepted levels. Further, a two or more speed unit with clutches could maintain the high efficiency for most of the speed range with a minimum of additional complexity. While multi-speeding adds some complexity and number of machined elements to the system the effects on overall efficiency increase are dramatic. See Figure 30, page 82.

POTENTIAL PROBLEM AREAS

Certain elements and features of the CVT design present potential problems and require special attention. These are: reaction to the tangential load on the cones (traction force), deflection of the cones and the associated traction contact pattern skew, hydraulic control response (piston motion and time), ratio change rate with the lead screw, binding effect of the axial force on the positioner imposed by the lead screw, piston relaxation time after pressure is reduced, and the accuracy and response time of the encoder/toothed disc monitor system. Addressing each item in sequence:

Reaction to the tangential load on the cones:

The traction force is reacted by the cone mounting bearings which are supported on the aft end by a quill in the transmission housing and on the forward end by the cone loading piston. This piston moves radially in plane with the cone/roller contact. The traction force generated in the traction conjunction causes a side load on the piston, which tends to bind the piston in the cylinder and prevent piston motion. To prevent the piston from actually binding an integral skirt is provided on either side of the piston to accept the side load. Further, the cast material will be a low friction material, such as 4032 aluminum, containing a high percentage of silicon. The magnitude of the side force will be always less then 1780 N (400 lbs) and the relaxation will lag the pressure drop. This always assures a load sufficient to maintain operation on the negative side of the optimum slip point. See page 74 for an alternative design.

Deflection of the Cone:

Bending moments imposed on the cone by the loading system will cause a curved shape of the cone, distorting the contact pattern in the traction conjunction. The roller is crowned with a 12.7cm (5.0 inch) crown radius. The drop from the point of the crown to the edge of the roller is .033 cm (.013 inches) which is much greater than the deflection of the cone for any loading condition. The roller is crowned to prevent edge loading under abnormal conditions and to provide an abbreviated major diameter of the contact ellipse. Crowning eliminates edge loading, provides reasonable contact ellipse dimensions, and reduces spin velocity.

Hydraulic control response:

Response of the hydraulic system to a computer output signal is determined by the modulator valve response time and the compliance in the hydraulic system. The response time will affect the slip rate and corrective traction force generation. If the response time is too great the output torque requirement may cause uncorrectable slip in the traction unit, thereby causing a runaway condition. The modulator valve responds in a matter of 1-5 ms (milliseconds) and the hydraulic system has at least the oil system pressure present at all times. The pressure lines are short with thick wall passages. Therefore, the response time is sufficiently short to allow all corrective motions of the piston to occur. The only feature to possibly cause a lag in the response motion is in the relaxing direction. The side load may be sufficient to prevent immediate reduction of the load thereby maintaining the traction load. See page 74 for an alternative design.

Ratio rate change with the lead screw:

The worm driven lead screw could limit the excursion time of the positioner from one end of the cone to the other end. The requirement to traverse the length of the cone from maximum ratio to minimum ratio, and vice versa, is 2.0 seconds. The lead screw requires 6.5 turns to produce the total excursion. The worm-wheel ratio is 16.5:1 which requires the drive motor to rotate 107 turns to move the positioner from one end of the cone to the other. The average speed of the motor would then be 3210 RPM. The positioner drive motor is 5,000 RPM reversible d.c. motor, which provides adequate margin to accomplish the excursion-time task.

It is recognized that the choice of a worm drive results in considerable loss in the worm-wheel set. The drive motor must therefore be sized to produce the required power for all control response inputs. The axial restraint of the roller at the traction conjunction is an unknown variable which must be evaluated on test; therefore the actual size of drive motor is an imperical factor. The worm-wheel design was done to maintain simplicity in concept and may require a lower power loss design in prototype and production units. See page 73 for an alternative design.

Binding effect of the axial force on the positioner:

Since the positioner lead screw drives the positioner axially at a considerable radial distance from the roller centerline, a bending moment is applied to the lead screw. The lead screw and drive motor may be unable to withstand the bending moment. The result would be binding in the screw at the positioner. In this event a second screw would be provided diametrically opposite the existing screw. Two screws thus situated would eliminate the imposed bending moment and apply a pure axial load to the positioner. See page 73 for an alternative design.

Piston relaxation time:

As previously described, the relaxation time required for the piston to unload the cone is a function of piston side load and friction. The piston is fitted with a flow control valve which serves a dual purpose: relieving the piston pressure to the lubricating system pressure of 34×10^4 N/m^2 (50 psi) and lubricating the cone support bearing. In the event that the lag time between load and relaxation is greater than the normal loading response time, the load would be maintained at a value in excess of what is required which would prevent excessive slip. However, this is not expected. When the pressure is relieved the load vanishes, thereby relieving the piston side load. Piston return would follow immediately. See page 74.

Accuracy and response time of the encoder/toothed disc monitor system:

This item is addressed in the section "Detail Control System Description", page 84 in the Appendix.

TECHNOLOGY ASSESSMENT

The mechanical transmission design embodies "conventional" automotive detail components; gears, bearings, shafting and housing. The unique elements are the traction components. Uniqueness is only in respect to the use of traction to accomplish variable speed instead of a torque converter and multispeed transmission. The traction roller and cone are fabricated of conventional materials using conventional processing. No new technology is required in their construction.

The traction conjunction physics are similar to gear tooth action or ball bearing action in that rolling and sliding exists in a lubricated conjunction. The use of a traction fluid for a lubricant imparts a greater traction force in the rolling-sliding conjunction than with conventional gear lubricants. Otherwise, the contacts are quite similar.

In the area of the control system, however, it was necessary to explore possible alternatives to the developed system presented herein. The use of electronic components that yield much higher response rates or activity rates was investigated. Alternates to the toothed disc and encoder are programmed magnetic film deposit with read head, digital signal generator and read head, and analog permanent magnet generator systems. While these components do not of themselves represent new technology, their use in the control system would require some development and test in order to be feasible.

CONCLUSIONS AND RECOMMENDATIONS

The design study has resulted in a computer controlled, continuously variable, transmission featuring multiple traction contracts, in a regenerative power. The traction elements are a crowned roller and four (4) cones in the regenerative design. The cones are aligned so that the cone axis is displaced at one half the cone angle from the transmission centerline. This puts the inner surfaces of the cones parallel to the roller axis. The roller is moved axially on a recirculating ball spline to affect a ratio change. Power is transmitted through the traction elements to an output planetary differential ring gear while feedback power is transmitted through the sun gear of the output planetary differential roller shaft. Traction ratio changes cause the output shaft speed to change.

The CVT designs presented herein result in lightweight, highly efficient, cost effective transmissions to be used in an electric vehicle. The designs enable the use of a power storage flywheel in conjunction with an electric motor, with an electric motor. Slight modification to the basic design provides immediate adaptability.

The computer control system provides exact ratio and speed changes to match the storage flywheel speed to the vehicle driveshaft speed. Power may be taken from the flywheel to propel the vehicle or it may be restored to the flywheel through braking. The flywheel may also be charged by the electric motor.

Study results indicate an overall operating efficiency of the regenerative CVT as 91.5% for the mean power condition, 16KW (22 HP) and 3,000 Rpm output. Calculated efficiency ranged from 92.1% at 15KW (20 HP), 14,000 Rpm in, 3,000 Rpm out, to 76.64% at wheel slip "Torque Limit" of 39.8KW (53.4 HP) with 28,000 Rpm input and 850 Rpm output.

The low weight and cost of a computer controlled traction CVT, coupled with its high efficiency, make it a viable transmission system for an electric vehicle. Those elements which represent relatively high risk areas have been addressed in detail. Any questions or potential shortcomings of the design capability at this point would be addressed during test and demonstration.

It is recommended that a follow-on program to conduct a detail design, fabrication and test program be conducted on the basic regenerative CVT or hybrid multispeed shown herein. Integration of the CVT with the computer control system into the electric vehicle would compliment the optimum propulsion system for the E.V.

List of References

1. Tevaarwerk, Joseph L., Traction Drive Performance Prediction for the Johnson and Tevaarwerk Traction Model. NASA Technical Paper 1430, October 1979.

2. Dudley, D.W. et al; Gear Handbook, McGraw Hill, First Edition, 1962.

3. Rohn, D.A., Loewenthal, S.H., Coy, J.J., Simplified Fatigue Life Analysis for Traction Drive Contacts. ASME Trans. Journal of Mechanical Design. Vol. 103, Apr. 1981, pp. 430-439.

4. Modern Methods of Gear Manufacture, National Broach and Machine Division/Lear Seigler Inc., Copyright 1972.

5. Bamberger, E.N. et al.; Life Adjustment Factors for Ball and Roller Bearings. ASME Design Guide. Copyright ASME 1971.

6. Jones, A.B., Analysis of Stresses and Deflections, New Departure, Division of GM Copyright 1946.

7. Daniels, B.K., Non-Newtonian Thermo-Viscoelastic EHD Traction from Combined Slip and Spin. Preprint No. 78-LC-2A-2 ASLE Preprint.

8. Daniels, B.K., Traction Contact Optimization. Preprint No. 79-LC-1A-1 ASLE Preprint.

APPENDIX LISTING

APPENDIX LISTING
(Continued)

APPENDIX A

STRUCTURAL ALTERNATIVES

Based on the detailed analysis of the current design the following considerations are made as means to improve design if required to resolve cited prospective problem areas.

1. Weight may be decreased and cost reduced by converting to a three cone system. An approximate 4% increase in cone radius provides the added power capacity for the regenerative design and no change is required for 3 cones in a multispeed arrangement. The restraints being compressive stress and cone bearing performance.

2. Change the shifting mechanism to a ball screw powered by a reversible-modulating wet clutch, driven by the input roller shaft. Or use a hydraulic cylinder to provide a less strenuous, rapid shift capability, and to eliminate bending loads on a screw. Strengthen the roller carrier by using a lightweight webbed assembly to provide continuous, uniform thrust on the roller carrier bearings, or include two or more screws.

"Gibs and ways" may be substituted for the linear ball bearings at the pads. Figure 25, page 73.

3. Convert the piston loading and cone mounting to a configuration as depicted in Figure 26, page 74. The self-aligning Spherical Liners insure proper bearing normal forces under even slight cone deflection or bending. The bearing liner recepticles being fabricated into the case for rigidity, (in lieu of one end being subject to deflection of the piston in the cylinder and cone loads inducing sid; forces on the control piston).

The gear end spherical liners were selected slightly larger in diameter to permit the cone to pass through the liner recepticle on assembly. The cone is merely passed through the hole and the lower journal slid into its bearing. The liner and gear end bearing properly centering the cone. The cone is free to move axially in its bearings and follows its center line angle toward the transmission center line until it contacts the roller.

The cone will contact the roller at a specific cone diameter depending on roller location on assembly.

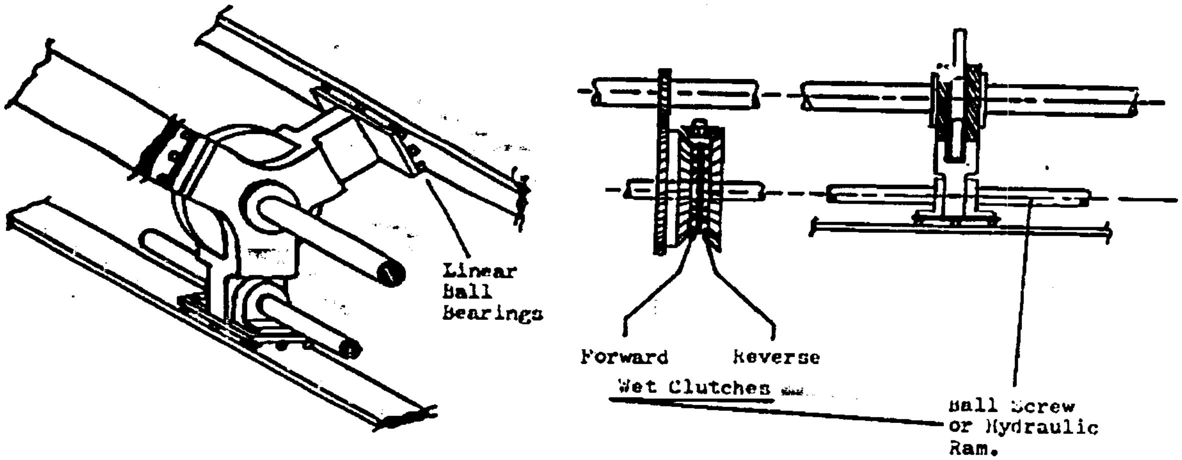

Alternate Roller Carrier
And Shifting Mechanism(s)

Figure 25.

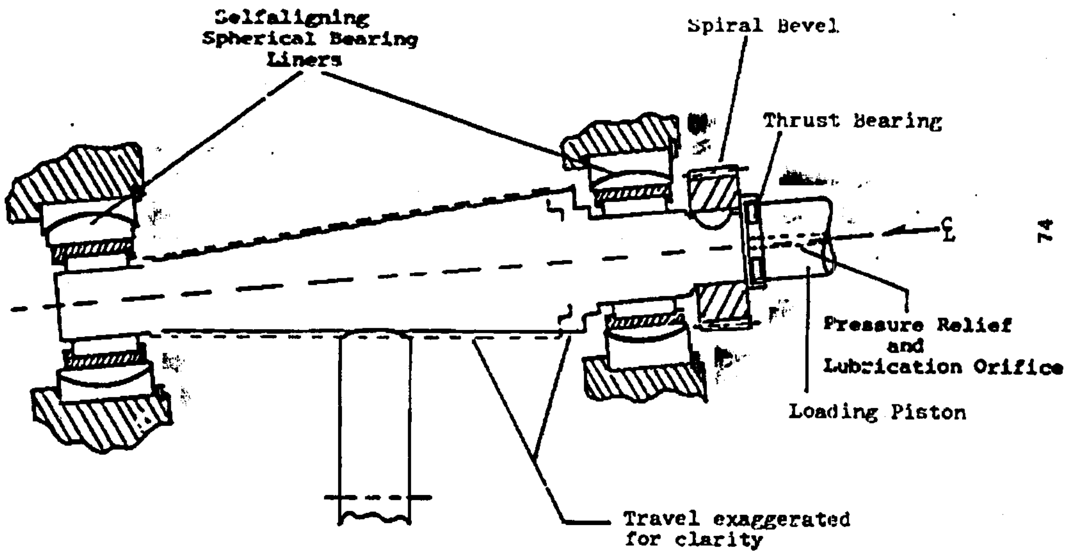

Pictoral of End Loaded Cone Mount

Figure 26:

The spiral bevel gear shoulder should be accurately located a given distance from the large cone shoulder or a "finish to fit" sleeve used to space the gear properly along a keyed output shaft for correct gear mesh at cone contact with the roller.

The technique provides simpler assembly with assured alignment and greater all around rigidity.

In addition the spiral bevel angle can be designed to provide thrust in the contact loading direction as a function of traction force (torque). One of the major complications to the optimized control system was the external load induced slip changes and response required to accommodate shock loads. Spiral bevel gear thrust with torque, insures that a rapid rise in external load, is countered with immediate rise in contact normal force. The load transient cannot induce slip without increased torque automatically providing increased normal load because of the traction force to slip relationship on the rising slope of the curve.

The spiral bevel angle should be selected carefully so as to place its response just slightly less than the corresponding Δ TCP/Δ CS slope selected for computer operations. (A slight "inadequacy" to maintain traction for the traction coefficient of the best fluid considered for use). Regular oil would then rely more heavily upon the computer to maintain proper traction.

The computer burden would be acutely reduced and its ability to respond greatly enhanced.

One added notation (and benefit) is the angle of the pressure piston. It is not perpendicular to the normal force but has a mechanical advantage of $1/\tan\theta$. For the current cone design $1/\tan\theta \approx (\theta = 9.24^{\circ}) = 6.147/1$. And the 5.5° cone has a 10.4/1 advantage. The required control pressure is reduced commensurately, bringing pressures into the range of the lubrication system. This eliminates the requirement for a high pressure system. Also the piston is free floating (restrained from rotating) and suffers no effects from cone forces due to load. Only minor travel is required for loading and unloading which is accommodated within normal gear backlash at the spiral bevel. A piston stop should limit the relaxation travel to restrain gear backlash to its maximum allowable value during initial startups, even though there is a spring in the cylinder to maintain minimum pressure.

Slip in the junction insures proper load sharing between the cones.

A small orifice through the piston injects lubrication to the lightly loaded thrust bearing separating the cone and piston.

A spring in the piston cylinder provides a minimum load to preclude bearing skidding under light loads and insures initial traction hence spiral gear reaction for baseline loading with limited response then needed from the computer.

4. Change power flow to provide conventional output shaft rotation using the same cone design and the same output speeds. (Figure 27, page 77). Stresses are the same as before because ratio expansion is the same. It requires a slightly larger planetary. Ring 140 teeth, sun 40 and planets 50 teeth, in comparison to the original of 100, 40 and 30 teeth respectively.

The increased size, however, is offset by the elimination of the spiral bevel-helical idler gears. The new spiral bevel junction is larger in pitch diameter (20/120) and should prove more efficient. However, just removing the idler gears and bearings saves 1-3% over the operating range.

5. The predominant loss is (at the highest reduction ratio) in the duplex cone bearings. Power loss curves closely resemble the bearing radial load curve. Figure 28, page 78 shows load distribution to the cone bearings, for the regenerative CVT. They share average loads equally but; 91% of the lightest load being carried by the piston bearing ($m = 1.27 \times .91 = 1.15$), and the duplex bearing must carry 85% of the highest loads, ($m - 4.24 \times .85 = 3.6$). The duplex bearings then have a peak service factor 3.13 times as large as the piston bearings, ($\div 2 = 1.565$). Cone bearing radial load distribution is enhanced by widening the support bearing stance. This becomes readily acceptable in the multispeed configuration where internal horsepower is reduced to a fraction of regenerative CVT horsepower over the operating range. This reduces cone bearing loss sensitivity to roller axial location and maintains a more stable loss/Hp in the bearing area.

Forward Speed Regenerative CVT

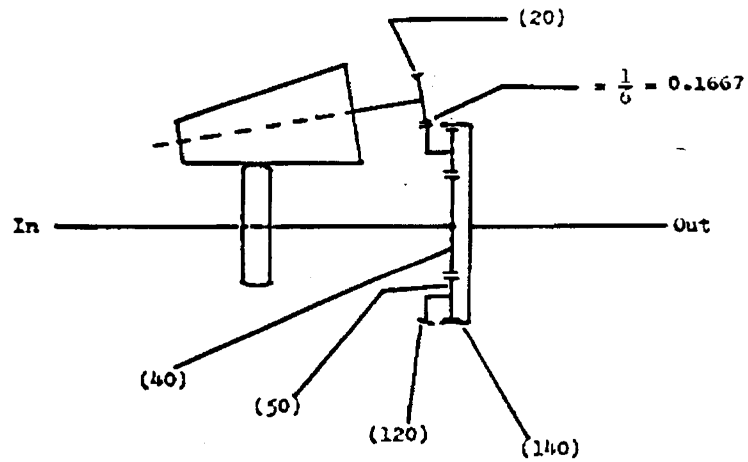

() Number of Teeth

Kinematic Diagram
(Less Input Reduction)

Figure 27:

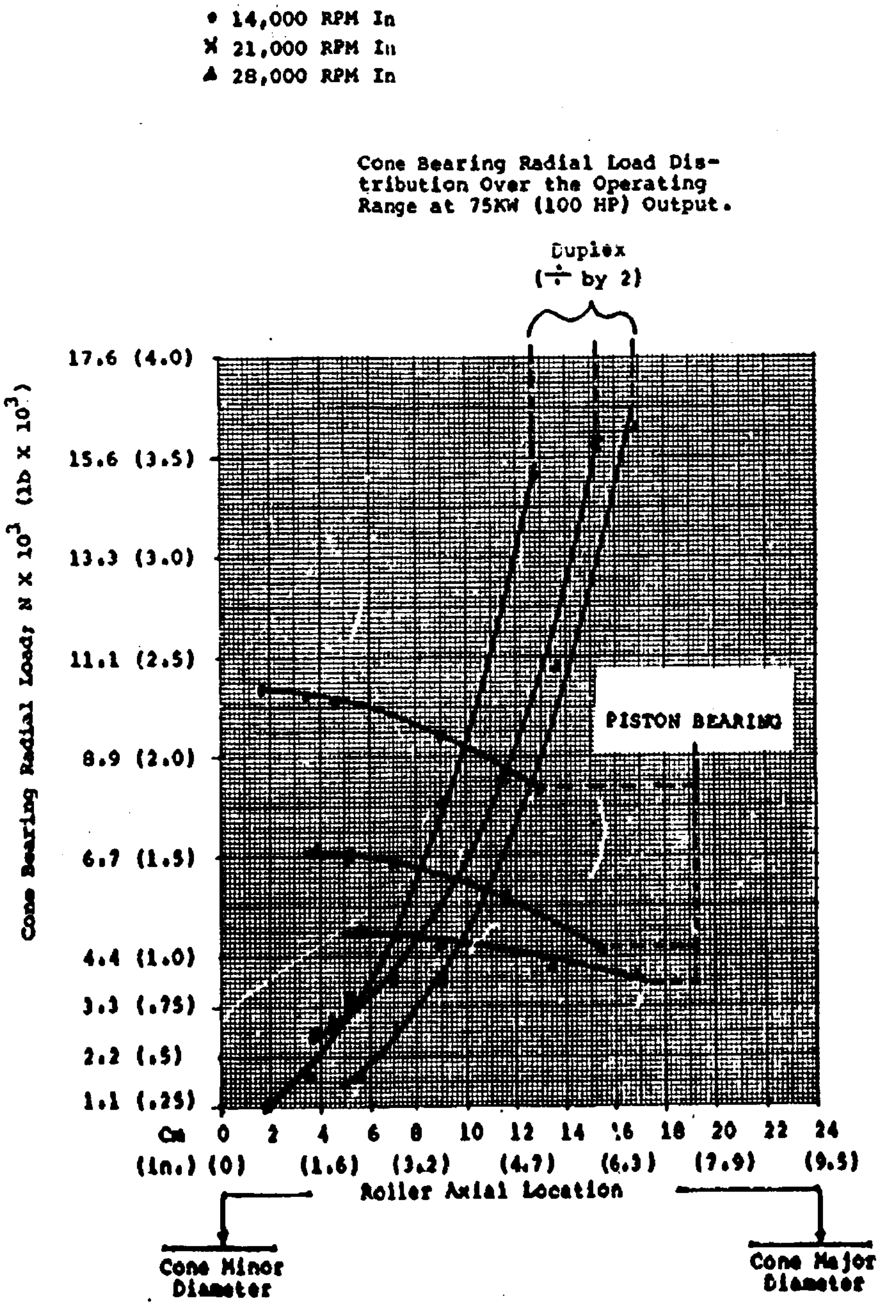

• 14,000 RPM In
X 21,000 RPM In
▲ 28,000 RPM In
Cone Bearing Radial Load Distribution Over the Operating Range at 75KW (100 HP) Output.
Duplex
(÷ by 2)
PISTON BEARING
17.6 (4.0)
15.6 (3.5)
13.3 (3.0)
11.1 (2.5)
8.9 (2.0)
6.7 (1.5)
4.4 (1.0)
3.3 (.75)
2.2 (.5)
1.1 (.25)
Cone Bearing Radial Load; N X 10^3 (lb X 10^3)
Cm 0 2 4 6 8 10 12 14 16 18 20 22 24
(in.) (0) (1.6) (3.2) (4.7) (6.3) (7.9) (9.5)
Roller Axial Location
Cone Minor Diameter
Cone Major Diameter

Figure 28:

APPENDIX B

MULTISPEEDING IMPACT ON DESIGN AND PERFORMANCE

Multispeeding step gear transmissions are common in the industry but multispeeding in conjunction with a limited range CVT is of current consideration. First, one primary feature of a CVT, the simplicity, may be lost by multispeeding. Second, the drivability must be carefully considered. Other considerations are cost, size, weight, control, efficiency and service life.

Size and weight appear to be reasonable with the overall design envelope being conducive to retrofit if desired. Cost, control, drivability and survivability all seem reasonable if the method of multispeeding is carefully considered. The efficiency and survivability of the traction components is greatly improved by multispeeding.

Control and drivability are best achieved by clutching the existing planetary to redirect powerflow to change range. Clutching the existing planetary also minimizes the number of parts added to the system, which is helpful from the size, weight, cost vantage point.

The addition of clutches should not be detrimental to survivability since clutching is designed to occur at points on the cone-roller junction wherein there is minimum or no speed differential at closing.

Figure 29, page 81, reflects the desired principle of the clutched planetary, power flow change, for achieving range changes. Ultimate efficiency is obtained by providing two direct cone drive ranges wherein power regeneration is avoided and in between these two ranges providing a regenerative power flow through the planetary to reverse the cone function so that a range change may be made without having to relocate the roller as part of the shift. While this has been successfully done on paper it does require a complex clutching arrangement and another approach is indicated where acceptable to the specific application. The clutching complexity is not intolerable and it does provide very low stress, light weight design of the traction components and operate continually at high efficiency.

A simpler approach, shown in Figure 31, page 83, is to use a lockable torque converter to provide neutral and high initial reduction rations, for range 1. The roller is located at the minor diameter of the cone and remains there until come minimum design speed is achieved. The torque converter provides a smooth increase in speed to the point that the CVT may come into use. This provides the same minimal stress designs as before but with only about half as many clutches and components.

Range 1 is with clutches "b" and "c" engaged and the torque converter in service. When the minimum speed (with some range overlap) is achieved, the torque converter begins to lock up. During this transition the roller only moves to maintain a surge free shift, by compensating the traction ratio downward to offset for the elimination of slip within the torque converter. This is a relatively minor roller motion and while longer than other shifts in the multispeed design, it is no longer than the shift of a conventional automatic transmission; plus does not induce the surge or shock of a conventional shift incurred by the step change between ranges.

The power flow in range 2 is through the input spiral bevel gear driving the cones, through the traction junction to the roller. With clutches "b" and "c" engaged and the torque converter locked, the output (sun gear) is forced to co-rotate with the roller and no relative gear motion is involved. As the roller is moved toward the major cone diameter the roller speed is increased and hence the output speed increases.

When the roller approaches the major cone diameter a point is reached where the roller Rpm exactly matches the input spiral bevel gear and clutch "a" may be closed without a closing speed differential. Clutch "c" is opened and power flow is now split with part flowing from the input spiral bevel gear driving the cones and part through clutch "a" driving the planetary carrier. The part flowing through the cones drives the roller which now only drives the planetary ring gear. As the roller is relocated toward the minor cone diameter the ring gear is slowed and it may be seen that power flowing through the planetary carrier induces a step up speed to the output sun gear. The split power mode provides range 3.

A range 4 may be used in some applications; which is direct motor drive accomplished by positioning the roller so that the input spiral bevel speed matches the roller speed, then engaging all clutches and locking the torque converter. By leaving the roller in this position the output speed is a direct function of motor speed and no traction contact losses or gear losses are generated; this could provide a useful openroad range.

To overcome the inherent thrust developed on the cones by the cone angle, in combination with torque and pressure, and to provide an excess of mechanical spiral bevel gear thrust loading with torque at the cones, the spiral angle would run from 15° to 25° as a function of other design variables and the fluid used. The computer then "unloads" the traction contact to optimize the power capacity and efficiency. Piston control pressures required in the structure are reduced to normal lubrication oil pressures thereby eliminating the high pressure oil system and further provides a failsafe control since the transmission will work without the benefit of optimization through unloading pressure.

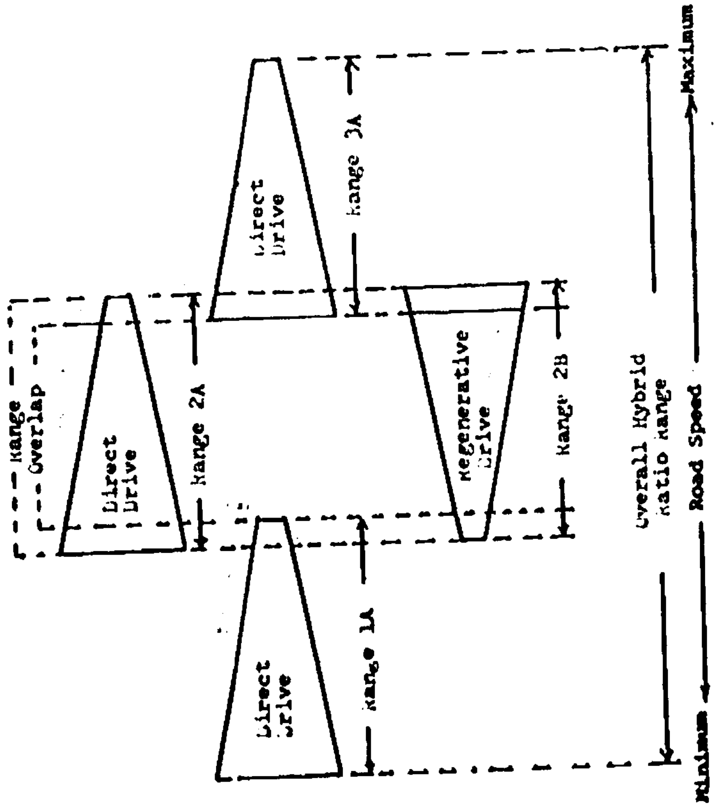

Multispeed Function Diagram

Figure 29:

RPM HP Flywheel/Power Conditions
A - 14,000/10
B - 21,000/40
C - 28,000/100*

▲ Regenerative CVT as Studied

● Typical Multispeed Design (See Fig. 31, pg 83)

Volumeteric Efficiency
Over the Operating Spectrum
of 7.5 KW(10 HP) to 75 KW(100 HP
or*Wheelslip Limit)

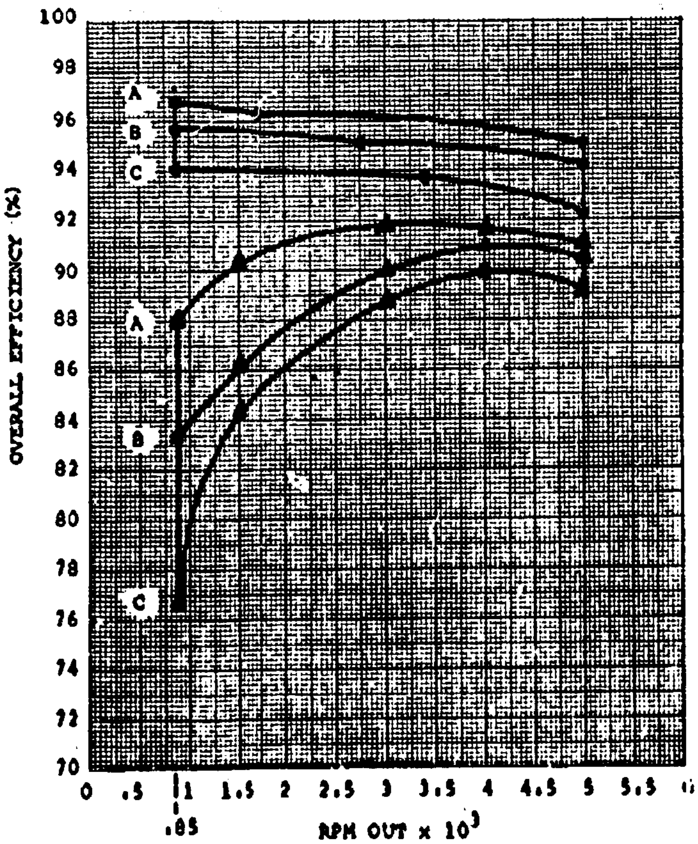

Figure 30:

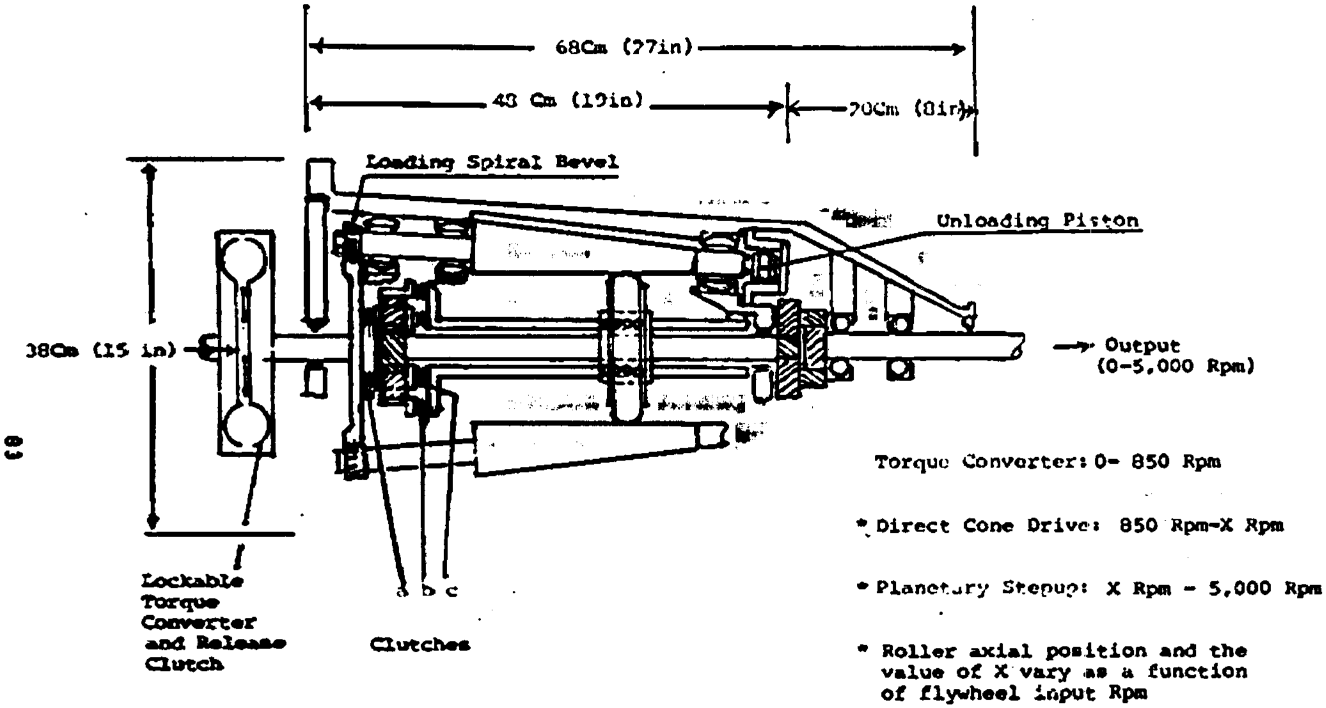

Figure: 31 Multispeed/CVT Functional Layout

APPENDIX C

CONTROL SYSTEM DETAIL

Referring to the analog flow diagram Figure 32, page 85 basic automatic slip control is achieved as herein described.

TSI; Traction Speed In (Roller) and Traction Speed Out (Cone); TSO, are either in the form of a voltage proportional to Speed (if permanent magnet generators are used) or pulses from an encoder are converted by a frequency to voltage converter (f/v).

At this point either TSI or TSO is applied to a high quality operational amplifier (OP amp) such as MC1741CL with the other signal being applied to a transconductance quadrant multiplier, for example, a MC1495L. The output of the MC1741CL is also applied to the MC1495L. The response of this loop is to multiply TSO output by TSI and this product is applied to the MC1741CL terminal as negative feedback. In this fashion the MC1495L multiplier in combination with the MC1741CL forms a divider with a net resulting output of

$Vy = \frac{-10Vz}{Vx}$ = MSR (Measured Speed Ratio).

MSR and TSR are then applied to the inputs of another divider network with the resulting output being MSR/TSR or vice versa. Either arrangement produces a final output that represents % speed.

For example if -10V out equals 100% (no-slip), then 95% would be -9.5V out. If the reciprocal mathematics were used, 95% speed would produce an output of -10.5v. In each case 5% slip produces 0.5v change in the processor output.

It may be seen that passing % speed into an "offset null" (OSN) shifting amplifier and adjusting 10v input to equal 0v out, the 0.5v change with 5% slip will produce +/- 0.5v output. (This step is not necessary as will be shown.) However to continue the slip control theme, traction physics is indifferent to slip +/- condition. Slip +/- should not be confused with +/- slip used previously. +/- slip denotes the quantity of slip as insufficient or excessive. Slip +/- is a function of the roller having a higher or lower peripheral velocity than the cone (leading or lagging). Such transitions can occur when the cone-roller junction goes from a retarting force to a driving force or during acceleration to braking transitions.

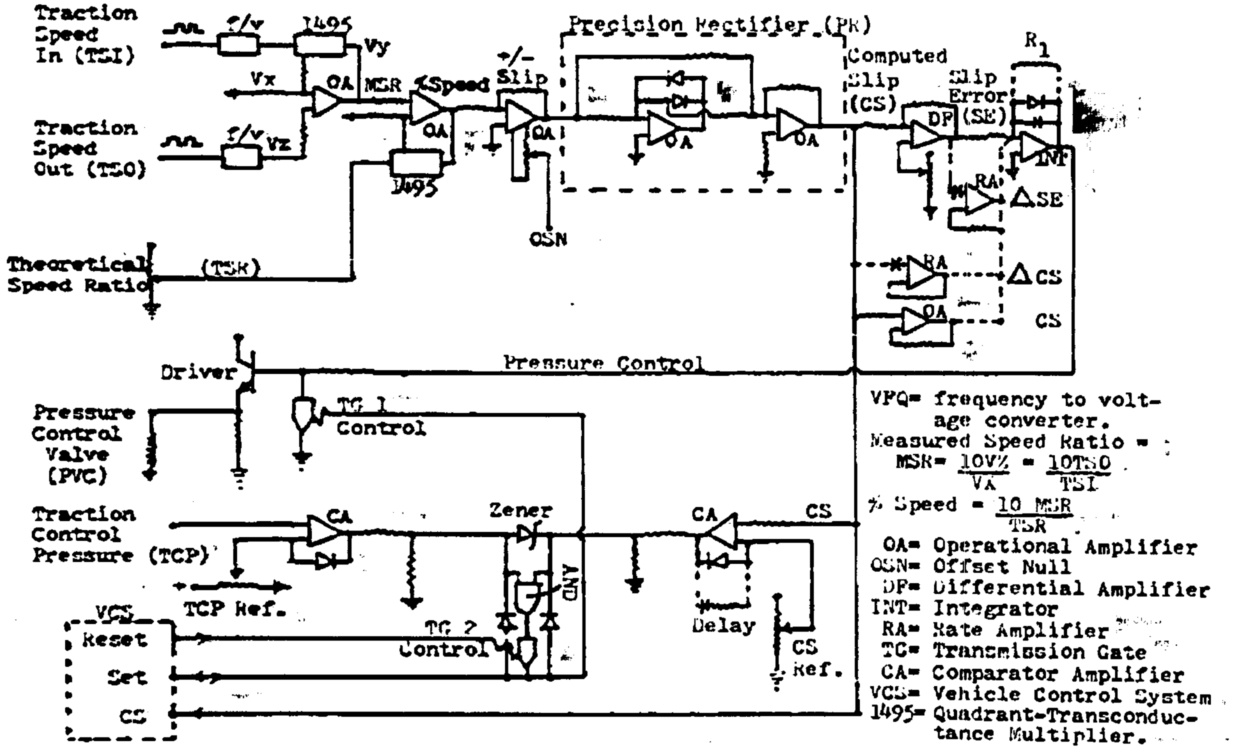

Figure 32. Basic Slip Control Schematic

Since traction is a function of +/- slip and is indifferent to whether the slip is in relation to the roller leading or lagging the cone (slip +/-). The (OSN) slip amplifier output is applied to a precision rectifier (PR) constructed of two Operational Amplifiers (OA). This insures detection and linear amplification of very small signals. (Caution: simple diode rectifiers cannot be used without very high gain of the slip signal because the diode PN junction has a low voltage breakover region where current flow is a non-linear function to voltage.) The P.R. arrangement is very important since out system is anlayzing low slip values, near zero voltage output. The alternative of making 1% equal 2V means high gain and is prone to produce oscillation, drift and instabilities that are generally to be avoided. And even at 1% = 2V, the PN Junction of some diodes are very non-linear from 0-0.4V which is 0.2% slip equivalent range that would become non-linear.

The output from the P.R. is computed slip (CS) and is applied to differential amplifier (DF). The other DF input is a slip reference voltage (RS). It doesn't matter if the - (inverting) or + (non-inverting) terminals are used. Whichever signal is applied to the - terminal is subtracted from the + signal and the output is proportional to the difference in the two respective inputs. The choice of + or - inputs for a particular signal must agree with final drive supply voltage and the proper response on demand.

The output swings +/- in proportion to the difference between CS and RS depending on which is larger and which terminals have been selected.

The DF output is slip error (SE) and is applied to an integrator, which is an OA with capacitive feedback coupling. The output goes up with even the slightest input current. The output rise is coupled to the - terminal and tries to suppress the rising output, but as the capacitor charges, the negative feedback current diminishes. With less feedback the output continues to rise. When the capacitor receives a full charge the output will be at maximum voltage. In this manner even 0.1% error continues to demand more and more corrective action until error is zero.

The diode is used to preclude the integrator from saturating in the opposite voltage. If slip were less than reference the integrator unwinds from its saturated pressure demand condition and would begin returning to zero. If the diode is not used the amplifier would go past zero and saturate at - voltage supply instead of plus volts supply. With a single ended +12v supply to the driver transistor the only ill effect would be time loss in response to error requiring renewed pressure demand.

The output from the integrator drives a power transistor in the emitter-follower mode to operate the pressure control valve (PVC) which ultimately causes a pressure change, and slip correction.

The capacitive effects of the integrator make its response slower than the detection and computation of error. R_1 added to the feedback loop of the integrator provides a more practical integrator which is much more stable. It provides "proportional band" control where demand for pressure is in response to error magnitude, supplemented by increased demand as long as error exists.

Examples of other control modifier signals (optional) are shown attached by broken lines.

The - terminal of OA's are electronically held to ground potential (not grounded but held to zero volts) by internal circuit. The OA functions are based on currents flowing in the system to hold the - terminal at zero. This is a very important feature in that several inputs may be tied to the - terminal simultaneously by input resistors. With the common side (- terminal) at ground potential each input remains effectively isolated. Their input currents produce a collective output or forms a summing function: (A + B).

The rate amplifier(s), (RA), with capacitive inputs contribute demand proportional to rate of change (Δ). Two are shown: Δ SE or Rate of Slip Error change and ΔCS, Rate of Computed Slip change. These subcircuits contribute stability to the overall control by altering the demand response under certain conditions. As the rate of error change gets larger an even greater correction demand is made to get the situation under contol.

Another modifier shown is CS, which simply provides some baseline pressure demand proportional to slip.

Obviously the combination of modifiers is virtually unlimited. For example, the peak traction point changes with temperature (oil viscosity) such that a temperature modifier would appear advisable. Traction, hence optimum slip varies with peripheral velocity (film thickness) of the components and a speed modifier should be added using TSI or TSO signals. The traction contact patch geometry changes over the ratio range settings hence a TSR modifier may be added. Even pressure (normal load) changes the contact patch and optimum slip and a Traction Control Pressure (TCP) modifier could be included.

Many of the traction variables will necessarily need to be determined empirically and the decision regarding control modifier circuits made as a function of cause-effect.

One other logic loop is shown which involves two comparator amplifiers (CA), and AND Gate, and Two Transmission Gates (TG). (TG's are electronic switches, controlled by the signal line shown on the side).

The CA's will saturate + anytime their + input exceeds the level set on the - input, and are clamped to zero anytime the + input is below the - input reference, by the negative feedback diodes.

One CA is monitoring slip and its reference would be set just above an empirically derived worst case (normal) operating condition. The resistor and capacitor shown in broken lines would provide an appropriate time delay, sensitive to the magnitude of the signals. A small transient would be given longer to be corrected than a large transient. If slip remains above normal limits this CA will go from zero to maximum voltage. Logically the output is viewed as a "1" or "0" in binary terms (on or off, resectively). The "1" or "0" output is applied to one input of the AND Gate.

The other CA operates in the same manner and is monitoring Traction Control Pressure (TCP). This is the actual pressure, not demand for pressure. Its reference is set just below the maximum control pressure available as dictated by the high pressure supply manifold adjustment.

The logic is that if slip is becoming excessive and maximum control capability is being approached, an unsafe operating condition is about to occur; a problem that must be corrected. The AND Gate will see both conditions and transmit a "1" output which opens transmission Gate 1 dropping pressure to zero and an auxiliary signal is sent to the Vehicle Control System (VCS) to shift the roller in a tracking mode to bring slip to zero and keep it there.

Diodes from the AND Gate output form a latch by supplying false "high slip" and "control capacity reached" inputs. The latch is reset by the Vehicle Control System opening TG 2 breaking the false signal supply.

A zener diode cross-couples the "high slip" CA output to the TCP limit input to the AND Gate. The purpose is that a faulty relief valve, scoured pump, faulty pressure control valve, plugged filter and many other problems could cause actual control pressure available to be less than normal, causing an inability to increase pressure on demand. In this case the high slip output would [illegible] the zener breakover point and shut the system down by sl[illegible]

An alternative to zener diode protection would be another pressure transducer on the high pressure supply manifold to vary the TCP reference but that adds cost and still would not protect against PCV failure or plugged filter problems.

Whereas the zener diode effectively determines the controls are not getting the job done and shuts the system down.

In this sense TCP need not be considered at all but its inclusion provides an early warning when the problem is vehicle overload or some problem other than hydraulic controls are creating the high slip condition.

Note that CS also is sent to the VCS system. This will be discussed in the VCS presentation.

Previously I mentioned that the OSN sequence was not necessary. This is because % speed is just as effective as % slip in control of the system. To eliminate that step the OSN becomes a D7 with a % speed reference in lieu of a % slip reference. If % speed is correct (equal to reference) the output is automatically zero and if % speed is greater or smaller than the reference the output swings + or - accordingly. Through the PR an error signal is then applied directly to the integrator.

If we supply a 95% speed reference we are by negative logic demanding 5% slip. The system can not tell the difference in terms of error and ultimate control.

One last point regarding the basic presentation. Transconductance multiplier circuits are quite delicate to calibrate and used as feedback modifiers to achieve division, become 100-fold greater a problem at small signal levels. Cascading two such networks presents undesirable calibration problems. This has been overcome by using TSR directly as a gain control resistor around the % speed amplifier, in lieu of the second MC1495L.

As shown in Figure 33, page 90, the gain of the % speed amplifier is expressed as:

$$\text{Gain} = \frac{Rx}{TSR + Rz}$$

Since TSR = MSR (without slip) Rx and Rz are adjusted to provide a constant % speed output for all TSR ratio settings if no slip is present.

For example, if the roller speed were 5,000 Rpm and the cone speed varies from 10,000 Rpm to 30,000 Rpm, then TSR

C - 2

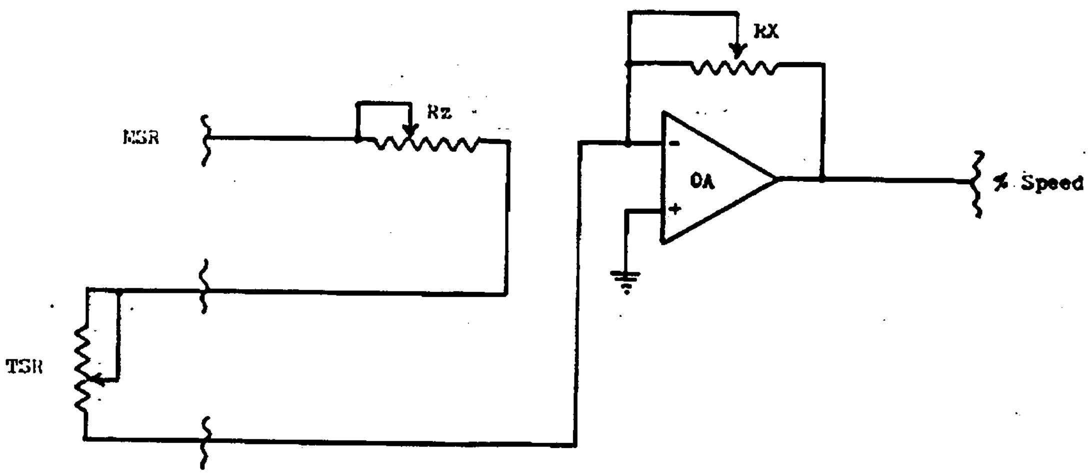

% Speed Optional
Divider Structure
(From Figure 32, page 85)

Figure 33

produces roller-cone ratios of 6/1 to 2/1; a cone speed variance of 3/1.

The conversion from true 6/2 ratio to 3/1 is accomplished by a scale adjustment at the CR, MSR divider and is not critical in that once set, a given ratio becomes 4v, 6v, 7.2v, or any relative value. The important point becomes matching the span of CR ratios (MSR without slip) output by calibration of TSR, Rx and Rz and not the absolute value or accuracy of ratio calculation.

If TSR travel with roller position varies in resistance from 10K ohms to 700Ω; for example, Rz and Rx values for proper performance may be found by:

1. $\frac{TSR}{10K\Omega} = 1/1$

2. $700\Omega = .7K = 3/1$

$$\frac{Rx}{\Delta TSR + Rz} = \int_1^3$$

$$\frac{Rx}{TSR_2 + Rz} = 3$$

$$Rx_1 = 3\ (.7K + Rz) = 2.1K + 3Rz$$

and:

$$\frac{Rx}{TSR_1 + Rz} = 1$$

$$Rx_2 = 10K + Rz$$

Since: $Rx_1 = Rx_2$

Therefore:

$$10K + Rz = 2.1K + 3\ Rz$$

$$10K - 2.1K = 3Rz - Rz$$

$$7.9K = 2Rz$$

$$\frac{7.9K}{2} = Rz$$

$$Rz = 3.95K$$

Hence: $Rx = 10K + Rz = 10K + 3.95K = 13.95K$

and $Rx = 2.1K + 3Rz = 2.1K + 3(3.95K) = 2.1K + 11.85K = 13.95K$

Likewise:

$$\frac{13.95K}{10K + 3.95K} = 1$$

and

$$\frac{13.95K}{.7K + 3.95K} = \frac{13.95K}{4.65K} = 3$$

Results:

$Rx = 13.95K$

$Rz = 3.95K$

For different ratio ranges or different values of TSR resistance over the ratio range these values will vary. But as outlined here for a given "no-slip" MSR, the % speed amplifier output will always remain constant as the transmission is shifted. If MSR is offset by virtue of the presence of slip, % speed output will change. To achieve this the TSR leads are reversed so that when MSR = 3/1; TSR = 1/1 and when MSR - 1/1; TSR = 3/1, thereby providing the constant % speed output with no actual slip.

<u>Optimized Traction Control (OTC)</u>:

In lieu of simple slip control which must be tuned to empirical parameters and for maximum effect or benefit must use additional sensing (such as temperature) another technique may be used.

That technique involves recognition that every traction fluid or oil has a peak traction point. This point (in terms of slip) varies from one fluid to another, temperature, peripheral velocity, one transmission design geometry to another, and even at differrnt ratio settings within a given transmission design. See Figure 34, page 93.

The control system just discussed can be calibrated to a specific transmission design. But to function over a wide range of environmental changes required added components to modify its response to such variables and would not work properly if a different fluid were substituted.

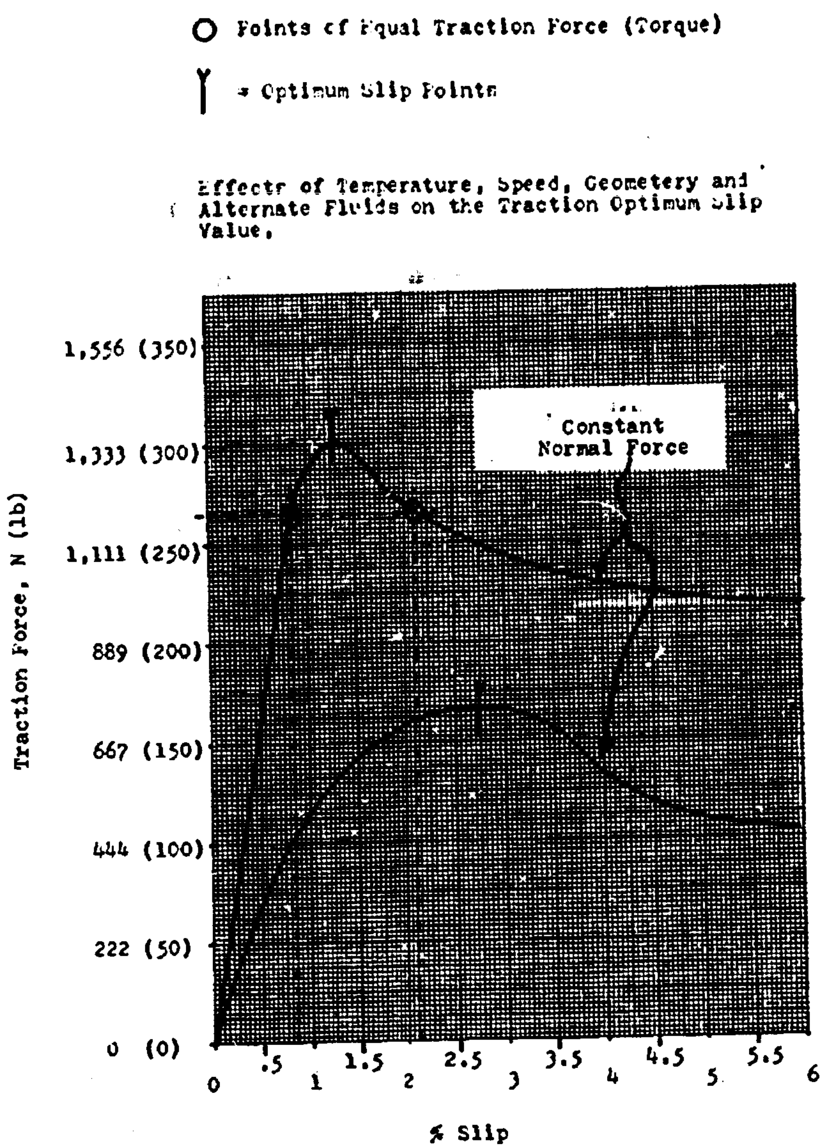

Figure 34: Typical Traction Curve (Constant Normal Force-Pressure).

The fact that every fluid has a peak, and variables only move the peak slip value, permits us to develop a controller that can be attached to any traction drive, using any fluid, in any workable environment, without the necessity of specific calibration, and will have much less sensitivity to calibration drift in the slip computer section.

It is shown in Figure 35 and 36, pages 95 , and 96 , respectively that regardless of the absolute slip magnitude for peak traction, the rate of slip change to rate of pressure change ($\Delta CS/\Delta TCP$) = ∞ .

THIS STATEMENT HOLDS TRUE FOR EVERY FLUID, EVERY KNOWN TRACTION DEVICE, AT ALL SPEEDS, TEMPERATURES OR RATIOS.

With that in mind we can start with CS and TCP signals of Figure 32 , page 85, and develop the Optimized Traction Control (OTC) system, Figure 37, page 97.

CS and TCP signals are converted into +/- ΔCS and +/- ΔTCP. These rate signals in turn are then applied to a PR resulting in Δ CS and ΔTCP signals. The previously described divider network then has an output that is proportional to Δ TCP /Δ CS which is a representation of slope. Slope identifies where on the traction curve the system is operating.

Unlike the basic slip system this system would prefer Δ TCP/ ΔCS instead of ΔCS/ ΔTCP because as shown a slope calculation of 0/X results in "0". If ΔCS/ ΔTCP were used then the peak is X/0 = ∞ and saturation of computer circuits would result in data loss near the peak.

The operating slope (OS) calculation and the desired slope reference (selected operating point at or near the peak) are applied to a DF. The DF output is +/- slope error (SE). SE is applied to the - terminal of an integrator such that - SE produces a + voltage rise out of the integrator. Referring to Figure 38, page 98 , it may be seen that - SE means a slope value less than the reference (SR), hence closer to the peak than desirable. The + integrator response will produce a demand for increased pressure which will reduce slip, bringing the operating point back toward SR_1.

Just as a typical traction curve reflects two equal torque (Traction Force) points for given values of slip and normal load, see Figure 34, page 93 , equal slope values also exist (See SR_1 and point 2 of Figure 35, page 95 . A shock load could transient the operating condition into the + slip regime. The problem is that reverse logic is produced by control systems for that slip condition. Such that at point 3, for example,

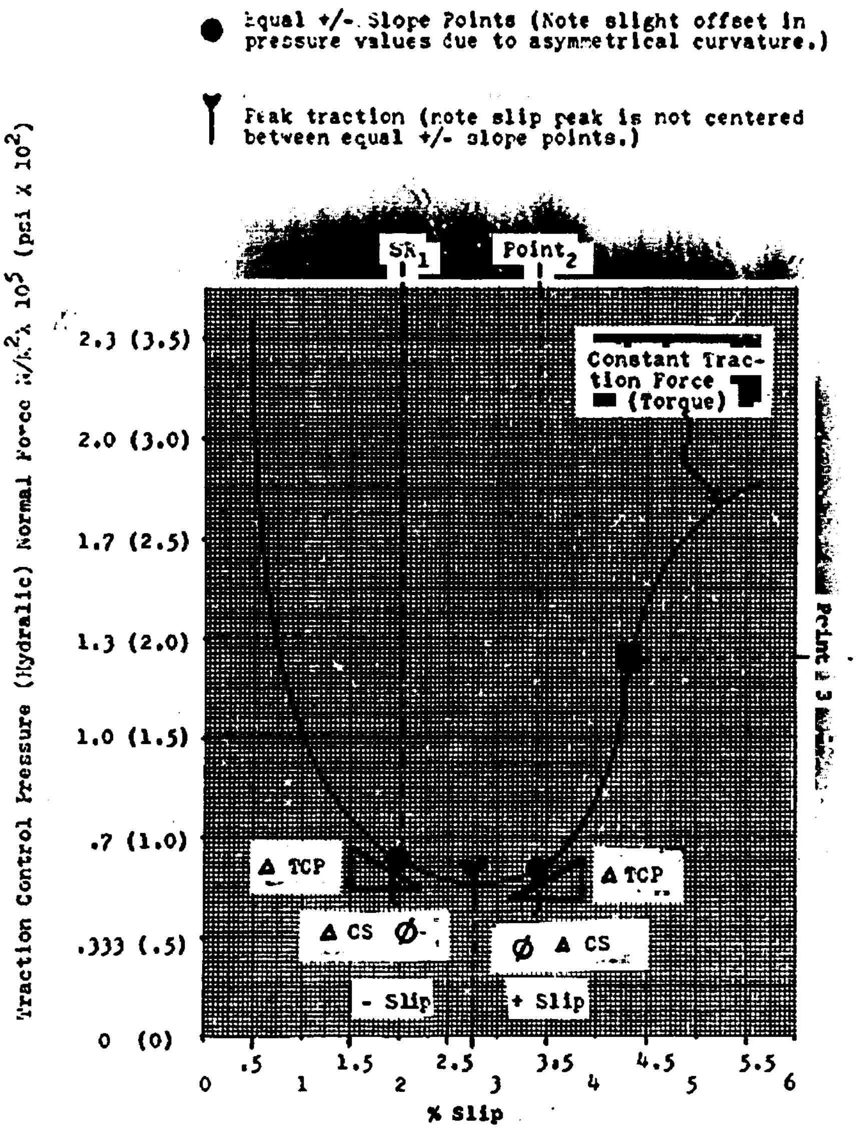

Typical
Traction Curve
Pressure VS % Slip

Figure 35

(Invert for $\Delta TCP/\Delta CS$, $\infty = 0$)

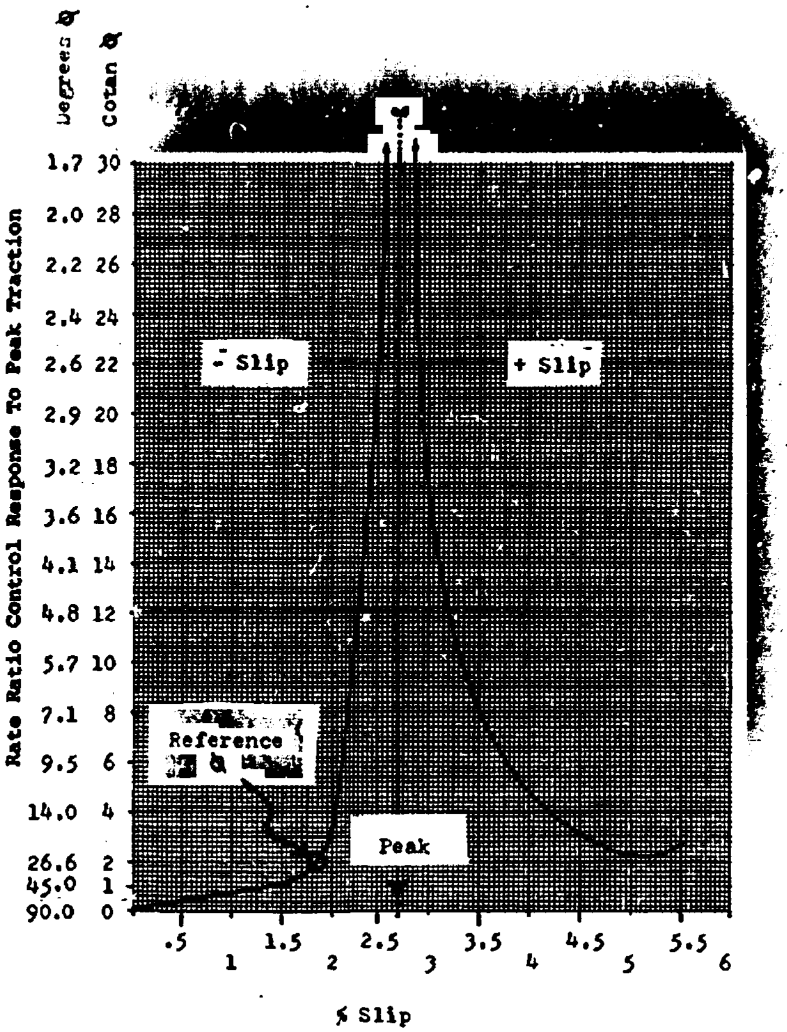

Typical Rate Control Curve

Figure 36 : ($\Delta CS/\Delta TCP$)

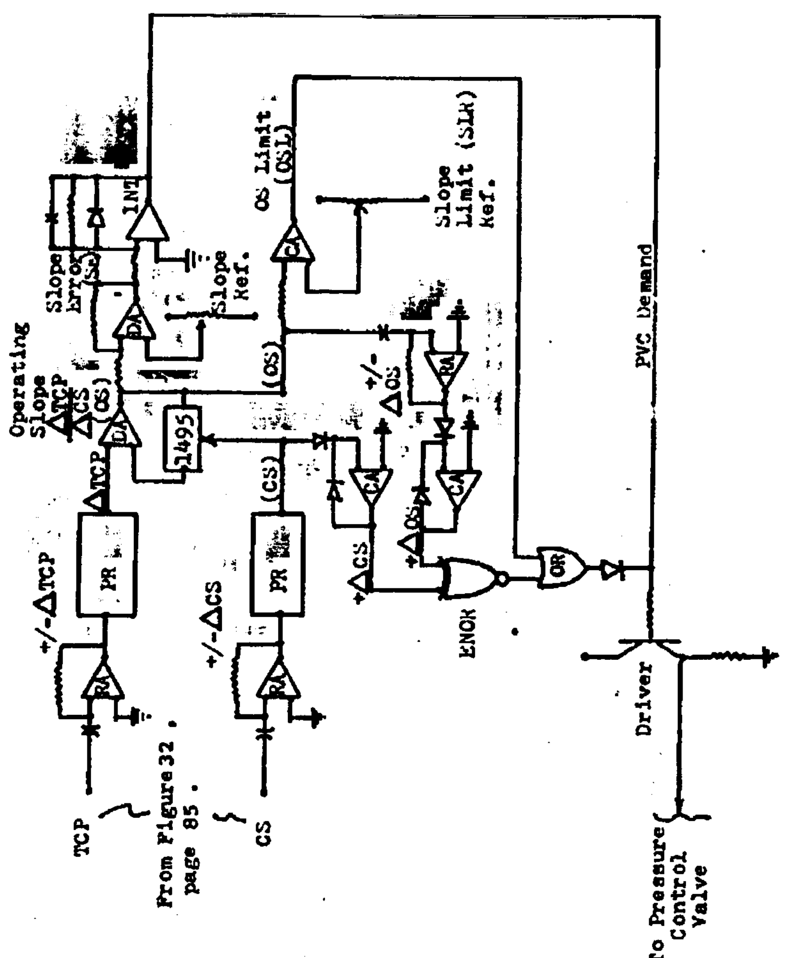

Figure 37: Optimized Traction Control (OTC) Diagram

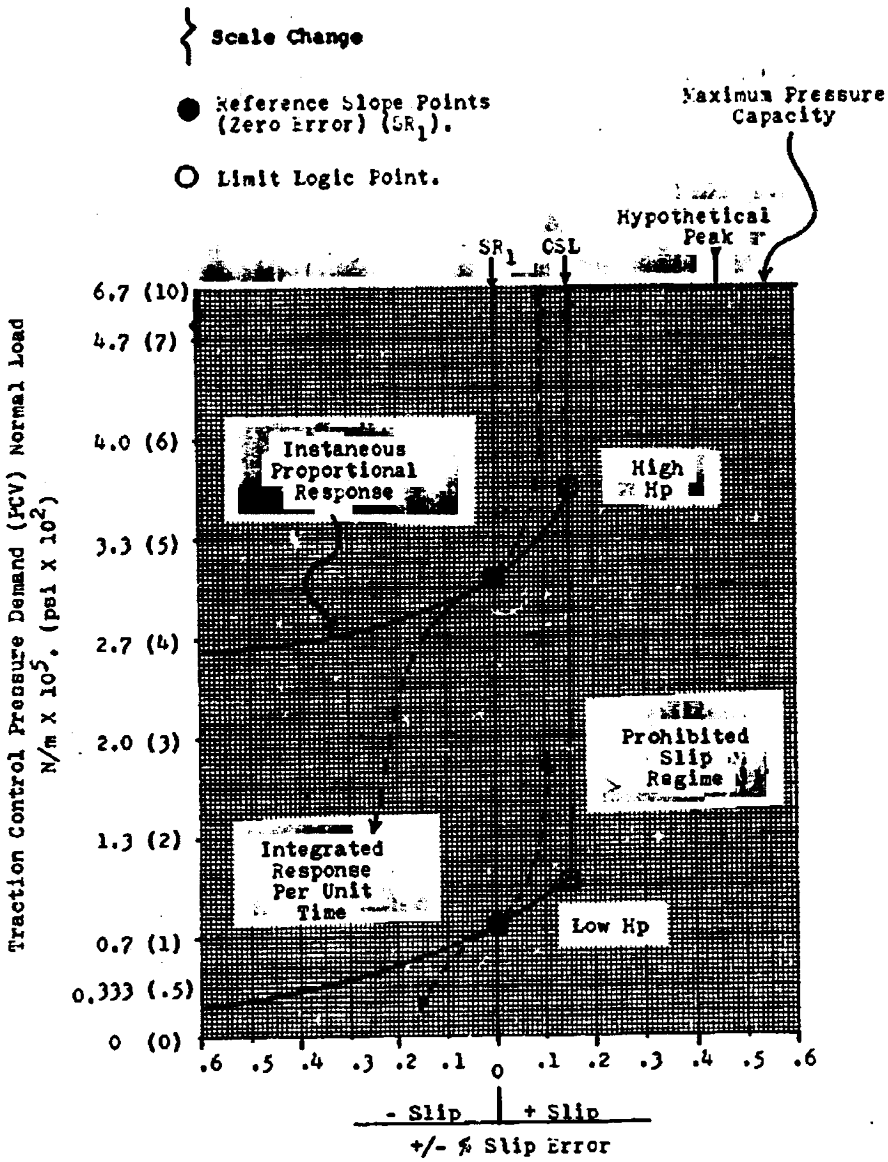

Computer Response To Error

Figure 38 :

the slope is too large and the normal response for correction in the - slip regime is to decrease pressure but in the + slip regime must increase pressure. That condition is disallowed by the system rather than developing reverse logic control.

This is accomplished first by driving a comparator with the OS signal. The Slope Limit Reference (SLR) will demand maximum correction anytime OS falls below the preset SLR. It will continue to demand maximum pressure for as long as OS calculations fall below the SLR settings.

With adequate hydromechanical response designed into the system initially the OS Limit (OSL) should preclude a + slip condition from occuring.

However, the closer to the peak we can operate the more dramatic the benefits of OTC. But consequently a greater hydromechanical response must be available to maintain control and the easier it becomes for shock loads to cause an uncontrollable transient into the + slip regime.

Therefore CS and OS signals are analyzed for their trends. It may be seen in Figure 35, page 95, that as the traction peak is approached in the - slip regime the slop values decrease with increased slip and slope values increase as slip decreases. But in the + slip regime slope values increase as slip increases and vice-versa. In the + slip regime "parity" occurs in the slope and slip trends.

This fact is used to identify and prohibit continued operation in the regime by constant demand for increased pressure.

This is accomplished by isolating +/-ΔCS from a comparator using a diode. Only +CS becomes applied to the CA input. The other input is grounded such that any +ΔCS caused maximum output. The feedback diode precludes spurious - saturation.

OS is applied to an RA to provide +/-ΔOS and an identical structure reduces the signal to an "0" or "1" (+ΔOS) output.

OS and CS logic signals are applied to an "Exclusive NOR" (ENOR) Gate. The ENOR output is "0" for any conditions except two "0" inputs or two "1" inputs. Anytime CS and ΔOS are the same, both "0" or both "1", we are operating in the + slip regime and ENOR response is a "1" output.

The ENOR output is applied to an OR Gate in conjunction with the OSL logic output. Anytime a "1" appears out the OR Gate, maximum pressure is demanded by the PCV Driver.

The result is a control system that controls pressure to maintain the traction junction operating at slope calculations around a reference value near peak traction. Once error in control exists beyond a preset CSL amount, full pressure is demanded until the return to the normal control range -- even if the peak is transiented in the interim. This may be insured by using a "sample and hold" of the slip value at the time OSL indicates the transient may be imminent (not shown), as a reference.

Just as in the basic slip controller other modifier signals are readily available for OTC.

Since basic slip control can only do what we tell it to do, and cannot tell if that is right or wrong, we must test empirically the effects of temperature, speed, etc., and modify the control response to maintain maximum benefit. The OTC system just described will control the pressure to maintain optimum conditions even if regular oil is substituted for traction fluid. And automatically compensates for all variable effects without the necessity of measuring those factors or without knowing what effect such variables have, because OTC analysis is of the traction slope produced, after the influence of such variables.

Figure 38, page 98 , is a typical control response to conditions in the junction. The area between the solid line and dashed line represents the effect of the integrator with time. The solid line therefore is an instantaneous response and if the error continues the demand for correction will correspondingly drive the PCV to full pressure or no pressure in an attempt to bring conditions exactly to the SR point.

The problem with the OTC system just described is that it only works with a fixed load condition where ΔCS is <u>only</u> in response to Δ TCP.

The automotive application presents varying external load conditions and slip would vary with that load, without a change in TCP. This would produce false $\Delta TCP / \Delta CS$ slope calculations and the system becomes lost.

Also the system would become lost under quiesent conditions of constant load where ΔTCP and Δ CS both equal zero. However, in this case the system produces its own change and will oscillate thereby producing its own Δ TCP which would cause a Δ CS response.

Many options exist to overcome these problems.

First, a torque sensing device could be installed to permit computation of the % of ΔCS due to load change and thereby leave the appropriate ΔCS for the $\Delta TCP / \Delta CS$ slope calculation. This adds cost and complexity.

A hybrid control philosophy can replace the need for torque sensing in light of the improved cone mounting using the spiral bevel to assist loading as a function of traction torque.

It can be seen that low slope values will result from operating too near the peak or from external load influences. But the correct response is increased pressure in both cases.

It can be seen that an external load increase causing slip to increase actually moves the operating point toward the peak and also produces the correct slope calculation change to produce a corrective response.

But a load decrease (which is in the safe direction) could falsely indicate near peak conditions and improper response (but safe) of increased pressure would result.

If a basic slip controller therefore were used as the primary control and slope calculations as a modifier are introduced, a system of pressure response to slip (load influence) around a selected slope point evolves.

In this technique slope error values would be averaged and applied to the slip circuit reference via a summing amplifier. An oscillator could be used to insure continuous Δ TCP by providing a fixed dither signal to the demand; although the use of the integrator in the system as well as dynamic loads may prove adequate on their own. See Figure 39, page 102.

In this manner a reasonable (safe) starting slip value may be established and the average slope error used to bring the reference into line with environmental conditions but under short term transient conditions, respond to ΔCS as load signals.

The net effect is a traction drive under torque feedback response with slip calculations used to fine tune control responses to operate at or near peak traction conditions. And slope logic as well as ΔCS and CS modifiers to preclude operation in + slip regime.

Unenhanced OTC control would necessitate a high degree of compliance to the dither signal as the slope values would need to be predominately based on controlled ΔTCP effects on ΔCS in time frames much faster than ΔCS produced by normal vehicle load changes.

This all becomes possible because for a given set of conditions there is a particular ΔCS in response to ΔTCP at specific operating slopes and lower frequency dither may now be applied and the baseline ΔTCP/ ΔCS filtered out. The remaining ΔTCP and ΔCS are vehicle load effects and slip

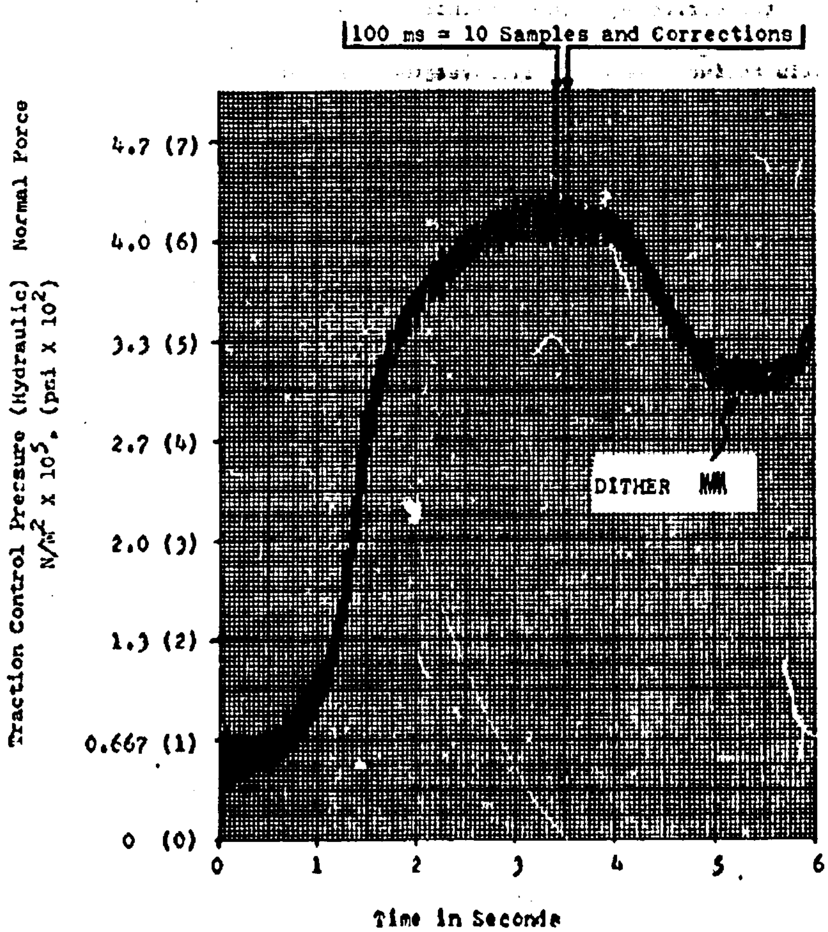

Load Transient Response

Figure 39:

control response induced. The specific relationship of Δ TCP to ΔCS need not be known as it will change as a function of environmental variables. But on the average that information filters into the basic slip control and updates the slip reference.

In terms of time, the system hydromechanical response from no pressure to maximum pressure is 50-100 milli-seconds.

The pressure available is calculated at twice that required to handle peak design horsepower. So from zero to full load control capability in 25-50 milli-seconds; usual vehicle load changes are much slower than that and even shock loads (transients) would range from 100-500 milli-seconds. Rubber tires, axles, drive shafts and the like, absorb most load spikes but <u>if necessary a torsional coupling may be added to smooth out road shock permitting the computer adequate time to respond</u>.

Optimum operating slip will only change over a period of 1-5 seconds with temperature, speeds or ratio setting and slope averaging would allow 0.5-1 second to make corrections to the slip reference.

These basic concepts were provided in analog form to better facilitate comprehension. Obviously such a system may be converted to digital and placed under the control of a microprocessor.

The analog system would suffer from calibration requirements, temperature drift, non-linearities and physical size. Its advantage is constant monitoring and a dedicated system performing control.

The microprocessor (MPU) (programmable) provides greater flexibility during development; smaller packaging and higher speed as well as is available to perform other tasks on a time sharing basis. It suffers from sensitivity to environmental electrical noise such as fans, turnlight flashers and spark plug firings. It can soon lose in terms of speed because of the program required to fulfill complex computations.

The best all around system would appear to be a hybrid between an MPU and analog conversions. By converting monitored data into analog form, then multiplex that data either directly or through a logrithmic converter, to an "analog to digital" converter, allows us to supply a high speed MPU with digital numbers that need only to be added or subtracted (4 computer cycles) to achieve addition, subtraction, multiplication, or division.

Without logrithmic data, multiplication and division time by the normal multiple precision addition or subtraction method will vary with the value of the number being processed and usually requires a few hundred cycles if numbers large enough to provide 0.1% accuracy or resolution are used, (i.e., 1,000 or greater is 10 Bits minimum in binary).

An alternative is to supply a ROM (Read Only Memory) for logrithmic values over operating-ranges and let input data address its logrithmic equivalent for use by the MPU. This would basically double MPU cycles to 8 but eliminates multiplexer and analog-logrithmic and analog ant' og conversions. This would be an overall preferred technique. It allows minimizing processing time without the bulk and complications of added external analog processing.

For example if the TSO and TSI disc has 60 aperatures and TSO is spinning at 10,000 Rpm, each aperature would occupy 0.0001 of a second or 100 μ seconds (100 millionths at a second). Using an internal clock frequency of 10 MHz (10 million cycles per second) 1,000 clock pulses would be counted per aperature. TSI at 5,000 Rpm means 2,000 counts would accumulate. If speed were important for display, the MPU would divide 10,000,000 by the counts accumulated.

10,000,000/1,000 = 10,000 Rpm

10,000,000/2,000 = 5,000 Rpm

However, that step is not necessary to control, as previously shown, since the system is looking at ratios. Therefore the counts would address a log equivalent memory and the respective logs would be subtracted. The $\log_{10}$ of 1,000 = 3.000 the $\log_{10}$ of 2,000 = 3.3010.

3.3010 - 3.000 = 0.3010. The antilog of 0.3010 = 2.000 or is equivalent to 10,000/5,000 = 2.000. If the clock frequency is not exact such that 10,000 = 8,260 for example.

8,260 Rpm = 1,210.65 counts (1,210) and the $\log_{10}$ 1,210 = 3.0828. 16,520 Rpm = 605. $\log_{10}$ 605 = 2.7818.

3.0828 - 2.7818 = 0.3010 the antilog of which = 2.000. Drift becomes relatively unimportant.

TSR (as well as TCP) would provide a variable voltage to a voltage controlled oscillator (VCO). The VCO would be calibrated to produce a frequency of 2,000 Hz at the 2/1 roller-cone position. One VCO cycle would be timed. At 2,000 Hz the pulse width would cause 5,000 counts to accumulate. This would be converted to $\log_{10}$ of 5,000 = 3.6990 and would be subtracted from a memory fixed of 4.000. ($\log_{10}$ of 10,000 counts) 4.000 - 3.6990 = 0.3010.

The 2/1 roller-cone ratio computed above in $\log_{10}$ form of 0.3010 is subtracted from TSR = 0.3010 and the results = 0.0000. The antilog of 0.000 = 1.000 or 1/1 = no slip!

Under the above assumptions it may be seen that if the roller speed was 5,000 Rpm but the cone speed of 10,000 Rpm was not present because of 5% slip + (a cone speed of 10,500 would exist) the cone count would equal 952.38 (952). The $\log_{10}$ 952 = 2.9786.

3.3010 - 2.9786 = 0.3224 as the $\log_{10}$ of roller-cone ratio. This ratio minus the predicted ratio by TSR of 0.3010 equals 0.3224 - 0.3010 = 0.0214. The antilog of 0.0214 = 1.05 or 5% more speed than there should be.

This philosophy can be extended throughout the system and need not be duplicated in this presentation. Due to the control complexity and the amount of multiplication and division data, $\log_{10}$ conversion before MPU processing is dictated. The appropriate Bytes of log ROM is preferred but may be achieved by other means.

A logrithmic amplified could convert analog inputs before the analog to digital conversion. In which case the frequency conversion would need to be made or preferably use small voltage generators. But since $\log_{10}$ 1.111 = 0.0457, $\log_{10}$ 11.11 = 1.0457, $\log_{10}$ of 111.1 - 2.0457 and $\log_{10}$ of 1,111 = 3.0457, a ranging unit can be used to assign the characteristic while digit decoding may be used to address the $\log_{10}$ of four (1's). This cuts memory capacity requirements to ¼.

To minimize mechanical fabrication requirements for extreme tollerance between open and closed duty cycle (See Figure 40, page 106, the MPU is edge triggered and begins counting the clock with positive or negative transition of the incoming signal. It continues to count until the next "like", rising or falling signal is received. It counts from leading edge to leading edge or trailing edge to trailing edge. This eliminates cutter size to disc circumference relationship problems otherwise required to keep the duty cycle balanced. In the preceding example only the aperature was considered and that also eliminates duty cycle balance but if the MPU is to wait for an

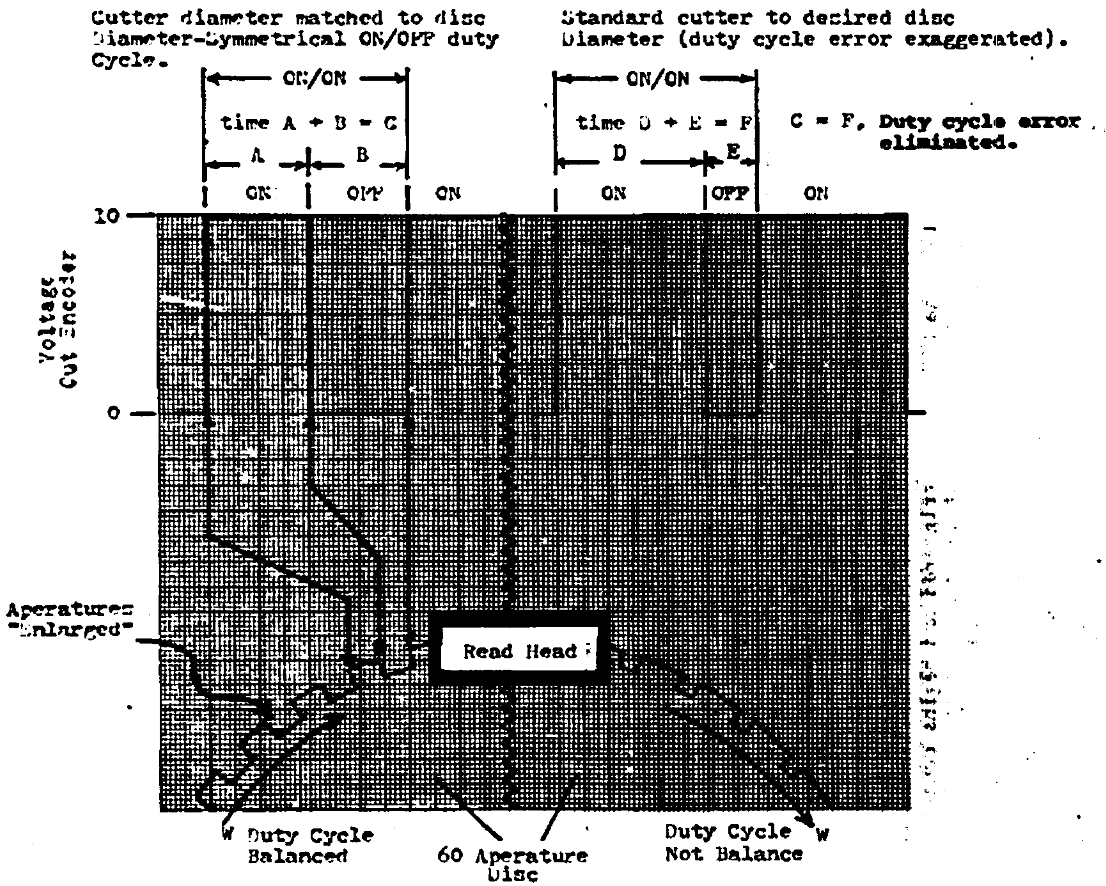

Figure 40 : Duty Cycle Error and Correction

aperature, it is preferable for it to count during that time since more counts improve resolution. Comparable counts are accomplished by going to 120 aperatures providing twice the sampling rate.

The final output integration will be accomplished by repeated addition of error value into an output accumulator. This accumulation is continuously applied to a digital to analog converter to drive the PCV amplifier.

Rates are developed by operating sampling on fixed cycles so that time need not be computed but is inherent to the data collection $(\text{Cycle}_1 - \text{Cycle}_2)$ / fixed sample time interval = Δ counts.

With a fixed sample time Δ may be used as rate, disregarding the sampling time used.

Keeping computer time to a minimum permits time for more computations. Some useful computations as far as traction goes would be ΔTCP/ ΔPCV. This is a measure of hydromechanical response not only inherent in any given design but is also sensitive to temperature and fluid used. Such that the computed pressure lag could be used in the program to vary the frequency of adding error into the output accumulator.

This causes the integrator to respond faster in cold weather (assuming oil viscosity change has caused an increase in hydromechanical response time).

Adding the slope over 10 cycles can reflect a change in terrain by successive excursions toward the peak. Unlike slip error +/- which would average zero for any given amount of error (+/- 1% or +/- 5% around a set point), slope is $\tan\theta$ and the trigometric function means the average will shift dramatically as the oscillations vary from +/- 1% or +/- 5% around the set point. Such that transient conditions and responses become easily detected. That information can be used to either offset the slip reference downward or preferably to increase PCV (integrator) response. This increases the tautband of the control by changing the error addition frequency into the integrator.

It is recommended therefore that a small programmable MPU be used, with a 10 MHz internal clock. And a minimum of 4 edge triggered I/O ports for TCP, TSR, TSI and TSO signals. A 10 Bit wide O port to provide better than 0.1% pressure control resolution, and at least 1,000 memories for $\log_{10}$ value storage; plus appropriate processing space.

Having developed the described control response in actual hardware a custom system can be developed on a single chip for mass production which uses ROM for the fixed program.

VCS (Vehicle Control System):

VCS units are already available commercially in terms of optimizing the performance of an electric motor or proper throttle setting for best BSFC of an IC engine. So only those aspects of VCS as applies in a unique way to the traction CVT and/or flywheel are discussed.

In the prior discussion it was noted that (computed slip) CS was made available to the VCS unit.

The purpose is several-fold.

1. Slip may be used to offset Transmission Speed Control (TSC), thereby reducing the rate of shift to preclude driver demand from placing uncontrollable slip conditions on the unit. This would not normally be a problem but it is possible that the driver could attach a trailer to the vehicle or in some other fashion induce abnormal vehicle loads into the system (such as attempting to push a second vehicle or operate with the brakes locked up). By interlocking the MPU demand for shift of the transmission, to slip in the traction junction, hundreds of potentially destructive possibilities are precluded. The transmission would only shift to the point that slip limits would allow. There it would stop trying and when maximum control pressure is reached an overload warning light would tell the driver his problem.

2. Also should any condition such as plugged filter or pump failure preclude continued control of pressure, the basic slip/OTC system would set the safety shutdown. The set signal would then instruct the MPU to operate TSC to maintain zero slip, or track output speed with no clamping pressure being applied.

Obviously ΔP monitoring should warn the driver well in advance that a filter problem is imminent but if that minor problem is not fixed we should still preclude the destruction of the transmission. Indeed if the problem is a slowly growing one, warnings and automatic steps could be taken to preclude the undesirable total shutdown on the open road. Such a possibility would be TSC feedback from filter ΔP. The vehicles performance would diminish demanding attention as well as providing a warning indication to the driver.

The TSC normally functions by the difference between vehicle speed out (VSO) and Vehicle Speed Demand (VSD). VSD is derived from the floor pedal and brake pedal pressure (BPD).

VSO may be developed by normal speed-o-meter means at the output shaft or it may be derived by the MPU.

The output speed of the planetary is a fixed relationship to the sun gear speed (TSI) and ring gear speed (TSO): Where:

WS = Sun Rpm = TSI
WR = Ring Rpm = TSO
WC = Carrier Rpm = Output = VSO
Sr = Sun radius
Rr = Ring radius
Cr = Carrier radius = center of planet gears to sun gear center.
K = Constant taking tire size, rear axle ratio, etc. into account for conversion into Mph

$$W_C = \frac{WSSr - WRRr}{2Cr}$$

Cone gear coupling ratio = (Cgr)

$$VSO = K \left(\frac{TSI(Sr) - TSO\ (Cgr)\ (Rr)}{2\ Cr} \right)$$

Since these signals are available the additional conventional speed-o-meter can be eliminated.

TSC is further modified to take into account the current operating conditions of the motor. In other words, a large differential between VSD and VSO would generally mean rapid shift of TSC to increase VSO, such that vehicle acceleration corresponds to driver demand. But TSC is offset if the engine is being overloaded (Rpm below optimum for demand) and a decision to downshift TSC and increase throttle could result. But the final vehicle response is still heavy acceleration for large demand differential to current speed.

If VSD-VSO is negative the results may be ignored and a coast down would occur. To best simulate today's driver feel the - result can cause a slow downshift of TSC or CREEP signal, duplicating normal vehicle coast down with the driver's foot removed from the pedal.

BPD becomes a modifier for Creep. As a larger BPD is detected creep is increased causing a more rapid downshift of TSC resulting in regenerative braking. BPD is set as "master" so that pressing both pedals produces braking.

The combination of regenerative braking with normal brakes provides a most suitable arrangement in that under gentle braking TSC is causing recovery of energy. But should more rapid braking be dictated and slip starts to override TSC then the increased pedal pressure (which is normal driver response even with power brakes) causes normal braking to become predominate. This is less efficient because regenerative energy is being lost but getting stopped safely is more important than capturing energy at this point. This system not only provides smooth transition from TSC regenerative braking to normal braking but insures maximum regeneration will be utilized and even with transmission failure leaves the driver with ample normal brakes as a safety backup.

Having TSC shift speed tied to the magnitude of VSD-VSO makes the response duplicate conventional driving of torque demand with an accelerator pedal.

Cruise may be accomplished in a conventional manner by storing VSO, at the moment cruise is set, into the memory for reference in lieu of VSD. VSD can override VSO memory for temporary increases in speed, larger value as demand result, by OR logic.

TSC = (VSO Memory or VSD) - VSO.

Notice that a - TSC means road speed greater than desired. In the cruise mode TSC may respond to maintain constant road speed resulting in slight regenerative braking in hilly country, to be used to climb the next hill.

BPD will clear cruise as normal. I would add to the usual array of buttons an Increment (increase) and Decrement (decrease) memory button. This would provide finite trimming of cruise speed to suit speed limits, traffic or weather conditions.

Logic may be provided to preclude going into reverse with + VSO computed and vice-versa. A bottom limit to this interlock should be provided to permit rocking the vehicle as a means of removal from mud or snow, i.e., below 2-3 mph.

With the computer on board one added safety feature can be easily accomplished.

By monitoring VSO, and comparing it with a frame accelerometer, skidding may be precluded. The computer would know when tire traction was being lost and could override normal TSC or BPD signals. To take advantage of the possibility for antiskid circuitry the direct pressure link between the pedal (BPD) and the wheels would need to be broken so that a composite pressure signal from the pedal and the computer activates cylinder pressure.

This excluding any desired startup or shutdown sequences, added safety, or auxillary indicator functions and flywheel monitoring and clutch control, would conclude a controls package for the CVT presented.

The flywheel may engage only during braking until an operating speed range is achieved, at which time it remains engaged. The motor controls in conjunction with TSC will maintain operating speed on the flywheel as well as control vehicle speed. A shutdown sequence by removing the key could cause an output clutch to disengage and engage the motor, causing it to brake the flywheel by generating into the batteries. (If the motor is designed to produce counter emf).

In the final analysis the control technology exists. The final design to be predicated by details of the application and desired features in performance, which must be weighed against size and cost of an MPU to achieve all the functions reliably in acceptable time frames.

APPENDIX D

GEAR WINDAGE POWER LOSS

$$P.L. = \left[\frac{\rho'}{\rho}\right](N^3)\ (D^5)\ (\ell^{.7})/10^{17}$$

$$\left[\frac{\rho'}{\rho}\right] = 1.5$$ FOR JET LUBRICATION NO ROTATING PARTS SUBMERGED.

BEVEL PINION:

$$P.L. = (1.5)\ (23479)^3\ (1.54)^5\ (.5)^{.7}/10^{17}$$

$$P.L. = .0001\ HP$$

BEVEL GEAR:

$$P.L. = (1.5)\ (16552)^3\ (2.1)^5\ (.5)^{.7}/10^{17}$$

$$P.L. = .00017\ HP$$

IDLER HELICAL:

$$P.L. = (1.5)\ (16552)^3\ (1.54)^5\ (.5)^{.7}/10^{17}$$

$$P.L. = .00004\ HP$$

APPENDIX E

BEARING LUBRICATION FACTOR(REF. 5)

BEARING	$m(\mu\,\alpha)^{.7}\ (N)^{.7}\ (Po)^{-.09} \Lambda\, F$
ROLLER CONE SUPPORT	$(6.5)(10^{4})\ (5.5)(10^{-8})\ (1146)(.59)(2.14) > 3.0$
BALL, DUPLEX CONE SUPPORT	$(8)(10^{4})\ (55)(10^{-8})\ (1080)(.65)(30.9) > 3.0$

APPENDIX F

TRANSMISSION RATIO ANALYSIS

N_{os} = OUTPUT SHAFT SPEED, SUN DRIVING = $(RPM_s)\ (R_p)$

$$R_p = \frac{N_s}{N_s + N_r} = \frac{40}{40 + 100} = .2857$$

RPM_s = SUN SPEED = Flywheel $RPM_n/2.9166$

$N_{os} = .2857\ RPM_s$

N_{or} = OUTPUT SHAFT SPEED, RING DRIVING = $(RPM_r)\ (R_r)$

$$R_r = \frac{N_r}{N_s + N_r} = \frac{100}{40 + 100} = .7143$$

$N_{or} = .7143\ RPM_r$

$RPM_r = (RPM_s)\ \frac{\text{ROLLER DIA}}{\text{CONE DIA}}$ (BEVEL IDLER RATIO)

$= (RPM_S)\ (R_C)\ (R_B)$

N_o = OUTPUT SHAFT SPEED
$= N_{or} - N_{os}$

$N_o = (.7143\ R_C\ R_B - .2857)\ RPM_S$

$$R_B = \frac{19}{27} \cdot \frac{21}{49} = .3016$$

$$\boxed{N_o = (.2154\ R_c - .2857)\ RPM_s}$$

Flywheel RPM	RPM_s	R_c	RPM_{out}
14,000	4800	4.65/.75	5038
21,000	7200	4.65/1.426	3000
28,000	9600	4.65/2.68	845

Table 10:

APPENDIX G

INPUT PLANETARY GEAR DATA

	SUN	PLANET	RING
N	48	22	92
P_T	20.0		
ϕ_T	22.5°		
ψ	30°		
P_N	23.09		
ϕ_N	19.73°		
C.D.	1.75		
D	2.40	1.10	4.60
D_o	2.50	1.20	4.70
D_R	2.28	.98	4.48
r_f	.02	.02	.02
t	.077	.077	.079
F	.50	.50	.50

Table 11:

APPENDIX H

INPUT PLANETARY SUN LOSS FACTOR

$$P_L = \frac{50\ f\ \cos^2\Psi}{\cos\phi_N}\left[\frac{H_T{}^2 + H_S{}^2}{H_T + H_S}\right]$$

$$H_S = \left(\frac{Mg + 1}{Mg}\right)\left[\sqrt{\left(\frac{r_o}{r}\right)^2 - \cos^2\phi_N} - \sin\phi_N\right]$$

$$= \left(\frac{41/19 + 1}{41/19}\right)\left[\sqrt{\left(\frac{1.05}{.95}\right)^2 - \cos^2 19.7339} - \sin 19.7339\right]$$

$$H_S = .353$$

$$H_T = (Mg + 1)\left[\sqrt{\left(\frac{R_o}{R}\right)^2 - \cos^2\phi_N} - \sin\phi_N\right]$$

$$= (41/19 + 1)\left[\sqrt{\left(\frac{2.15}{2.05}\right)^2 - \cos^2\ 19.7339} - \sin 19.7339\right]$$

$$H_T = .394$$

$$P_L = \frac{(50)\ (.03)\ (\cos^2 30^\circ)}{\cos 19.7339}\left[\frac{.353^2 + .394^2}{.353 + .394}\right]$$

$$P_L = .448\%$$

APPENDIX I

INPUT PLANETARY RING GEAR LOSS FACTOR

$$P_L = \frac{50\ f\ \cos^2 \psi}{\cos\ \phi N} \left[\frac{H_T{}^2 + H_S{}^2}{H_T + H_S} \right]$$

$$H_S = \frac{Mg - 1}{Mg} \left[\sqrt{\left(\frac{r_o}{r}\right)^2 - \cos^2 \phi_N} - \sin \phi_N \right]$$

$$= \frac{79/19 - 1}{79/19} \left[\sqrt{\left(\frac{1.05}{.95}\right)^2 - \cos^2 19.7339} - \sin 19.7339 \right]$$

$$H_S = .1835$$

$$H_T = (Mg - 1) \left[\sqrt{\left(\frac{R_o}{R}\right)^2 - \cos^2 \phi_N} - \sin \phi_N \right]$$

$$= (79/19 - 1) \left[\sqrt{\left(\frac{3.95}{3.85}\right)^2 - \cos^2 19.7339} - \sin 19.7339 \right]$$

$$H_T = .2228$$

$$P_L = \frac{(50\ (.03)\ (\cos^2 30)}{\cos 19.7339} \left[\frac{.1835^2 + .2228^2}{.1835 + .2228} \right]$$

P_L = .245% (PER MESH)

APPENDIX J

INPUT PLANETARY ASSY POWER DERIVATION

$$T_{in} = \frac{6300\ HPin}{RPMin}$$

AT MEAN CONDITION:

$$T_{in} = \frac{(6300)(22)}{21000}$$

$$= 66\ IN.LB.$$

$$W_{T_S} = \frac{2\ T_{in}}{(D_s)\ (No.\ PLANETS)}$$

$$= \frac{2\ T_{in}}{(2.05)(3)}$$

$$= .325\ T_{in}$$

$$T_{pc} = (W_{Ts})\ R_{PL}$$

$$= (W_{Ts})\ \frac{.95}{2}$$

$$= .154\ T_{in}$$

Table 12:

FLYWHEEL RPM	PLANET
28000	39780
21000	29830
14000	19890

APPENDIX K

OUTPUT PLANETARY GEAR DATA

	SUN	PLANET	RING
N	40	30	100
P_T	20		
ϕ_T	22.796°		
ψ	30°		
D_P	2.00	1.500	5.00
D_o	2.10	1.60	4.90
D_R	1.86	1.36	5.14
R_f	.03	.03	.03
F	.50	.75	.50
t	.077	.077	.081
P_N	23.094		
ϕ_N	20°		

Table 13:

APPENDIX L

OUTPUT PLANET SPEED DERIVATION

$$RPM_{PL} = \left(\frac{N_r}{N_p}\right) RPM_r + \left(\frac{N_s}{N_p}\right) RPM_s$$

$$RPM_r = (RPM_s)\ (R_c)\ (R_B)$$

$$= (RPM_s)\ (R_c)\ (.3016)$$

$$RPM_{PL} = \left[(.3016)\left(\frac{100}{40}\right)R_c + 1\right] RPM_s$$

$$= \left(.754\ R_c + 1\right)\ RPM_s$$

RPM_{PL}

$^*RPM_s \longrightarrow$ / $RPM_o \downarrow$	9600	7200	4800
5000	36700	31901	27102
4000	33204	28405	23602
3000	29701	24903	20102
1500	24453	19654	14851
850	22173	17374	12578

*RPMs = Flywheel $RPM_n/2.9166$

Table 14 :

APPENDIX M

OUTPUT PLANETARY SUN-PLANET POWER LOSS FACTOR

$$P_L = \frac{50\ f\ \cos^2 \gamma}{\cos \phi_N} \left[\frac{H_S^{\,2} + H_T^{\,2}}{H_S + H_T}\right]$$

$$H_T = \frac{Mg + 1}{Mg}\left[\sqrt{\left(\frac{r_o}{r}\right)^2 - \cos^2} - \sin\right]$$

$$= \frac{40/30 + 1}{40/30}\left[\sqrt{\left(\frac{1.6}{1.5}\right)^2 - \cos^2 20} - \sin 20\right]$$

$$H_T = .2847$$

$$H_S = (40/30 + 1)\left[\sqrt{\left(\frac{2.1}{2.70}\right)^2 - \cos^2 20} - \sin 20\right]$$

$$H_S = .2951$$

$$P_L = \frac{(50)(.03)(\cos^2 30)}{\cos 20}\left[\frac{(.2847)^2 + (.2951)^2}{.2847 + .2951}\right]$$

$$P_L = .347\%$$

APPENDIX N

OUTPUT PLANETARY PLANET-RING POWER LOSS FACTOR

$$P_L = \frac{(50)\ (.03)\ (\cos^2 \gamma)}{\cos 20} \quad \frac{H_S^2 + H_T^2}{H_S + H_T}$$

$$H_T = \frac{Mg - 1}{Mg} \left[\sqrt{\left(\frac{r_o}{r_i}\right)^2 - \cos^2 \phi} - \sin \phi \right]$$

$$= \frac{100/30 - 1}{100/30} \left[\sqrt{\left(\frac{1.6}{1.5}\right)^2 - \cos^2 20} - \sin 20 \right]$$

$$H_T = .1139$$

$$H_S = (100/30 - 1) \left[\sqrt{\left(\frac{5.1}{5.0}\right)^2 - \cos^2 20} - \sin 20 \right]$$

$$H_S = .1276$$

$$P_L = \frac{(50)(.03)(\cos^2 30)}{\cos 20} \left[\frac{(.1139)^2 + (.1276)^2}{.1139 + .1276} \right]$$

$$P_L = .145\%$$

APPENDIX O

OUTPUT PLANETARY ASSY POWER DERIVATION

$$T_o = \frac{63000\ HP_o}{RPM_o}$$

$$T_s = \frac{T_o}{3.50} = .2857\ T_o$$

$$W_T = \frac{2\ Ts}{Ds}$$

$$T_{PL} = \left(W_{Ts}\right)\left(R_{PL}\right)$$

$$= \frac{2\ Ts}{Ds}\left(R_{PL}\right)$$

$$= \frac{2\ T_o}{(3.5)\ Ds}\left(R_{PL}\right)$$

$$= \frac{63000\ HP_o}{(3.5)(RPM_o)}\left(\frac{Dp}{Ds}\right)$$

$$= \frac{13500\ \ HP_o}{RPM_o}$$

$$HP_{PL} = \frac{T_{PL}\ RPM_{PL}}{(63000)(4)} \qquad \text{(FOR 4 PLANETS)}$$

$$= \frac{13500\ HP_o}{RPM_o} \qquad \frac{RPM_{PL}}{(63000)(4)}$$

$$HP_{PL} = .0536\ (HP_o)\left(\frac{RPM_{PL}}{RPM_o}\right)$$

APPENDIX P

OUTPUT PLANET POWER

$$HP_{PL} = .0536\ HP_o \left(\frac{RPM_{PL}}{RPM_o}\right)$$

7.5KW (10 HP)

RPM_n → / RPM_o ↓	28,000	21,000	14,000
5000	3.93	3.42	2.91
4000	4.45	3.81	3.16
3000	5.31	4.45	3.59
1500	8.74	7.02	5.31
850	13.98	10.96	7.93

15KW (20 HP)

5000	7.87	6.84	5.81
4000	8.89	7.61	6.33
3000	10.61	8.90	7.18
1500	17.48	14.05	10.61
850	27.96	21.91	15.86

30KW (40 HP)

5000	15.74	13.68	11.62
4000	17.78	15.23	12.65
3000	21.23	17.80	14.37
1500	34.95	28.09	21.23
850	55.93	43.82	31.73

Table 15:

APPENDIX P (continued)

52KW (70 HP)			
5000	27.54	23.94	20.34
4000	31.12	26.64	22.14
3000	37.15	31.15	25.14
1500	61.16	49.16	37.15
850	*97.87	*76.69	*55.52
75KW (100 HP)			
5000	39.34	34.20	29.05
4000	44.45	38.06	31.63
3000	53.07	44.49	35.92
1500	*87.38	*70.23	*53.07
850	*139.82	*109.56	*79.32

*NOTE: The values shown do not reflect the limiting wheelslip torque of 330 FT. LBS.

Table 15: (Continued)

APPENDIX Q

SPIRAL BEVEL GEAR DATA

	PINION	GEAR
N	19	27
P	13.570	
ϕ	22° 30'	
ψ	30°	
D_P	1.400	1.990
F	.600	.600
SHAFT ANGLE	9° 41'	
OUTER CONE DISF.	10.522	
WHOLE DEPTH	.136	.136
HAND OF SPIRAL	RH	LH
OUTSIDE DIA.	1.539	2.095

Table 16:

APPENDIX R

SPIRAL BEVEL GEAR POWER LOSS FACTOR

$$P_L = 50\ f\ (\cos\Gamma + \cos\gamma)\ \frac{\cos\psi^2}{\cos\phi}\left[\frac{H_S^{\,2} + H_T^{\,2}}{H_S + H_T}\right]$$

$\Gamma = 5.433^\circ$

$\gamma = 3.817^\circ$

$\psi = 30^\circ$

$\phi = 22.5^\circ$

$f = .03$

$$H_T = \frac{Mg + 1}{Mg}\left[\sqrt{\left(\frac{r_o}{r}\right)^2 - \cos^2\phi_N} - \sin\phi\right]$$

$$= \frac{27/19 + 1}{27/19}\left[\sqrt{\left(\frac{1.539}{1.400}\right)^2 - \cos^2 22.5} - \sin 22.5\right]$$

$H_T = .3629$

$$H_S = (Mg + 1)\left[\sqrt{\left(\frac{R_o}{R}\right)^2 - \cos^2\phi} - \sin\phi\right]$$

$$H_S = (27/19 + 1)\left[\sqrt{\left(\frac{2.095}{1.99}\right)^2 - \cos^2 22.5} - \sin 22.5\right]$$

$H_S = .2955$

$$P_L = (50)(.03)(\cos 5.433 + \cos 3.817)\left[\frac{.3629^2 + .2955}{.3629 + .2955}\right]$$

$P_L = .807\%$

APPENDIX S

HELICAL IDLER GEAR DATA

	PINION	GEAR
N	21	49
P_T	14.894	
ϕ_T	21.789°	
ψ	24.427°	
D_P	1.41	3.2899
D_O	1.544	3.4242
D_R	1.222	3.1019
R_f	.035	.035
F	.50	.50
t	.104	.103
P_N	16.358	
ϕ_N	20°	
C	2.350	

Table 17:

APPENDIX T

HELICAL IDLER POWER LOSS FACTOR

$$P_c = \frac{50\ f\ \cos^2\psi}{\cos\ N}\left[\frac{H_S^{\ 2} + H_T^{\ 2}}{H_S + H_T}\right]$$

$$H_S = \frac{Mg + 1}{Mg}\left[\sqrt{\left(\frac{r_o}{r}\right)^2 - \cos\phi^2} - \sin\phi\right]$$

$$= \frac{49/21 + 1}{49/21}\left[\sqrt{\left(\frac{1.544}{1.41}\right)^2 - \cos^2 20^\circ} - \sin 20^\circ\right]$$

$$H_S = .3146$$

$$H_T = (Mg + 1)\left[\sqrt{\left(\frac{R_o}{R}\right)^2 - \cos^2\phi_N} - \sin\phi\right]$$

$$= (49/21\ H)\left[\sqrt{\left(\frac{3.4242}{3.2899}\right)^2 - \cos^2 20} - \sin 20\right]$$

$$H_T = .3517$$

$$P_L = \frac{(50)(.03)(\cos^2 24.427)}{\cos 20}\left[\frac{(.3146)^2 + (.3517)^2}{.3146 + .3517}\right]$$

$$P_L = .444\%$$

APPENDIX U

CONE BENDING STRESS

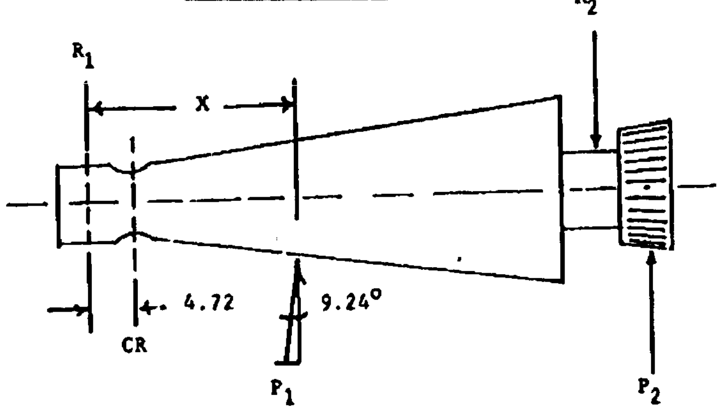

MEAN CONDION:

R_1 = RESULTANT LOAD $=$ $\overset{a.}{29.35} \overset{*}{\rightarrow\!\!+\!\!\rightarrow} \overset{b.}{345.6}$ $=$ 345.8 LB.

$M_{cr} = (R_1)\,(\ell) = (346.8)(.472) = 163.8$ IN. LB.

$I = .049\ D^4 = (.049)(.67)^4 = .0099$ IN.4

$S_B = \frac{Mc}{I} = \frac{(163.8)(.335)}{.0099} = \underline{5560}$ PSI

MAXIMUM CONDION:

$S_B = M'\frac{c}{I} = R_1'\,\ell\,\frac{c}{I} = \frac{(2350)(.472)(.335)}{.0099}$

$S_B = 37{,}530$ PSI

$* \rightarrow\!\!+\!\!\rightarrow = \sqrt{a^2 + b^2}$

APPENDIX V

CONE HORSEPOWER DERIVATION

HP_c FORMULA:

$$T_o = \frac{(HP_o)(6300)}{RPM_o}$$

$$T_r = (T_o)(1 - R_p)$$

$$HP_c = \frac{(T_c)(RPM_c)}{(63000)(4)}$$

$$= \frac{(T_r)(R_b)(RPM_c)}{(63000)(4)}$$

$$= \frac{\dfrac{(HP_o)(63000)(RPM_c)(1 - R_p)}{(RPM_o)}}{(63000)(4)}$$

$$HP_c = \frac{(HP_o)(R_b)(RPM_c)(1 - R_p)}{(4)(.2154\ R_c - .2857)(RPM_s)}$$

$$HP_c = \frac{(HP)(.3016)(R_c)(.7143)}{(4)(.2154\ R_c - .2857)}$$

$$HP_c = \frac{(.0539)(HP_o)(R_c)}{(.2154\ R_c - .2857)}$$

APPENDIX W

TRACTION CONE LIFE AT MEAN CONDITION (REF.3)

$$L = K_4 \, (K_2)^{.9} \, (Q)^{-3} \, (E)^{-6.3} \, (R)^{-.9}$$

$$K_4 = 6.43 \times 10^8$$

$$K_2 = 1.3 \times 10^6$$

$$Q = 498.5 \text{ LB.}$$

$$E = \frac{1}{2.325} + \frac{1}{5} + \frac{1}{.722} = 2.015$$

$$L = (6.43 \times 10^8)(1.3 \times 10^6)^{.9} \, (498.5)^{-3} \, (2.015)^{-6.3} \, (.722)^{-.9}$$

$$= 2.68 \times 10^4 \, (\text{MR})$$

$$L_{10} = \frac{2.68 \times 10^4 \text{ MR}}{(60)\,(23479)} = 19{,}020 \text{ HOURS (Single cone life)}$$

APPENDIX X

TRACTION ROLLER LIFE AT MEAN CONDITION (REF. 3)

$$L = K_4 \,(K_2)^{.9}\,(Q)^{-3}\,(E)^{-6.3}\,(R)^{-.9}$$

$$K_4 = 6.43 \times 10^8$$

$$K_2 = 1.3 \times 10^6$$

$$Q = 498.5 \text{ LB.}$$

$$E = \frac{1}{2.325} + \frac{1}{5} + \frac{1}{.722} = 2.015$$

$$L = (6.43 \times 10^8)(1.3 \times 10^6)^{.9}\,(498.5)^{-3}\,(2.015)^{-6.3}\,(2.325)^{-.9}$$

$$L = 9.36 \times 10^3 \text{ MR}$$

$$L_{10} = \frac{(9.36 \times 10^3)(10^6)}{(7200)\,(60)\,(4)} = 5420 \text{ HOURS}$$

APPENDIX Y

TRACTION CONTACT COMPOSITE LIFE
AT MEAN CONDITION

$$L_c = \left[\frac{N_c}{(H_1)^{10/9}} + \frac{N_r}{(H_2)^{10/9}}\right]^{-9/10}$$

N_c = NUMBER OF CONES = 4

N_r = NUMBER OF ROLLERS = 1

H_1 = INDIVIDUAL CONE LIFE, HRS. 19020

H_2 = ROLLER LIFE, HRS. = 5420

$$L_c = \left[\frac{4}{(19020)^{10/9}} + \frac{1}{(5420)^{10/9}}\right]^{-\frac{9}{10}}$$

L_c = 2920 HOURS

APPENDIX Z

CONE TORQUE (IN. LB.)

$$T_c = HP_c \times \frac{63025}{RPM_c}$$

7.5KW (10 HP)

RPM_o ↓ \ RPM_n →	28,000	21,000	14,000
5000	6.79	6.79	6.79
4000	8.49	8.49	8.49
3000	11.32	11.32	11.32
1500	22.63	22.63	22.63
850	39.99	39.99	39.99
15KW (20 HP)			
5000	13.58	13.58	13.58
4000	16.98	16.98	16.98
3000	22.64	22.64	22.64
1500	45.26	45.26	45.26
850	79.98	79.98	79.98
30KW (40 HP)			
5000	27.16	27.16	27.16
4000	33.96	33.96	33.96
3000	45.28	45.28	45.28
1500	90.52	90.52	90.52
850	159.96	159.96	159.96

Table 181

APPENDIX Z (continued)

52KW (70 HP)				
	5000	47.53	47.53	47.53
	4000	59.43	59.43	59.43
	3000	79.24	79.24	79.24
	1500	158.41	158.41	158.41
39.8KW(53.4 Hp)	850	279.93*	279.93*	279.93*
75KW (100 HP)				
	5000	67.90	67.90	67.90
	4000	84.90	84.90	84.90
	3000	113.20	113.20	113.20
70.4KW(94.3 Hp)	1500	226.30*	226.30*	226.30*
39.8KW(53.4 Hp)	850	399.90*	399.90*	399.90*

* THE NUMBERS SHOWN ARE THEORETICAL ONLY. THE MAXIMUM WHEEL SLIP TORQUE OF 330 FT. LBS. LIMITS THE CONE TORQUE.

Table 13: Continued

APPENDIX AA

SINGLE CONE HORSEPOWER (HP)

$$HP = \frac{(.0539)(HPo)(Rc)}{(.2154)(Rc) - .2857}$$

7.5KW (10 HP) RPM_n → RPM_o ↓	28,000	21,000	14,000
5000	3.88	3.53	3.19
4000	4.22	3.79	3.36
3000	4.79	4.22	3.65
1500	7.08	5.93	4.79
850	10.59	8.56	6.54
15KW (20 HP)			
5000	7.75	7.06	6.38
4000	8.43	7.58	6.72
3000	9.58	8.44	7.29
1500	14.15	11.86	9.58
850	21.17	17.13	13.07
30KW (40 HP)			
5000	15.50	14.13	12.75
4000	16.87	15.16	13.44
3000	19.16	16.87	14.58
1500	28.30	23.73	19.16
850	42.34	34.25	26.15

Table 19:

ORIGINAL PAGE IS
OF POOR QUALITY

APPENDIX AA (continued)

52KW (70 HP)			
5000	27.13	24.72	22.32
4000	29.53	26.52	23.52
3000	33.53	29.53	25.52
1500	49.53	41.53	33.53
850	74.10 (56.53)	59.94 (45.73)	45.76 (34.91)
75KW (100 HP)			
5000	38.75	35.39	31.89
4000	42.18	37.89	33.60
3000	47.90	42.18	36.46
1500	70.63(66.69)	59.32(55.91)	47.90 (45.15)
850	105.85(56.53)	85.63(45.73)	65.37 (34.91)

NOTE: THE MAXIMUM WHEEL SLIP TORQUE OF 330 FT. LBS. LIMITS THE CONE HORSEPOWER TO THE VALUES IN PARENTHESIS.

Table 19: Continued

APPENDIX BB

TOTAL CONE HORSEPOWER (HP): FOUR (4) CONES

$$HP = \frac{(.539)(HPo)(Rc)}{(.2154)(Rc)-.2857} \times 4 \qquad "n" = \frac{\text{Total cone power}}{\text{Power out}}$$

RPM$_o$ ↓ \ RPM$_n$ →	28,000	21,000	14,000
7.5KW (10 HP)			
5000	15.52	14.12	12.76
4000	16.88	15.16	13.44
3000	19.16	16.88	14.60
1500	28.32	23.72	19.16
850	42.36	34.24	26.16
15KW (20 HP)			
5000	31.00	28.24	25.52
4000	33.72	30.32	26.88
3000	38.32	33.76	29.16
1500	56.60	47.44	38.32
850	84.68	68.52	52.28
30KW (40 HP)			
5000	62.00	56.56	51.00
4000	67.48	60.64	53.76
3000	76.64	67.48	58.32
1500	113.20	94.92	76.64
850	169.36	137.0	104.6

Table 201

APPENDIX BB (continued)

<u>52KW (70 HP)</u>			
5000	108.5	98.88	89.28
4000	118.1	106.1	94.08
3000	134.1	118.1	102.1
1500	198.1	166.1	134.1
850	296.4(226.1)	239.8(182.9)	183(139.6)
<u>75KW (100 HP)</u>			
5000	155.0	141.6	127.6
4000	168.7	151.6	134.4
3000	191.6	168.7	145.8
1500	282.5(266.8)	237.3(223.6)	191.6(180.6)
850	423.4(226.1)	342.5(182.9)	261.5(139.6)

NOTE: THE MAXIMUM WHEEL SLIP TORQUE OF 330 FT. LBS. LIMITS THE CONE HORSEPOWER TO THE VALUES IN PARENTHESES ().

Table 20: Continued

APPENDIX CC

CONE NORMAL LOAD (LB.)

$$W_N - \frac{2\ T_c}{.07\ D_{cone}}$$

7.5KW (10 HP)

RPM_o \ RPM_n →	28,000	21,000	14,000
5000	156.20	189.82	256.95
4000	170.11	203.67	271.03
3000	193.09	226.81	294.03
1500	285.34	318.98	386.01
850	426.81	460.53	527.99

15KW (20 HP)

5000	312.40	379.65	513.91
4000	340.21	407.34	542.06
3000	386.18	436.62	588.05
1500	570.67	637.96	772.02
850	853.62	921.06	1055.98

30KW (40 HP)

5000	624.80	759.30	1027.81
4000	680.42	814.68	1084.12
3000	772.37	907.23	1176.10
1500	1141.34	1275.92	1544.05
850	1707.24	1842.11	2111.96

52KW (70 HP)

5000	1093.40	1328.77	1798.68
4000	1190.74	1425.69	1897.21
3000	1351.64	1587.66	2058.18
1500	1997.35	2234.86	2702.09
850	2987.99 (2273.33)	3224.04 (2452.93)	3696.33 (2812.25)

Table 21

APPENDIX CC (continued)

<u>75KW (100 HP)</u>			
5000	1562.00	1898.24	2569.54
4000	1701.06	2036.70	2710.30
3000	1930.92	2268.08	2940.26
1500	2853.36 (2685.66)	3189.79 (3002.32)	3860.13 (3633.26)
850	4268.10 (2273.33)	4605.28 (2452.93)	5279.90 (2812.25)

NOTE: THE MAXIMUM WHEEL SLIP TORQUE OF 330 FT. LB. LIMITS THE CONE NORMAL LOAD TO THE VALUES SHOWN IN PARENTHESES.

Table 21: Continued

APPENDIX DD

CONE BEARING LOSS

(4 cones)

7.5 KW (10 HP)

RPM_o ↓ \ RPM_n →	28,000	21,000	14,000
5000	.394	.383	.420
4000	.260	.360	.310
3000	.266	.342	.250
1500	.320	.340	.230
850	.390	.311	.242
15 KW (20 HP)			
5000	.720	.700	.680
4000	.460	.510	.600
3000	.480	.500	.560
1500	.760	.700	.540
850	.950	.800	.580
30 KW (40 HP)			
5000	1.240	1.368	1.840
4000	.960	1.180	1.640
3000	1.158	1.206	1.510
1500	2.140	1.870	1.550
850	2.737	2.295	1.573
52 KW (70 HP)			
5000	2.66	3.32	4.60
4000	2.20	2.60	3.92
3000	2.54	2.75	3.70
1500	4.44	4.15	3.71
(39.8 KW) 850 (53.4 HP)	6.50 (4.3)	5.55 (3)	3.82 (1.9)
75 KW (100 HP)			
5000	4.31	5.46	8.10
4000	3.83	4.54	6.37

Table 22:

APPENDIX DD

CONE BEARING LOSS (CONTINUED)

(4 CONES)

	3000	4.13	4.47	6.22
(90KW)	1500 (94.3 HP)	6.45 (6.4)	6.20 (4.8)	6.95 (3.4)
(39.8KW)	850 (53.4 HP)	11.11 (4.3)	9.29 (3)	7.65 (1.9)

( ) WHEEL SLIP TORQUE LIMITED VALUES.

Table 22: Continued

APPENDIX EE

SPIN VELOCITY DERIVATION

$$\text{TANGENTIAL VELOCITY} = \frac{D_{roll}}{2} \cdot (RPM_s)$$

RPM_s = Flywheel $RPM_n/2.9166$

$$\nu = \left(\frac{2\pi}{60}\right)\left(\frac{1}{2}\right)\left(\frac{4.65}{39.37}\right)(RPM_s)$$

$$\nu = .00618\ (RPM_s)\ M/SEC$$

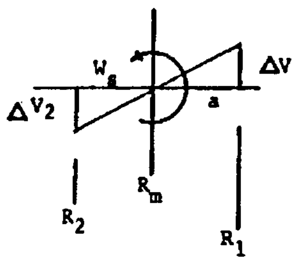

$$W_s = \frac{\Delta V1}{a}$$

$$\Delta V1 = W_c\left(R_1\right) - \left(W_R\right)R_{Roll}$$

$$\Delta V1 = W_c\left(R_{cone} + a\ TAN\,\alpha\right) - \left(W_R\right)R_{Roll}$$

$$\alpha = (\text{CONE ANGLE})/2$$

$$W_s = \frac{W_c\ (R_{cone} + a\ TAN\,\alpha) - (W_R)\ R_{Roll}}{a}$$

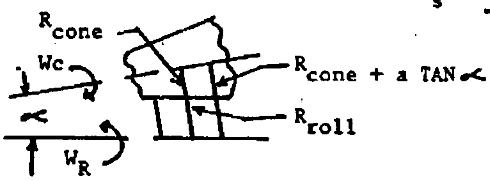

$$W_c = R_c\left(W_R\right)$$

$$R_{cone} = R_{roll}/R_c$$

$$W_s = R_c\left(W_R\right)TAN\,\alpha$$

$*RPM_n \longrightarrow$	28000	21000	14000
$*RPM_s \longrightarrow$	9600	7200	4800
$W_{Roll}\ \frac{RAD}{SEC}$	1005	754	503
V (M/SEC)	59.37	44.53	29.69

$$W_s = (RAD/SEC) = (R_c)(W_{roll})\ TAN\,\alpha$$

RPM_o	RPM_s 9600	7200	4800
5000	612	558	504
4000	533	479	425
3000	454	400	346
1500	335	281	227
850	284	230	176

Table 23:

APPENDIX FF

J_6, DIMENSIONLESS SPIN TORQUE FACTOR (REF. 1)

RPM_o ↓ \ RPM_h →	28,000	21,000	14,000
7.5 KW (10 HP)			
5000	.009	.007	.004
4000	.008	.0065	.0035
3000	.007	.006	.0028
1500	.0065	.005	.0022
850	.006	.004	.002
15 KW (20 HP)			
5000	.012	.009	.006
4000	.010	.008	.0045
3000	.009	.007	.0038
1500	.008	.006	.0032
850	.0075	.005	.0027
30 KW (40 HP)			
5000	.014	.010	.007
4000	.013	.009	.006
3000	.012	.008	.005
1500	.011	.007	.004
850	.010	.006	.0035
52 KW (70 HP)			
5000	.016	.012	.008
4000	.015	.011	.007
3000	.014	.009	.006
1500	.013	.008	.005
850	.012	.007	.004
75 KW (100 HP)			
5000	.019	.015	.0085
4000	.018	.012	.0075
3000	.017	.010	.0065
1500	.016	.009	.0055
850	.015	.008	.0045

Table 24:

APPENDIX GG

TRACTION LOAD DETERMINATION

MEAN CONDITION:

HP_{out} = 22 HORSEPOWER

RPM_{out} = 3000 RPM

$$T_o = \frac{(HP_{out})(63000)}{RPM_{out}} = 462 \text{ in. lb.}$$

$$T_{sun} = (T_o)(Rp) = (462)(.2857) = 132 \text{ in. lb.}$$

$$T_{ring} = (T_o)(1\text{-}Rp) = (462)(1-.2857) = 330 \text{ in lb.}$$

$$T_{cone} = (T_{ring})(R_B) = (330)(.3016) = 99.5 \text{ in. lb.}$$

FOR 4 CONES:

$$T_{cone} = \frac{99.5}{4} = 24.88 \text{ in. lb./cone}$$

$$W_{T_{cone}} = \frac{T}{R_{cone}} = \frac{24.88}{\left(\frac{1.426}{2}\right)} = 34.9 \text{ lbs.}$$

$$W_{N_{cone}} = \frac{W_T}{\mu} = \frac{34.9}{.07} = 498.5 \text{ lbs.}$$

MAXIMUM CONDITION:

HP_{out} = 100 HP
T_o = 330 FT. LB. = 3960 IN. LB.
RPM_o = 100 x 63025/3960 = 1592 RPM
RPM_{in} = 14,000 RPM

$$R_c = \frac{\frac{n_o}{RPM_s} + .2857}{.2154} = \frac{\frac{1592}{4800} + .2857}{.2154} = 2.866$$

APPENDIX GG

TRACTION LOAD DETERMINATION (CONTINUED)

$D_c = 4.65/R_c = 4.65/2.866 = 1.622$ in.

$RPM_c = R_c\ RPM_x = 2.866\ (4800) = 13757$ RPM

$T_{ring} = T_o\ (1-R_p) = 3960\ (1 - .2857) = 2829$ IN. LB.

$T_{cone} = T_{ring}\ R_B = 2829\ (.3016) = 853$ IN. LB. (4 cones)

PER CONE:

$T_{cone} = 853/4 = 213$ IN. LB.

$$W_{N_{cone}} = \frac{W_T}{\mu} = \frac{T_{cone}}{\frac{D_c \mu}{2}} = \frac{213}{1.622}\ \frac{(2)}{(.07)} = 3750 \text{ LB.}$$

APPENDIX HH

TRACTION POWER LOSS (HP, FOR 4 CONTACTS) (REFERENCE 2)

$$\text{POWER LOSS} = \frac{(.015)^{J_7/J_4}\,(HP_c)}{\sqrt{K}}$$

$RPM_o \downarrow$ \ $RPM_n \rightarrow$	28,000	21,000	14,000
7.5 KW (10 HP)			
5000	.25	.23	.21
4000	.27	.25	.22
3000	.31	.27	.24
1500	.46	.38	.31
850	.69	.56	.42
15 KW (20 HP)			
5000	.50	.46	.41
4000	.55	.49	.44
3000	.62	.55	.47
1500	.92	.77	.62
850	1.37	1.11	.85
30 KW (40 HP)			
5000	1.00	.91	.83
4000	1.09	.98	.89
3000	1.24	1.10	.94
1500	1.83	1.54	1.24
850	2.74	2.22	1.70
52 KW (70 HP)			
5000	1.75	1.60	1.45
4000	1.91	1.72	1.55
3000	2.17	1.92	1.65
1500	3.21	2.69	2.17
850	4.80 (3.69)	3.89 (2.99)	2.97 (2.24)
75 KW (100 HP)			
5000	2.50	2.80	2.07
4000	2.73	2.45	2.22

Table 25:

APPENDIX HH

TRACTION POWER LOSS (HP, FOR 4 CONTACTS) (REFERENCE)(CONTINUED)

$$\text{POWER LOSS} = \frac{(.015)\ J_7/J_4\ (HP_c)}{\sqrt{K}}$$

3000	3.10	2.74	2.36
1500	4.58 (4.33)	3.84 (3.58)	3.10 (2.92)
850	6.86 (3.69)	5.55 (2.99)	4.24 (2.24)

NOTE: THE MAXIMUM WHEEL SLIP TORQUE OF 330 FT. LBS LIMITS THE POWER LOSS TO THE VALUES SHOWN IN PARENTHESES.

Table 25: Continued

APPENDIX II

CONTACT ELLIPSE DIMENSIONS, a/b (IN.) (REF. 6)

RPM_o ↓ / RPM_n →	$b = \mu g$ 28,000	$a = \nu g$ 21,000	14,000
		a/b in.	
7.5 KW (10 HP)			
5000	.0456/.0101	.0492/.0098	.0507/.0086
4000	.0462/.0109	.0499/.0108	.0561/.0105
3000	.0478/.0122	.0508/.0120	.0566/.0118
1500	.0531/.0155	.0556/.0155	.0600/.0153
850	.0601/.0188	.0618/.0188	.0656/.0188
15 KW (20 HP)			
5000	.0574/.0127	.0619/.0124	.0702/.0120
4000	.0581/.0138	.0630/.0136	.0708/.0132
3000	.0600/.0153	.0645/.0153	.0713/.0148
1500	.0670/.0195	.0702/.0192	.0758/.0193
850	.0757/.0237	.0779/.0237	.0825/.0236
30 KW (40 HP)			
5000	.0723/.0160	.0780/.0157	.0886/.0151
4000	.0733/.0174	.0793/.0171	.0892/.0167
3000	.0758/.0193	.0806/.0191	.0900/.0187
1500	.0843/.0246	.0884/.0246	.0955/.0244
850	.0953/.0299	.0981/.0299	.1041/.0298
52 KW (70 HP)			
5000	.0872/.0192	.0941/.0189	.1068/.0182
4000	.0884/.0209	.0956/.0207	.1073/.0201
3000	.0914/.0233	.0972/.0230	.1085/.0226
1500	.1017/.0296	.1067/.0297	.1150/.0293
850	.1147/.0360 (.1047/.0329)	.1183/.0360 (.1079/.0328)	.1253/.0359 (.1145/.0328)

Table 26:

APPENDIX II

CONTACT ELLIPSE DIMENSIONS, a/b (IN.) (REF. 6) (CONTINUED)

75 KW (100 HP)			
5000	.0980/.0216	.1060/.0213	.1201/.0205
4000	.0995/.0236	.1075/.0232	.1210/.0226
3000	.1028/.0262	.1096/.0259	.1222/.0254
1500	.1145/.0334 (.1121/.0327)	.1200/.0334 (.1177/.0327)	.1295/.0330 (.1269/.0324)
850	.1292/.0405 (.1047/.0329)	.1332/.0405 (.1079/.0328)	.1412/.0404 (.1145/.0328)

NOTE: THE MAXIMUM WHEEL SLIP TORQUE OF 330 FT. LB LIMITS "b/a" TO THE VALUES SHOWN IN PARENTHESES.

Table 26: Continued

g (REF. 6)

RPM_o ↓ \ RPM_n →	28,000	21,000	14,000
7.5 KW (10 HP)			
5000	.0190	.0193	.0197
4000	.0201	.0205	.0201
3000	.0218	.0221	.0227
1500	.0264	.0268	.0274
850	.0312	.0315	.0322
15 KW (20 HP)			
5000	.0239	.0243	.0248
4000	.0253	.0259	.0265
3000	.0274	.0281	.0286
1500	.0333	.0338	.0346
850	.0393	.0397	.0405
30 KW (40 HP)			
5000	.0301	.0306	.0313
4000	.0319	.0326	.0334
3000	.0346	.0351	.0361
1500	.0419	.0426	.0436
850	.0495	.0500	.0511
52 KW (70 HP)			
5000	.0363	.0369	.0377
4000	.0385	.0393	.0402
3000	.0417	.0423	.0435
1500	.0505	.0514	.0525
850	.0596 (.0544)	.0603 (.0550)	.0615 (.0562)
75 KW (100 HP)			
5000	.0408	.0416	.0424
4000	.0433	.0442	.0453

Table 27:

APPENDIX JJ

g (REF. 6) (CONTINUED)

3000	.469	.0477	.0490
1500	.0569 (.0557)	.0578 (.0567)	.0591 (.0579)
850	.0671 (.0544)	.0679 (.0550)	.0693 (.0562)

NOTE: THE MAXIMUM WHEEL SLIP TORQUE OF 330 FT. LB. LIMITS "g" TO THE VALUES SHOWN IN PARENTHESES.

Table 27:

APPENDIX KK

ELASTOHYDRODYNAMIC (EHD) FILM THICKNESS AT TRACTION CONTACT (REF. 7)

$$h = 2.04\left(1 + \frac{2R_1}{3R_2}\right)\left(\mu_0 \alpha \frac{(u_1 + u_2)}{2}\right)^{.74}\left(R_1\right)^{.407}\left(\frac{F}{(1 - \nu^2)Q}\right)^{.074}$$

AT MEAN CONDITION:

$$R_1 = \frac{1}{\frac{1}{2.325} + \frac{1}{.722}} = .551$$

$$R_2 = \frac{1}{\frac{1}{5.0} + \frac{1}{\infty}} = 5.0$$

$\mu_0 = .87 \times 10^{-6}$ AT 176°F

$\alpha = 1.5 \times 10^{-4}$

$$\frac{u_1 + u_2}{2} = \pi(4.65)\left(\frac{7200}{60}\right) = 1753 \text{ IN./SEC.}$$

Q = 498.5 LB.

$$h = 2.04\left(1 + \frac{3(.551)}{2(5.0)}\right)^{-.74}\left(.87 \times 10^{-6} \times 1.5 \times 10^{-4} \times 1753\right)^{.74}$$

$$\left(.551\right)^{.407}\cdot\left(\frac{30 \times 10^6}{(1 - .3^2)(498.5)}\right)^{.74} = 39.6\,\mu\text{ in.}$$

$h = 39.6\,\mu$ in.

$$\sigma = \left(\sigma_1^2 + \sigma_2^2\right)^{.5} = \left(6^2 + 6^2\right)^{.5} = 8.49$$

$h/\sigma = 39.6/8.49 = 4.66$

APPENDIX KK

EHD FILM THICKNESS AT

TRACTION CONTACT (REF. 7)

(CONTINUED)

AT MAXIMUM CONDITION:

$$R_1 = \frac{1}{\frac{1}{2.325} + \frac{1}{.822}} = .607 \text{ IN.}$$

$$R_2 = 5.0 \text{ IN.}$$

$$Q = 3750 \text{ LB.}$$

$$\frac{u_1 + u_2}{2} = \frac{\pi(4.65)\ (4800)}{60} = 1169 \text{ IN./SEC.}$$

$$h = 2.04 \left(1 + \frac{2(.607)}{3(5.0)}\right)^{-.74} \left(.87 \times 10^{-6} \times 1.5 \times 10^{-4} \times 1169\right)^{.74}$$

$$\left(.607\right)^{.407} \left(\frac{30 \times 10^6}{(1 - .3^2)(3750)}\right)^{.074} = 27.8\,\mu \text{ in.}$$

$h = 27.8\,\mu$ IN.

$h/\sigma = 27.8/8.49 = 3.27$

APPENDIX LL

HERTZIAN TRACTION CONTACT STRESS (REF. 6)

MEAN CONDITION:

$P = 498.5$ LB.

$R_{A1} = 2.235$ IN.

$R_{A2} = 5.0$ IN.

$R_{B1} = 1.426 \Big/ (2 \cos 9.24^{o}) = .722$ IN.

$R_{B2} = \infty$

$$g = .00459 \left(\frac{498.5}{\frac{1}{2.325} + \frac{1}{5} + \frac{1}{.722}} \right)^{1/3} = .0288$$

$$\cos \tau = \frac{\frac{1}{2.325} - \frac{1}{5.0} + \frac{1}{.722}}{\frac{1}{2.35} + \frac{1}{5.0} + \frac{1}{.722}} = .8015$$

$\mu = 2.300$

$\nu = .543$

$b = \mu g = (2.300)(.0287) = .0662$

$a = \nu g = (.543)(.0287) = .0156$

ASPECT RATIO = .0662/.0156 = 4.24

$$S_{max} = \left(\frac{3}{2\pi}\right)\left(\frac{498.5}{(.0662)(.0156)}\right) = 230,480 \text{ PSI (MEAN)}$$

MAXIMUM CONDITION:

$P = W_N = 3750$ LB.

APPENDIX LL

TRACTION CONTACT STRESS (CONTINUED)
(REF. 6)

$$R_{B-1} = 1.622/(2 \cos 9.24^{\circ}) = .822 \text{ IN.}$$

$$g = (.00459)\left(\frac{3750}{\frac{1}{2.325} + \frac{1}{5} + \frac{1}{.822}}\right)^{1/3} = .0581$$

$$\cos \tau = \frac{\frac{1}{2.325} - \frac{1}{5} + \frac{1}{.822}}{\frac{1}{2.325} + \frac{1}{5} + \frac{1}{.822}} = .783$$

$$\mu = 2.208$$

$$\nu = .566$$

$$b = \mu g = 2.208\ (.0581) = .1283$$

$$a = \nu g = 0.556\ (.0581) = .0323$$

$$\text{ASPECT RATIO} = .1283/.0323 = 3.972$$

$$S_{max} = \frac{3}{2\pi}\ \frac{3750}{(.1283)(.0323)} = 432{,}060 \text{ PSI (MAX)}$$

APPENDIX MM

EXAMPLE: TRACTION LOSS CALCULATION

From Reference 1 , page 15.

$$\text{Loss factor} = \frac{3\pi}{8} \cdot \sqrt{k} \cdot \frac{m}{\mu} \cdot \left(\frac{\text{power loss}}{\text{power input}}\right)$$

$$\text{Power Loss} = \text{Loss factor } (8)\ (\text{power input}) \Big/ 3\pi \cdot \sqrt{k} \cdot \left(\frac{m}{\mu}\right)$$

$$\text{Loss factor} = J_7/J_4$$

$$\text{Power Loss} = \frac{.849\ (J_7/J_4)\ (\text{power input})}{\sqrt{k} \cdot \left(\frac{m}{\mu}\right)}$$

For four contacts, and assuming $m/\mu = 220$

$$\text{Power loss} = \frac{.015\ (J_7/J_4)\ (\text{power input})}{\sqrt{k}}$$

$$J_7/J_4 = \left(J_6 \times J_3\right) + \left(J_4 \times J_1\right) \qquad \text{(Ref. 1, page 15)}$$

$$J_1 = \frac{3\pi}{8} \cdot \frac{m}{\mu} \cdot \frac{\Delta u}{u} \cdot \sqrt{k} \qquad \text{(Slip Factor, Ref. 1 , page 9)}$$

Assuming $\frac{\Delta u}{u} = .016$

$$J_1 = 4.15\sqrt{k} = 8.30$$

k = aspect ratio of Hertzian contact = 4.0

$$J_3 = \frac{3\pi}{8} \cdot \frac{m}{\mu} \cdot \frac{Ws}{u} \cdot \sqrt{a.b} \cdot \sqrt{k} \qquad \text{(Spin Factor, Ref. 1 , page 9)}$$

For Ws = 600 rad/sec. (Spin Velocity)

APPENDIX MM

EXAMPLE: TRACTION LOSS CALCULATION (CONTINUED)

and u = 60 m/sec (Velocity)

and since k = a/b

$J_3 = 2592\ b$

For b = .0013 m

$J_3 = 3.37$

$J_1/J_3 = 8.30/3.37 = 2.46$

From Reference 1, page 30:

$J_4 = 1.0$

From Reference 1, page 33:

$J_6 = .06$

$$J_7/J_4 = \frac{J_6 \times J_3 + J_4 \times J_1}{J_4}$$

$$= \frac{.06 \times 3.37 + 1.0 \times 8.30}{1.0}$$

$J_7/J_4 = 8.50$

Therefore,

$$\text{Power Loss} = \frac{.015\ (8.50)\ (\text{power input})}{\sqrt{4}}$$

Power loss = .064 (power input)

APPENDIX MM

EXAMPLE: TRACTION LOSS CALCULATION (CONTINUED)

Where power loss is per four contacts and power input is horsepower per contact.

APPENDIX NN

$J_7 \,/\, J_4$

LOSS FACTOR (REF. 1)

$$J_7/J_4 = \frac{J_6 \cdot J_3 + J_4 \cdot J_1}{J_4}$$

RPM_o ↓ \ RPM_n →	28,000	21,000	14,000
5000	8.78	9.32	10.22
4000	8.44	9.09	9.70
3000	8.21	8.44	9.23
1500	7.71	7.78	8.21
850	7.47	7.60	7.69

Table 28:

APPENDIX OO

J_1, DIMENSIONLESS SLIP FACTOR (Ref.1)

$$J_1 = \left(\frac{3\pi}{8}\right)\left(\frac{M}{\mu}\right)\left(\frac{\Delta u}{u}\right)\sqrt{K}$$

$$J_1 = \left(\frac{3\pi}{8}\right)(220)(.016)\sqrt{K} = 4.15\sqrt{K}$$

RPM_o ↓ \ RPM_s →	9600	7200	4800
5000	8.82	9.26	10.05
4000	8.54	8.92	9.59
3000	8.21	8.54	9.09
1500	7.68	7.86	8.22
850	7.42	7.52	7.75

Table 29:

APPENDIX PP

J_3

DIMENSIONLESS SPIN FACTOR (REF. 1)

$$J_3 = \left(\frac{3\pi}{8}\right)\left(\frac{M}{\mu}\right)\left(\frac{W_s}{U}\right)(a \cdot b)\sqrt{K}$$

$$\left(\frac{3\pi}{8}\right)\ (220)\ \left(\frac{W_s}{U}\right)(a \cdot b)\sqrt{K}$$

$J_3 = 4.366\ W_s \cdot b$ (AT 28,000 RPM_n)

$J_3 = 3.275\ W_s \cdot b$ (AT 21,000 RPM_n)

$J_3 = 2.183\ W_s \cdot b$ (AT 14,000 RPM_n)

(b is in meters)

7.5 KW (10 HP)			
RPM_o ↓ \ RPM_n ⟶	28,000	21,000	14,000
5000	3.09	2.24	1.42
4000	2.73	1.99	1.32
3000	2.41	1.69	1.09
1500	1.97	1.30	.76
850	1.89	1.18	.64
15 KW (20 HP)			
5000	3.90	2.87	1.96
4000	3.43	2.51	1.67
3000	3.02	2.15	1.37
1500	2.49	1.64	.95
850	2.38	1.49	.81
30 KW (40 HP)			
5000	4.91	3.62	2.48
4000	4.33	3.16	2.10
3000	3.82	2.68	1.73

Table 30:

J_3

DIMENSIONLESS SPIN FACTOR (REF. 1) (CONTINUED)

1500	3.13	2.07	1.20
850	3.00	1.88	1.02
52 KW (70 HP)			
5000	5.92	4.37	2.98
4000	5.23	3.81	2.53
3000	4.60	3.23	2.08
1500	3.78	2.49	1.45
850	3.61 (3.30)	2.26 (2.06)	1.22 (1.12)
75 KW (100 HP)			
5000	6.65	4.92	3.36
4000	5.88	4.28	2.85
3000	5.18	3.65	2.34
1500	4.25 (4.16)	2.80 (2.75)	1.63 (1.60)
850	4.07 (3.30)	2.55 (2.06)	1.38 (1.12)

( ) NOTE: Values at wheelslip torque limit values.

Table 30: (Continued)

APPENDIX QQ

RPM_o \ RPM_n →	28,000	21,000	14,000
	$g/(W_N)^{1/3}$ (REF. 6)*		
5000	.00352	.00336	.00310
4000	.00363	.00349	.00325
3000	.00377	.00363	.00342
1500	.00401	.00393	.00377
850	.00414	.00408	.00398
	$R_B - 1 = D_c/(2 \cos 9.24^\circ)$ in.*		
5000	.629	.518	.382
4000	.722	.603	.453
3000	.849	.722	.557
1500	1.148	1.027	.849
850	1.356	1.257	1.096
	$\cos \gamma$ *		
5000	.820	.843	.877
4000	.801	.825	.859
3000	.779	.801	.835
1500	.734	.751	.779
850	.707	.719	.741
	μ *		
5000	2.402	2.549	2.832
4000	2.297	2.432	2.670
3000	2.191	2.297	2.494
1500	2.013	2.076	2.191
850	1.925	1.962	2.038

Table 31:

APPENDIX QQ

$g/(W_N)^{1/3}$ (REF. 6)* (CONTINUED)

ν *

RPM_o ↓ \ RPM_n →	28,000	21,000	14,000
5000	.530	.512	.483
4000	.544	.526	.499
3000	.559	.544	.519
1500	.587	.577	.559
850	.604	.597	.583

Table 31:(Continued)

APPENDIX RR

$$\underline{RPM_s = \text{Flywheel } RPM_n/2.9166}$$

Flywheel RPM_n ⟶	28,000	21,000	14,000
RPM_s ⟶	9,600	7,200	4,800

Table 32:

APPENDIX SS

BEARING AND GEAR

COMPUTER DATA.

```
BALL AND ROLLER BEARING DISPLACEMENT, LOAD AND LIFE DETERMINATION
 NASA CVT STUDY INPUT PLANET BEARINGS
  7.33 HP AT 29500 RPM
* INPUT DATA FOR SYSTEM NO.  1
 BEARING    BEARING    NUMBER OF   BALL/ROLL     PITCH       RACE CURVATURES        CONTACT     INTERNAL    DISTANCE
              TYPE    BALLS/ROLLS     DIA.        DIA.       OUTER       INNER       ANGLE      CLEARANCE   TO ORIGIN
   NO.
   1         ROLLER    1.1000E 01  1.0000E-01  5.0000E-01  0.0         0.0         0.0         3.0000E-04  0.0
   2         BALL      7.0000E 00  1.0000E-01  1.4200E 00  5.2000E-01  5.2000E-01  1.0000E 01 -2.0000E-04 -2.0000E 00
                                                BALL/ROLL   MODULUS OF ELASTICITY      POISSON'S RATIO       FRICTION
 BEARING    BEARING    EFFECTIVE     TOTAL       DENSITY   BALLS/ROLLS    RACES     BALLS/ROLLS   RACES     COEFFICIENT
   NO.        TYPE    ROLL LENGTH ROLL LENGTH
   1         ROLLER    3.4500E-01  3.7500E-01  2.8300E-01  2.9000E 07  2.9000E 07  2.5000E-01  2.5000E-01  0.0
   2         BALL      0.0         0.0         2.8300E-01  2.9000E 07  2.9000E 07  2.5000E-01  2.5000E-01  7.5000E-02
                                      SHIM THICKNESS          - - - INITIAL DISPLACEMENTS AT BEARING CENTER - - -
 BEARING    BEARING      PHASE       OUTER       INNER      ALONG X     ALONG Y     ALONG Z     ABOUT Y     ABOUT Z
   NO.        TYPE       FACTOR
   1         ROLLER    0.0         0.0         0.0         0.0         0.0         0.0         0.0         0.0
   2         BALL      0.0         0.0         0.0         0.0         0.0         0.0         0.0         0.0
                                               RADIAL SPRING RATES       FATIGUE CONSTANT         VALUE OF LAMBDA
 BEARING    BEARING     PRELOAD      AXIAL      ALONG Y     ALONG Z      OUTER       INNER       OUTER       INNER
   NO.        TYPE    SPRING RATE   PRELOAD
   1         ROLLER    0.0         0.0         0.0         0.0         4.9500E 04  4.9500E 04  6.1000E-01  6.1000E-01
   2         BALL      0.0         0.0         1.0000E 00  1.0000E 00  7.1400E 03  7.1400E 03  0.0         0.0
* INPUT DATA FOR LOAD CASE NO.  1, SYSTEM NO.  1
  LOAD      - - - - - EXTERNAL LOADS APPLIED TO SHAFT - - - - -        DISTANCE TO    RPM OF      RPM OF
   NO.      ALONG X     ALONG Y     ALONG Z     ABOUT Y     ABOUT Z      ORIGIN       OUTER       INNER
   1      -6.0000E 01  1.1100E 02  0.0         0.0         0.0         0.0          2.9500E 04  0.0
  OUTER RACES ROTATE WITH RESPECT TO LOAD
  INNER RACES FIXED WITH RESPECT TO LOAD
  THIS LOAD CASE IS EFFECTIVE FOR 100.0000 PERCENT OF TIME
* OUTPUT DATA FOR LOAD CASE NO.  1, SYSTEM NO.  1
 BEARING      - - - - - REACTIONS OF BEARINGS ON SHAFT - - - - -        FRICTION   FATIGUE LIFE (90 PERCENT SURVIVAL)
   NO.      ALONG X     ALONG Y     ALONG Z     ABOUT Y     ABOUT Z      TORQUE      OUTER       INNER      BEARING
   1       0.0        -1.1103E 02 -2.1240E-02  0.0         0.0         0.0         3.9426E 04  4.3789E 03  4.0762E 03
   2       5.9999E 01 -8.4975E-04  5.2071E-04  1.2875E-04 -2.4128E-04  1.1774E-01  5.2985E 01  2.0001E 01  1.5382E 01
 BEARING      DISPLACEMENTS OF INNER RACE WITH RESPECT TO OUTER      DISPLACEMENTS OF FLOATING OUTER RACE
   NO.      ALONG X     ALONG Y     ALONG Z     ABOUT Y     ABOUT Z     ALONG X     ALONG Y     ALONG Z
   1       0.0        -2.4825E-04  8.0752E-06  0.0         0.0         0.0         0.0         0.0
   2       8.1323E-04  [illegible]-09 -1.0643E-09  1.1825E-12 -2.0485E-09  0.0        -2.4823E-04  8.1468E-06
 BEARING     - - - - - - - - - - PARTIAL NON-LINEAR SPRING RATES OF INDIVIDUAL BEARINGS - - - - - - - - - -
   NO.      DFX/DX      DFX/DY      DFX/DZ      DFX/DALY    DFX/DALZ    DFY/DY      DFY/DZ      DFY/DALY    DFY/DALZ
   1       0.0         0.0         0.0         0.0         0.0         1.5095E 06  1.4600E 05  0.0         0.0
   2       1.3644E 05 -5.2734E-01  8.2031E-02  6.6406E-02 -2.6172E-01  3.6649E 05 -1.6797E-01 -4.2969E-02  9.2185E 04
 BEARING      - - - - - PARTIAL NON-LINEAR SPRING RATES (CONTINUED) - - - - -
   NO.      DFZ/DZ      DFZ/DALY    DFZ/DALZ    DMY/DALY    DMY/DALZ    DMZ/DALZ
   1       3.0083E 05  0.0         0.0         0.0         0.0         0.0
   2       3.6649E 05  9.2185E 04 -3.5156E-02  3.4584E 04 -1.5625E-02  3.4584E 04
```


PRECEDING PAGE BLANK NOT FILMED

DISPLACEMENTS OF REFERENCE LINE AT ORIGIN

ALONG X	ALONG Y	ALONG Z	ABOUT Y	ABOUT Z
8.1323E-04	-2.4824E-04	8.1458E-06	1.3855E-11	-2.3665E-09

* OUTPUT DATA FOR BEARING NO. 1, LOAD CASE NO. 1, SYSTEM NO. 1

ELEMENT NO.	ELEMENT AZIMUTH	CONTACT FORCE OUTER	CONTACT FORCE INNER	OPERATING CONTACT ANGLE OUTER	OPERATING CONTACT ANGLE INNER	CONTACT AREA LENGTH OUTER	CONTACT AREA LENGTH INNER	CONTACT AREA WIDTH OUTER	CONTACT AREA WIDTH INNER
8	2.2909E 02	1.9084E 01	1.7231E 01	0.0	0.0	3.6500E-01	3.6500E-01	1.0164E-03	7.8855E-04
9	2.6182E 02	5.8208E 01	5.6335E 01	0.0	0.0	3.6500E-01	3.6500E-01	1.7750E-03	1.4261E-03
10	2.9455E 02	4.8272E 01	4.6419E 01	0.0	0.0	3.6500E-01	3.6500E-01	1.6164E-03	1.2942E-03
OTHERS		1.8529E 00	0.0	0.0	0.0	3.6500E-01	0.0	3.1669E-04	0.0

ELEMENT NO.	CENTRIFUGAL FORCE	GYROSCOPIC MOMENT	ORBITAL VELOCITY	ROTATIONAL VELOCITY	ROLLING VELOCITY OUTER	ROLLING VELOCITY INNER	CONTROLLING RACE	MEAN COMPRESSIVE STRESS OUTER	MEAN COMPRESSIVE STRESS INNER
8	1.8528E 00	0.0	1.7700E 04	7.0805E 04	5.9005E 04	-8.8505E 04		5.1443E 04	5.9868E 04
9	1.8530E 00	0.0	1.7699E 04	7.0815E 04	5.9014E 04	-8.8514E 04		8.9843E 04	1.0827E 05
10	1.8529E 00	0.0	1.7700E 04	7.0812E 04	5.9012E 04	-8.8512E 04		8.1816E 04	9.8262E 04
OTHERS	1.8529E 00	0.0	1.7700E 04	7.0809E 04	5.9008E 04	0.0		1.6029E 04	0.0

ELEMENT NO.	MAX. ORTHOGONAL SHEAR OUTER	MAX. ORTHOGONAL SHEAR INNER	MAX. ORTH. SHEAR DEPTH OUTER	MAX. ORTH. SHEAR DEPTH INNER	MAXIMUM SHEAR STRESS OUTER	MAXIMUM SHEAR STRESS INNER	DEPTH TO MAXIMUM SHEAR OUTER	DEPTH TO MAXIMUM SHEAR INNER
8	1.6375E 04	1.9057E 04	2.5409E-04	1.9714E-04	1.7668E 04	2.2889E 04	3.9951E-04	3.0996E-04
9	2.8598E 04	3.4463E 04	4.4376E-04	3.5651E-04	3.4350E 04	4.1395E 04	6.9772E-04	5.6055E-04
10	2.6043E 04	3.1278E 04	4.0411E-04	3.2356E-04	3.1281E 04	3.7569E 04	6.3539E-04	5.0874E-04
OTHERS	5.1021E 03	0.0	7.9170E-05	0.0	6.1283E 03	0.0	1.2448E-04	0.0

* OUTPUT DATA FOR BEARING NO. 2, LOAD CASE NO. 1, SYSTEM NO. 1

ELEMENT NO.	ELEMENT AZIMUTH	CONTACT FORCE OUTER	CONTACT FORCE INNER	OPERATING CONTACT ANGLE OUTER	OPERATING CONTACT ANGLE INNER	CONTACT AREA LENGTH OUTER	CONTACT AREA LENGTH INNER	CONTACT AREA WIDTH OUTER	CONTACT AREA WIDTH INNER
1	0.0	2.4979E 01	2.4287E 01	2.0274E 01	2.0667E 01	3.4089E-02	3.4122E-02	4.3566E-03	4.0231E-03
2	5.1429E 01	2.4979E 01	2.4284E 01	2.0274E 01	2.0667E 01	3.4089E-02	3.4121E-02	4.3565E-03	4.0230E-03
3	1.0286E 02	2.4979E 01	2.4284E 01	2.0274E 01	2.0667E 01	3.4089E-02	3.4121E-02	4.3565E-03	4.0230E-03
4	1.5429E 02	2.4979E 01	2.4284E 01	2.0274E [illegible]	2.0667E 01	3.4089E-02	3.4121E-02	4.3565E-03	4.0230E-03
5	2.0571E 02	2.4979E 01	2.4284E 01	2.0274E 01	2.0667E 01	3.4089E-02	3.4121E-02	4.3565E-03	4.0230E-03
6	2.5714E 02	2.4979E 01	2.4267E 01	2.0274E 01	2.0667E 01	3.4089E-02	3.4122E-02	4.3566E-03	4.0231E-03
7	3.0857E 02	2.4979E 01	2.4287E 01	2.0274E 01	2.0667E 01	3.4089E-02	3.4122E-02	4.3566E-03	4.0231E-03

ELEMENT NO.	CENTRIFUGAL FORCE	GYROSCOPIC MOMENT	ORBITAL VELOCITY	ROTATIONAL VELOCITY	ROLLING VELOCITY OUTER	ROLLING VELOCITY INNER	CONTROLLING RACE	MEAN COMPRESSIVE STRESS OUTER	MEAN COMPRESSIVE STRESS INNER
1	7.3806E-01	4.4827E-03	1.5722E 04	2.0865E 05	1.9567E 05	-2.2326E 05	OUTER	2.1415E 05	2.2526E 05
2	7.3806E-01	4.4827E-03	1.5722E 04	2.0865E 05	1.9567E 05	-2.2326E 05	OUTER	2.1415E 05	2.2526E 05
3	7.3806E-01	4.4827E-03	1.5722E 04	2.0865E 05	1.9567E 05	-2.2326E 05	OUTER	2.1415E 05	2.2526E 05
4	7.3806E-01	4.4827E-03	1.5722E 04	2.0865E 05	1.9567E 05	-2.2326E 05	OUTER	2.1415E 05	2.2526E 05
5	7.3806E-01	4.4827E-03	1.5722E 04	2.0865E 05	1.9567E 05	-2.2326E 05	OUTER	2.1415E 05	2.2526E 05
6	7.3806E-01	4.4827E-03	1.5722E 04	2.0865E 05	1.9567E 05	-2.2326E 05	OUTER	2.1415E 05	2.2526E 05
7	7.3806E-01	4.4827E-03	1.5722E 04	2.0865E 05	1.9567E 05	-2.2326E 05	OUTER	2.1415E 05	2.2526E 05

ELEMENT NO.	BALL CENTER COORDINATES X	BALL CENTER COORDINATES Z	SPINNING VELOCITY	SPINNING TORQUE OUTER	SPINNING TORQUE INNER	GYRO SLIP COEFFICIENT	SV VALUE	PATH HEIGHT/BALL DIA. OUTER	PATH HEIGHT/BALL DIA. INNER
1	3.9988E-04	5.3036E-05	-1.1751E 04	1.2264E-02	1.1900E-02	3.5892E-03	2.9558E 05	1.1823E-01	1.2061E-01
2	[illegible]	[illegible]	[illegible]	[illegible]	[illegible]	[illegible]	[illegible]	[illegible]	[illegible]

2	3.9900E-04	5.3035E-05	-1.1751E 04	1.2263E-02	1.1899E-02	3.5892E-03	2.9557E 05	1.1823E-01	1.2061E-01
3	3.9900E-04	5.3035E-05	-1.1751E 04	1.2263E-02	1.1899E-02	3.5892E-03	2.9558E 05	1.1823E-01	1.2061E-01
4	3.9900E-04	5.3035E-05	-1.1751E 04	1.2263E-02	1.1899E-02	3.5892E-03	2.9558E 05	1.1823E-01	1.2061E-01
5	3.9900E-04	5.3035E-05	-1.1751E 04	1.2263E-02	1.1899E-02	3.5892E-03	2.9558E 05	1.1823E-01	1.2061E-01
6	3.9900E-04	5.3037E-05	-1.1751E 04	1.2264E-02	1.1900E-02	3.5892E-03	2.9558E 05	1.1823E-01	1.2061E-01
7	3.9900E-04	5.3036E-05	-1.1751E 04	1.2264E-02	1.1900E-02	3.5892E-03	2.9558E 05	1.1823E-01	1.2061E-01

ELEMENT NO.	UPPER EDGE OF PATH OUTER	UPPER EDGE OF PATH INNER	L.E. EDGE OF PATH [illegible]	L.E. EDGE OF PATH INNER	GOTHIC ARCH CLEARANCE OUTER	GOTHIC ARCH CLEARANCE INNER	SPIN/ROLL RATIO	ROLLING TORQUE OUTER	ROLLING TORQUE INNER
1	3.9400E 01	3.9820E 01	1.1402E 00	1.5134E 00	0.0	0.0	5.2633E-02	8.6277E-04	8.4044E-04
2	3.9400E 01	3.9819E 01	1.1403E 00	1.5137E 00	0.0	0.0	5.2633E-02	8.6274E-04	8.4041E-04
3	3.9400E 01	3.9819E 01	1.1403E 00	1.5137E 00	0.0	0.0	5.2633E-02	8.6274E-04	8.4041E-04
4	3.9400E 01	3.9819E 01	1.1403E 00	1.5137E 00	0.0	0.0	5.2633E-02	8.6274E-04	8.4041E-04
5	3.9400E 01	3.9819E 01	1.1403E 00	1.5137E 00	0.0	0.0	5.2633E-02	8.6275E-04	8.4041E-04
6	3.9400E 01	3.9820E 01	1.1402E 00	1.5135E 00	0.0	0.0	5.2633E-02	8.6277E-04	8.4045E-04
7	3.9400E 01	3.9820E 01	1.1402E 00	1.5135E 00	0.0	0.0	5.2633E-02	8.6277E-04	8.4044E-04

ELEMENT NO.	MAX. ORTHOGONAL SHEAR OUTER	MAX. ORTHOGONAL SHEAR INNER	MAX. ORTH. SHEAR DEPTH OUTER	MAX. ORTH. SHEAR DEPTH INNER	MAXIMUM SHEAR STRESS OUTER	MAXIMUM SHEAR STRESS INNER	DEPTH TO MAXIMUM SHEAR OUTER	DEPTH TO MAXIMUM SHEAR INNER
1	7.9985E 04	8.4184E 04	1.0762E-03	9.9557E-04	-1.0319E 05	-1.0817E 05	1.6560E-03	1.5355E-03
2	7.9985E 04	8.4184E 04	1.0762E-03	9.9556E-04	-1.0319E 05	-1.0817E 05	1.6560E-03	1.5355E-03
3	7.9985E 04	8.4183E 04	1.0762E-03	9.9556E-04	-1.0319E 05	-1.0817E 05	1.6560E-03	1.5355E-03
4	7.9985E 04	8.4184E 04	1.0762E-03	9.9556E-04	-1.0319E 05	-1.0817E 05	1.6560E-03	1.5355E-03
5	7.9985E 04	8.4184E 04	1.0762E-03	9.9556E-04	-1.0319E 05	-1.0817E 05	1.6560E-03	1.5355E-03
6	7.9985E 04	8.4184E 04	1.0762E-03	9.9557E-04	-1.0319E 05	-1.0817E 05	1.6560E-03	1.5355E-03
7	7.9985E 04	8.4184E 04	1.0762E-03	9.9557E-04	-1.0319E 05	-1.0817E 05	1.6560E-03	1.5355E-03

ELEMENT NO.	VECTOR ATTITUDE
1	1.8963E 01
2	1.8963E 01
3	1.8963E 01
4	1.8963E 01
5	1.8963E 01
6	1.8963E 01
7	1.8963E 01

BALL AND ROLLER BEARING DISPLACEMENT, LOAD AND LIFE DETERMINATION
NASA CVT STUDY HELICAL-BEVEL CLUSTER . 11-20-79
HEAD CONDITIONS AT 10.00 HP 14320 RPM

* INPUT DATA FOR SYSTEM NO. 1

BEARING NO.	BEARING TYPE	NUMBER OF BALLS/ROLLS	BALL/ROLL DIA.	PITCH DIA.	RACE CURVATURES OUTER	RACE CURVATURES INNER	CONTACT ANGLE	INTERNAL CLEARANCE	DISTANCE TO ORIGIN
1	ROLLER	8.0000E 00	1.3750E-01	6.8000E-01	0.0	0.0	0.0	3.0000E-04	5.0000E-01
2	ROLLER	8.0000E 00	1.3750E-01	6.8000E-01	0.0	0.0	0.0	3.0000E-04	-5.0000E-01
3	BALL	7.0000E 00	1.0000E-01	1.4200E 00	5.2000E-01	5.2000E-01	1.0000E 01	-2.0000E-04	-2.0000E 00

BEARING NO.	BEARING TYPE	EFFECTIVE ROLL LENGTH	TOTAL ROLL LENGTH	BALL/ROLL DENSITY	MODULUS OF ELASTICITY BALLS/ROLLS	MODULUS OF ELASTICITY RACES	POISSON'S RATIO BALLS/ROLLS	POISSON'S RATIO RACES	FRICTION COEFFICIENT
1	ROLLER	1.3750E-01	1.7720E-01	2.8300E-01	2.9000E 07	2.9000E 07	2.5000E-01	2.5000E-01	0.0
2	ROLLER	1.3750E-01	1.7720E-01	2.8300E-01	2.9000E 07	2.9000E 07	2.5000E-01	2.5000E-01	0.0
3	BALL	0.0	0.0	2.8300E-01	2.9000E 07	2.9000E 07	2.5000E-01	2.5000E-01	7.5000E-02

BEARING NO.	BEARING TYPE	PHASE FACTOR	SHIM THICKNESS OUTER	SHIM THICKNESS INNER	- - - INITIAL DISPLACEMENTS AT BEARING CENTER - - - ALONG X	ALONG Y	ALONG Z	ABOUT Y	ABOUT Z
1	ROLLER	0.0	0.0	0.0	0.0	0.0	0.0	0.0	0.0
2	ROLLER	0.0	0.0	0.0	0.0	0.0	0.0	0.0	0.0
3	BALL	0.0	0.0	0.0	0.0	0.0	0.0	0.0	0.0

BEARING NO.	BEARING TYPE	PRELOAD SPRING RATE	AXIAL PRELOAD	RADIAL SPRING RATES ALONG Y	RADIAL SPRING RATES ALONG Z	FATIGUE CONSTANT OUTER	FATIGUE CONSTANT INNER	VALUE OF LAMBDA OUTER	VALUE OF LAMBDA INNER
1	ROLLER	0.0	0.0	0.0	0.0	4.9500E 04	4.9500E 04	6.1000E-01	6.1000E-01
2	ROLLER	0.0	0.0	0.0	0.0	4.9500E 04	4.9500E 04	6.1000E-01	6.1000E-01
3	BALL	0.0	0.0	1.0000E 00	1.0000E 00	7.1400E 03	7.1400E 03	0.0	0.0

* INPUT DATA FOR LOAD CASE NO. 1, SYSTEM NO. 1

LOAD NO.	- - - - - EXTERNAL LOADS APPLIED TO SHAFT - - - - - ALONG X	ALONG Y	ALONG Z	ABOUT Y	ABOUT Z	DISTANCE TO ORIGIN	RPM OF OUTER	RPM OF INNER
1	-6.4700E 01	1.0910E 02	0.0	4.1400E 01	0.0	0.0	0.0	1.6369E 04

OUTER RACES ROTATE WITH RESPECT TO LOAD
INNER RACES FIXED WITH RESPECT TO LOAD
THIS LOAD CASE IS EFFECTIVE FOR 100.0000-PERCENT OF TIME

* OUTPUT DATA FOR LOAD CASE NO. 1, SYSTEM NO. 1

BEARING NO.	- - - - - REACTIONS OF BEARINGS ON SHAFT - - - - - ALONG X	ALONG Y	ALONG Z	ABOUT Y	ABOUT Z	FRICTION TORQUE	FATIGUE LIFE (90 PERCENT SURVIVAL) OUTER	INNER	BEARING
1	0.0	-5.4698E 01	-3.7420E 01	0.0	0.0	0.0	2.0720E 05	1.4452E 04	1.3839E 04
2	0.0	-5.4272E 01	3.7695E 01	0.0	0.0	0.0	2.0914E 05	1.4573E 04	1.39[illegible]E 04
3	6.4600E 01	-5.0334E-04	1.2331E-03	-4.3033E 00	-1.4630E-02	1.2734E-01	8.3279E 01	2.9314E 01	2.[illegible]935E 01

BEARING NO.	DISPLACEMENTS OF INNER RACE WITH RESPECT TO OUTER ALONG X	ALONG Y	ALONG Z	ABOUT Y	ABOUT Z	DISPLACEMENTS OF FLOATING OUTER RACE ALONG X	ALONG Y	ALONG Z
1	0.0	-2.2934E-04	-1.7505E-04	0.0	0.0	0.0	0.0	0.0
2	0.0	-2.2817E-04	1.7605E-04	0.0	0.0	0.0	0.0	0.0
3	8.3510E-04	2.4182E-07	9.9172E-05	-3.5110E-04	-1.1842E-06	0.0	-2.2704E-04	6.1285E-04

BEARING NO.	- - - PARTIAL NON-LINEAR SPRING RATES OF INDIVIDUAL BEARINGS - - - DFX/DX	DFX/DY	DFX/DZ	DFX/DALY	DFX/DALZ	DFY/DY	DFY/DZ	DFY/DALY	DFY/DALZ
1	0.0	0.0	0.0	0.0	0.0	5.0644E 05	1.7473E 05	0.0	0.0
2	0.0	0.0	0.0	0.0	0.0	5.0595E 05	-1.7422E 05	0.0	0.0

3 [illegible]

- - - - - PARTIAL NON-LINEAR SPRING RATES (CONTINUED) - - - - -

BEARING NO.	DFZ/DZ	DFZ/DALY	DFZ/DALZ	DMY/DALY	DMY/DALZ	DMZ/DALZ
1	4.7404E 05	0.0	0.0	0.0	0.0	0.0
2	4.7503E 05	0.0	0.0	0.0	0.0	0.0
3	3.7273E 05	9.4409E 04	6.7969E-01	3.4871E 04	2.1602E 00	3.6221E 04

DISPLACEMENTS OF REFERENCE LINE AT ORIGIN

ALONG X	ALONG Y	ALONG Z	ABOUT Y	ABOUT Z
8.3531E-04	-2.2004E-04	4.3159E-07	-3.3079E-04	-1.0314E-06

* OUTPUT DATA FOR BEARING NO. 1, LOAD CASE NO. 1, SYSTEM NO. 1

ELEMENT NO.	ELEMENT AZIMUTH	CONTACT FORCE OUTER	CONTACT FORCE INNER	OPERATING CONTACT ANGLE OUTER	OPERATING CONTACT ANGLE INNER	CONTACT AREA LENGTH OUTER	CONTACT AREA LENGTH INNER	CONTACT AREA WIDTH OUTER	CONTACT AREA WIDTH INNER
5	1.8000E 02	7.1446E 00	6.7710E 00	0.0	0.0	1.5750E-01	1.5750E-01	1.2036E-03	9.2557E-04
6	2.2500E 02	4.3720E 01	4.3335E 01	0.0	0.0	1.5750E-01	1.5750E-01	2.9777E-03	2.3420E-03
7	2.7000E 02	2.4019E 01	2.4001E 01	0.0	0.0	1.5750E-01	1.5750E-01	2.2250E-03	1.7440E-03
OTHERS		3.7290E-01	0.0	0.0	0.0	1.5750E-01	0.0	2.7498E-04	0.0

ELEMENT NO.	CENTRIFUGAL FORCE	GYROSCOPIC MOMENT	ORBITAL VELOCITY	ROTATIONAL VELOCITY	ROLLING VELOCITY OUTER	ROLLING VELOCITY INNER	CONTROLLING RACE	MEAN COMPRESSIVE STRESS OUTER	MEAN COMPRESSIVE STRESS INNER
5	3.7288E-01	0.0	6.2889E 03	-3.3442E 04	-2.7153E 04	4.3522E 04		3.7688E 04	4.4453E 04
6	3.7297E-01	0.0	6.2892E 03	-3.3440E 04	-2.7159E 04	4.3528E 04		9.3237E 04	1.1754E 05
7	3.7292E-01	0.0	6.2890E 03	-3.3445E 04	-2.7156E 04	4.3525E 04		6.9467E 04	8.7526E 04
OTHERS	3.7290E-01	0.0	6.2890E 03	-3.3443E 04	-2.7154E 04	0.0		8.6101E 03	0.0

ELEMENT NO.	MAX. ORTHOGONAL SHEAR OUTER	MAX. ORTHOGONAL SHEAR INNER	MAX. ORTH. SHEAR DEPTH OUTER	MAX. ORTH. SHEAR DEPTH INNER	MAXIMUM SHEAR STRESS OUTER	MAXIMUM SHEAR STRESS INNER	DEPTH TO MAXIMUM SHEAR OUTER	DEPTH TO MAXIMUM SHEAR INNER
5	1.1996E 04	1.4786E 04	3.8091E-04	2.3139E-04	1.4409E 04	1.7760E 04	4.7312E-04	3.6382E-04
6	2.9670E 04	3.7413E 04	7.4444E-04	5.8549E-04	3.5640E 04	4.4939E 04	1.1705E-03	9.2057E-04
7	2.2176E 04	2.7860E 04	5.5625E-04	4.3599E-04	2.6634E 04	3.3464E 04	8.7459E-04	6.8551E-04
OTHERS	2.7405E 03	0.0	6.8742E-05	0.0	3.2917E 03	0.0	1.0808E-04	0.0

* OUTPUT DATA FOR BEARING NO. 2, LOAD CASE NO. 1, SYSTEM NO. 1

ELEMENT NO.	ELEMENT AZIMUTH	CONTACT FORCE OUTER	CONTACT FORCE INNER	OPERATING CONTACT ANGLE OUTER	OPERATING CONTACT ANGLE INNER	CONTACT AREA LENGTH OUTER	CONTACT AREA LENGTH INNER	CONTACT AREA WIDTH OUTER	CONTACT AREA WIDTH INNER
1	0.0	7.4430E 00	7.0710E 00	0.0	0.0	1.5750E-01	1.5750E-01	1.2284E-03	9.4580E-04
7	2.7000E 02	2.4021E 01	2.3640E 01	0.0	0.0	1.5750E-01	1.5750E-01	2.2070E-03	1.7297E-03
8	3.1500E 02	4.3402E 01	4.3309E 01	0.0	0.0	1.5750E-01	1.5750E-01	2.9762E-03	2.3407E-03
OTHERS		3.7290E-01	0.0	0.0	0.0	1.5750E-01	0.0	2.7498E-04	0.0

ELEMENT NO.	CENTRIFUGAL FORCE	GYROSCOPIC MOMENT	ORBITAL VELOCITY	ROTATIONAL VELOCITY	ROLLING VELOCITY OUTER	ROLLING VELOCITY INNER	CONTROLLING RACE	MEAN COMPRESSIVE STRESS OUTER	MEAN COMPRESSIVE STRESS INNER
1	3.7288E-01	0.0	6.2889E 03	-3.3442E 04	-2.7153E 04	4.3522E 04		3.8469E 04	4.7468E 04
7	3.7292E-01	0.0	6.2890E 03	-3.3445E 04	-2.7156E 04	4.3525E 04		6.9105E 04	8.6808E 04
8	3.7297E-01	0.0	6.2892E 03	-3.3448E 04	-2.7159E 04	4.3528E 04		9.3188E 04	1.1748E 05
OTHERS	3.7290E-01	0.0	6.2890E 03	-3.3443E 04	-2.7154E 04	0.0		8.6101E 03	0.0

ELEMENT NO.	MAX. ORTHOGONAL SHEAR OUTER	MAX. ORTHOGONAL SHEAR INNER	MAX. ORTH. SHEAR DEPTH OUTER	MAX. ORTH. SHEAR DEPTH INNER	MAXIMUM SHEAR STRESS OUTER	MAXIMUM SHEAR STRESS INNER	DEPTH TO MAXIMUM SHEAR OUTER	DEPTH TO MAXIMUM SHEAR INNER
1	1.2245E 04	1.5109E 04	3.8715E-04	2.3645E-04	1.4708E 04	1.8148E 04	4.8293E-04	3.7177E-04
7	2.1997E 04	2.7633E 04	5.5176E-04	4.3241E-04	2.6421E 04	3.3189E 04	8.6753E-04	6.7989E-04
8	2.9663E 04	3.7394E 04	7.4405E-04	5.8518E-04	3.5629E 04	4.4915E 04	1.1699E-03	9.2008E-04

OTHERS	2.7405E 03	0.0	6.8742E-05	0.0	3.2917E 03	0.0	1.0000E-04	0.0

* OUTPUT DATA FOR BEARING NO. 3, LOAD CASE NO. 1, SYSTEM NO. 1

ELEMENT NO.	ELEMENT AZIMUTH	CONTACT FORCE OUTER	CONTACT FORCE INNER	OPERATING CONTACT ANGLE OUTER	OPERATING CONTACT ANGLE INNER	CONTACT AREA LENGTH OUTER	CONTACT AREA LENGTH INNER	CONTACT AREA WIDTH OUTER	CONTACT AREA WIDTH INNER
1	0.0	2.4001E 01	2.5034E 01	1.7142E 01	1.7302E 01	3.4545E-02	3.4835E-02	4.4179E-03	4.1036E-03
2	5.1429E 01	2.3631E 01	2.3466E 01	1.8450E 01	1.8624E 01	3.4381E-02	3.4667E-02	4.3958E-03	4.0852E-03
3	1.0286E 02	2.3808E 01	2.5645E 01	2.1414E 01	2.1614E 01	3.4463E-02	3.4745E-02	4.4031E-03	4.0977E-03
4	1.5429E 02	2.4977E 01	2.6035E 01	2.3795E 01	2.4009E 01	3.4979E-02	3.5262E-02	4.4641E-03	4.1618E-03
5	2.0571E 02	2.4984E 01	2.6822E 01	2.3805E 01	2.4019E 01	3.4982E-02	3.5265E-02	4.4645E-03	4.1621E-03
6	2.5714E 02	2.3815E 01	2.5632E 01	2.1437E 01	2.1637E 01	3.4466E-02	3.4748E-02	4.4035E-03	4.0981E-03
7	3.0857E 02	2.5620E 01	2.5463E 01	1.8449E 01	1.8643E 01	3.4380E-02	3.4666E-02	4.3956E-03	4.0851E-03

ELEMENT NO.	CENTRIFUGAL FORCE	GYROSCOPIC MOMENT	ORBITAL VELOCITY	ROTATIONAL VELOCITY	ROLLING VELOCITY OUTER	ROLLING VELOCITY INNER	CONTROLLING RACE	MEAN COMPRESSIVE STRESS OUTER	MEAN COMPRESSIVE STRESS INNER
1	1.7404E-01	-1.0260E-03	7.6343E 03	-1.1574E 05	-1.0842E 05	1.2405E 05	OUTER	2.1692E 05	2.3010E 05
2	1.7423E-01	-1.1028E-03	7.6384E 03	-1.1575E 05	-1.0848E 05	1.2399E 05	OUTER	2.1593E 05	2.2894E 05
3	1.7469E-01	-1.2754E-03	7.6487E 03	-1.1577E 05	-1.0862E 05	1.2384E 05	OUTER	2.1654E 05	2.2934E 05
4	1.7511E-01	-1.4130E-03	7.6500E 03	-1.1579E 05	-1.0875E 05	1.2370E 05	OUTER	2.1987E 05	2.3263E 05
5	1.7511E-01	-1.4134E-03	7.6501E 03	-1.1579E 05	-1.0875E 05	1.2370E 05	OUTER	2.1989E 05	2.3267E 05
6	1.7469E-01	-1.2769E-03	7.6480E 03	-1.1577E 05	-1.0862E 05	1.2383E 05	OUTER	2.1656E 05	2.2936E 05
7	1.7423E-01	-1.1039E-03	7.6384E 03	-1.1575E 05	-1.0848E 05	1.2399E 05	OUTER	2.1593E 05	2.2893E 05

ELEMENT NO.	BALL CENTER COORDINATES X	BALL CENTER COORDINATES Z	SPINNING VELOCITY	SPINNING TORQUE OUTER	SPINNING TORQUE INNER	GYRO SLIP COEFFICIENT	SV VALUE	PATH HEIGHT/BALL DIA. OUTER	PATH HEIGHT/BALL DIA. INNER
1	2.8909E-04	7.4060E-05	5.1696E 03	1.2936E-02	1.2922E-02	7.8919E-04	1.3560E 05	1.0222E-01	1.0401E-01
2	3.3590E-04	7.8352E-05	5.5565E 03	1.2692E-02	1.2677E-02	8.6052E-04	1.4432E 05	1.0887E-01	1.1077E-01
3	4.0121E-04	4.0786E-05	6.4006E 03	1.2810E-02	1.2795E-02	9.8851E-04	1.6711E 05	1.2616E-01	1.2833E-01
4	5.2605E-04	1.0859E-05	7.0461E 03	1.3590E-02	1.3570E-02	1.0476E-03	1.8970E 05	1.4249E-01	1.4486E-01
5	5.2642E-04	1.0730E-05	7.0609E 03	1.3594E-02	1.3583E-02	1.0477E-03	1.8981E 05	1.4256E-01	1.4494E-01
6	4.4203E-04	4.0696E-05	6.4151E 03	1.2814E-02	1.2799E-02	9.8927E-04	1.6731E 05	1.2631E-01	1.2848E-01
7	3.3663E-04	7.8122E-05	5.5620E 03	1.2690E-02	1.2675E-02	8.6146E-04	1.4445E 05	1.0897E-01	1.1082E-01

ELEMENT NO.	UPPER EDGE OF PATH OUTER	UPPER EDGE OF PATH INNER	LOWER EDGE OF PATH OUTER	LOWER EDGE OF PATH INNER	GOTHIC ARCH CLEARANCE OUTER	GOTHIC ARCH CLEARANCE INNER	SPIN/ROLL RATIO	ROLLING TORQUE OUTER	ROLLING TORQUE INNER
1	3.6542E 01	3.6871E 01	-2.2576E 00	-2.2682E 00	0.0	0.0	4.1674E-02	9.2204E-04	9.3152E-04
2	3.7735E 01	3.8096E 01	-8.5400E-01	-8.4747E-01	0.0	0.0	4.4815E-02	9.0041E-04	9.0946E-04
3	4.0766E 01	4.1131E 01	2.0612E 00	2.0966E 00	0.0	0.0	5.1751E-02	9.1093E-04	9.1993E-04
4	4.3499E 01	4.3829E 01	4.1415E 00	4.1895E 00	0.0	0.0	5.7124E-02	9.8068E-04	9.9053E-04
5	4.3460E 01	4.3841E 01	4.1499E 00	4.1980E 00	0.0	0.0	5.7147E-02	9.8110E-04	9.9097E-04
6	4.0792E 01	4.1156E 01	2.0824E 00	2.1180E 00	0.0	0.0	5.1804E-02	9.1135E-04	9.2035E-04
7	3.7773E 01	3.8114E 01	-8.3487E-01	-8.2814E-01	0.0	0.0	4.4859E-02	9.0025E-04	9.0930E-04

ELEMENT NO.	MAX. ORTHOGONAL SHEAR OUTER	MAX. ORTHOGONAL SHEAR INNER	MAX. ORTH. SHEAR DEPTH OUTER	MAX. ORTH. SHEAR DEPTH INNER	MAXIMUM SHEAR STRESS OUTER	MAXIMUM SHEAR STRESS INNER	DEPTH TO MAXIMUM SHEAR OUTER	13E-

```
                    STD AND NON STD EXTERNAL HELICAL
                    GEARS - MAX BENDING STRESS
                 I N P U T   D A T A   S E C T I O N
                 NASA CVT STUDY  INPUT PLANETARY HELICALS
NO. OF TEETH    CENTER DISTANCE     HORSEPOWER   RPM-PINION     KO          KV          KS          KM
PINION  GEAR     STD       NON STD
  20     40    1.500000   1.500000   7.330000   29500.00    1.000000    1.000000    1.000000    1.000000
  NORMAL PLANE            HELIX       BACKLASH        FACE WIDTH - MIN      MAX TIP BREAK
  PHI N      PND          ANGLE      MIN      MAX     PINION      GEAR      PINION     GEAR
19.733007 23.093994    30.000000   0.0020   0.0040   0.250000   0.250000    0.0        0.0
OUTSIDE DIA - MIN          ROOT DIA - MIN          ARC TOOTH THK          L
 PINION      GEAR         PINION       GEAR        PINION       GEAR
1.099999  2.099999       0.000000    1.879999     0.077000    0.077000     0
SHAPED OR     H          ROOT FILLET RAD-MIN         MAX UNDERCUT          KT          KR          RN          DENSITY
HOBBED                   PINION       GEAR         PINION       GEAR                                          LB/CU.IN.
SHAPED        0          0.02000     0.02000       0.0          0.0       1.00000     1.00000     1.00000     0.28300
       XDINP=    0.02338
       XDING=    0.03038
       TUP  =    0.04605
       TUG  =    0.05225
       RFMIP=    0.02000
       RFMIG=    0.02000
       HP   =    0.09649
       HG   =    0.08985
       JP   =    0.46393
       JG   =    0.53795
       YCP  =    0.50912
       YCG  =    0.73386
       KFP  =    1.38560
       KFG  =    1.69859
       FLP  =    0.54770
       FLHG =    0.40004
       BHEP =    0.0
       BHEG =    0.0
       FCONP=    1.06103
SURFACE COMPRESSIVE STRESS=   57948.80859  P.S.I.
                POWER LOSS=       0.03923      HP.
               PINION LEAD=       5.44140      IN.
                 GEAR LEAD=      10.88281      IN.
                BASE HELIX=       0.49001     RAD.
  LENGTH OF LINE OF ACTION=       0.22343      IN.
     PROFILE CONTACT RATIO=       1.53962
        LOAD SHARING RATIO=       0.60324
AGMA BENDING STRESS,PINION=    3424.24219  P.S.I.
AGMA BENDING STRESS,  GEAR=    4464.63672  P.S.I.
   AGMA HELICAL FACTOR, CH=       1.43619
```

```
      ----- OUTPUT  DATA -----
TOOTH GEOMETRY
   PHI (PRESSURE ANGLE
        TRANSVERSE PLANE)    =  22.49998

   CIRCULAR PITCH           =   0.15708
   DIAMETRAL PITCH          =  20.00000
                                PINION      GEAR
   PITCH DIA                    1.00000    2.00000
   BASE CIRCLE DIA              0.92388    1.84776
   BEGIN CONTACT DIA            0.93680    2.10000
   END   CONTACT DIA            1.10000    1.92817
   WEAKEST SECTION DIA          0.90550    1.90637
   ARC TOOTH THK AT
   OPERATING DP                 0.07700    0.07700
   CH                           1.20516    1.20619
   YC                           0.38331    0.47816
   KF                           1.38560    1.69859
   J                            0.30056    0.34999
   BENDING STRESS
              BC (HPC)       6917.39     5935.38
 BENDING STRESS PINION-AT HPC IS LESS
THAN THE ENDURANCE LIMIT OF 175000. PSI - INFINITE LIFE.
 BENDING STRESS GEAR  -AT HPC IS LESS
THAN THE ENDURANCE LIMIT OF 175000. PSI - INFINITE LIFE.
   BENDING STRESS (COMBINED)
              BC (HPC)       6951.88     5969.19
```

SPIRAL BEVEL GEAR DIMENSIONS NO. 100.004C

PART NO. - NASA CVT STUDY SUN DRIVE+.63ROLL

	PINION	GEAR
NUMBER OF TEETH	19	27
DIAMETRAL PITCH		13.570
FACE WIDTH	0.600"	0.600"
PRESSURE ANGLE	22D 30M	
SHAFT ANGLE	9D 14M	
TRANSVERSE CONTACT RATIO . .		1.209
FACE CONTACT RATIO		1.341
MODIFIED CONTACT RATIO . . .		1.958
OUTER CONE DISTANCE		10.522"
MEAN CONE DISTANCE		10.222"
PITCH DIAMETER	1.400"	1.990"
CIRCULAR PITCH	0.232"	
WORKING DEPTH	0.122"	
WHOLE* DEPTH	0.136"	0.136"
CLEARANCE	0.014"	0.014"
ADDENDUM	0.070"	0.053"
DEDENDUM	0.067"	0.083"
**DEDENDUM ANGLES MODIFIED PER 1971 FORMULAS		
THEORETICAL CUTTER RADIUS . .	6.000"	
CUTTER RADIUS	6.000"	
CALC. GEAR FINISH. PT. WIDTH .		0.040"
GEAR FINISHING POINT WIDTH . .		0.040"
ROUGHING POINT WIDTH	0.035"	0.040"
OUTER SLOT WIDTH	0.035"	0.040"
MEAN SLOT WIDTH	0.035"	0.040"
INNER SLOT WIDTH	0.035"	0.040"
FINISHING CUTTER BLADE POINT	0.020"	0.025"
STOCK ALLOWANCE	-0.000"	-0.000"
MAX. RADIUS-CUTTER BLADES . .	0.018"	0.023"
MAX. RADIUS-MUTILATION . . .	0.043"	0.044"
MAX. RADIUS-INTERFERENCE . .	0.020"	0.029"
CUTTER EDGE RADIUS	0.015"	0.020"
CALC. CUTTER NUMBER	0	0
MAX. NO. BLADES IN CUTTER . .		0.0
CUTTER BLADES REQUIRED . . .	STD DEPTH	STD DEPTH
GEAR ANGULAR FACE - CONCAVE .		0D 0M
GEAR ANGULAR FACE - CONVEX .		0D 0M
GEAR ANGULAR FACE - TOTAL .		0D 0M

FORM J

		PINION		GEAR
OUTSIDE DIAMETER		1.539"		2.095"
PITCH APEX TO CROWN		10.494"		10.470"
MEAN CIRCULAR THICKNESS . .		0.119"		0.100"
OUTER NORMAL TOP LAND . . .		0.039"		0.038"
MEAN NORMAL TOP LAND		0.038"		0.040"
INNER NORMAL TOP LAND . . .		0.038"		0.037"
PITCH ANGLE		38 49M		50 26M
FACE ANGLE OF BLANK		38 58M		50 32M
ROOT ANGLE		38 42M		50 17M
DEDENDUM ANGLE		0D 7M		0D 9M
OUTER SPIRAL ANGLE				32D 21M
MEAN SPIRAL ANGLE				30D 0M
INNER SPIRAL ANGLE				27D 40M
HAND OF SPIRAL	RH		LH	
DRIVING MEMBER	PIN			
DIRECTION OF ROTATION-DRIVER	CW			
OUTER NORMAL BACKLASH	MIN	0.003"	MAX	0.005"
TOOTH TAPER		**TRLM		
CUTTING METHOD			SB	
GEAR TYPE				GENERATED
FACE WIDTH IN PERCENT OF CONE DISTANCE . .				5.702
GEOMETRY FACTOR-STRENGTH-J .		0.3299		0.3295
STRENGTH FACTOR-Q		51.028		35.946
SIZE FACTOR - KS		0.521		
FACTOR	KI	1.0213		
STRENGTH BALANCE DESIRED . .	STRS			
STRENGTH BALANCE OBTAINED .	STRS			0.003
GEOMETRY FACTOR-DURABILITY-I		0.0751		
DURABILITY FACTOR-Z		13463.		11293.
GEOMETRY FACTOR-SCORING-G . .*		0.003630		
SCORING FACTOR - X		0.4446		
ROOT LINE FACE WIDTH		0.600"		0.600"
PROFILE SLIDING FACTOR . . .		0.002016		0.002311
RATIO OF INVOLUTE/OUTER CONE		1.020		
AXIAL FACTOR-DRIVER CW . . .	IN	0.800	OUT	0.641
AXIAL FACTOR-DRIVER CCW . .	OUT	0.894	IN	0.548
SEPARATING FACTOR-DRIVER CW	SEP	0.758	SEP	0.436
SEPARATING FACTOR-DRIVER CCW	SEP	0.645	SEP	0.549
DUPLEX SUM OF DEDENDUM ANG .		0D 16M		
ROUGHING RADIAL		8.897"		

*THIS FACTOR IS USED IN THE 1966 SCORING FORMULA

```
                 STD AND NON STD EXTERNAL HELICAL
                 GEARS - MAX BENDING STRESS
              I N P U T   D A T A   S E C T I O N
              IDLER HELICAL GEARMESH
NO. OF TEETH    CENTER DISTANCE    HORSEPOWER   RPM-PINION     KO          KV          KS          KM
PINION  GEAR     STD       NON STD
  21     49    2.349999   2.349999    10.799999   16522.00    1.000000   1.000000   1.000000   1.000000
  NORMAL PLANE            HELIX         BACKLASH          FACE WIDTH - MIN      MAX TIP BREAK
  PHC D       PHD         ANGLE       MIN       MAX       PINION      GEAR     PINION     GEAR
20.000000 16.357986   24.426987   0.0030    0.0050    0.500000   0.500000   0.0        0.0
OUTSIDE DIA - MIN          ROOT DIA - MIN         ARC TOOTH THK          L
 PINION       GEAR       PINION       GEAR       PINION      GEAR
 1.300000  3.424199     1.221999   3.108999    0.104000   0.103000      0
SHAPED OR      D         ROOT FILLET RAD-MIN      MAX UNDERCUT          KT         KR         NN       DENSITY
HOBBED                   PINION       GEAR       PINION      GEAR                                      LB/CU.IN.
SHAPED         0         0.03500     0.03500     0.0         0.0        1.00000    1.00000    1.00000  0.28300
       XBINP=   0.02973
       XBING=   0.04087
       TWP  =   0.06190
       TWG  =   0.07134
       RFWIP=   0.03500
       RFNIG=   0.03500
       HP   =   0.12087
       HG   =   0.12454
       JP   =   0.31236
       JG   =   0.61867
       YCP  =   0.31740
       YCG  =   0.48191
       KFP  =   1.36696
       KFG  =   1.49260
       FLP  =   0.33188
       FLNG =   0.45537
       DHEP =   0.0
       DHEG =   0.0
       FCONT=   1.18296
  SURFACE COMPRESSIVE STRESS=  46204.67378  P.S.I.
                  POWER LOSS=      0.06006    HP.
                 PINION LEAD=      9.75277    IN.
                   GEAR LEAD=     22.73645    IN.
                  BASE HELIX=      0.39911   RAD.
    LENGTH OF LINE OF ACTION=      0.31032    IN.
      PROFILE CONTACT RATIO=       1.58434
         LOAD SHARING RATIO=       0.61218
  AGMA BENDING STRESS,PINION=   3396.02026  P.S.I.
  AGMA BENDING STRESS,  GEAR=   2813.56201  P.S.I.
     AGMA HELICAL FACTOR, CH=      1.39612
```

```
[illegible]
   AGMA HELICAL FACTOR, CM=      1.37612
             ----- O U T P U T   D A T A -----
   TOOTH GEOMETRY
      PHI (PRESSURE ANGLE
           TRANSVERSE PLANE)   =  21.78917

      CIRCULAR PITCH           =   0.21093
      DIAMETRAL PITCH          =  14.89362
                                  PINION       GEAR
      PITCH DIA                   1.41000      3.29000
      BASE CIRCLE DIA             1.30925      3.05491
      BEGIN CONTACT DIA           1.33410      3.42420
      END   CONTACT DIA           1.54400      3.19222
      WEAKEST SECTION DIA         1.24739      3.15601
      ARC TOOTH THK AT
      OPERATING DP                0.10400      0.10300
      CH                          1.27934      1.29123
      YC                          0.35333      0.46847
      KF                          1.36676      1.49260
      J                           0.35201      0.42502
     . BENDING STRESS
                 BC (HPC)       3863.26      3171.78
  BENDING STRESS PINION-AT HPC IS LESS
 THAN THE ENDURANCE LIMIT OF 175000. PSI - INFINITE LIFE.
  BENDING STRESS GEAR  -AT HPC IS LESS
 THAN THE ENDURANCE LIMIT OF 175000. PSI - INFINITE LIFE.
      BENDING STRESS (COMBINED)
                 BC (HPC)       3876.94      3183.31
OBI24: END OF FILE
```

```
                    STD AND NON STD EXTERNAL HELICAL
                    GEARS - MAX BENDING STRESS
                 I N P U T   D A T A   S E C T I O N
                 OUTPUT PLANETARY GEARS
NO. OF TEETH      CENTER DISTANCE     HORSEPOWER   RPM-PINION     KO         KV         KS         KM
PINION  GEAR      STD        NON STD
  40     30     1.750000   1.750000    9.799999   18677.00   1.000000   1.000000   1.000000   1.000000
  NORMAL PLANE          HELIX        BACKLASH       FACE WIDTH - MIN     MAX TIP BREAK
  PHI N      PND        ANGLE     MIN      MAX      PINION      GEAR     PINION      GEAR
20.000000 23.093994   30.000000  0.0030   0.0050   0.500000   0.750000   0.0        0.0
OUTSIDE DIA - MIN       ROOT DIA - MIN         ARC TOOTH THK        L
 PINION      GEAR     PINION      GEAR      PINION      GEAR
 2.099999  1.599999   1.860000  1.360000   0.077000   0.077000      0
SHAPED OR      H      ROOT FILLET RAD-MIN       MAX UNDERCUT        KT         KR         MN        DENSITY
HOBBED                PINION      GEAR      PINION      GEAR                                         LB/CU.IN.
SHAPED         0      0.03000     0.03000   0.0         0.0      1.00000    1.00000    1.00000    0.28300
       XDINP=   0.03041
       XDING=   0.02785
       TWP  =   0.05330
       TWG  =   0.05114
       RFNIP=   0.03000
       RFNIG=   0.03000
       HP   =   0.09342
       HG   =   0.09300
       JP   =   0.43422
       JG   =   0.46549
       YCP  =   0.73591
       YCG  =   0.68419
       KFP  =   1.46344
       KFG  =   1.42917
       FLN  =   0.40420
       FLNG =   0.50027
       DNEP =   0.0
       DNEG =   9.0
       FCONT=   2.12206
  SURFACE COMPRESSIVE STRESS=  36116.99844  P.S.I.
                  POWER LOSS=      0.04144     HP.
                 PINION LEAD=     10.88281     IN.
                   GEAR LEAD=      0.16211     IN.
                  BASE HELIX=      0.48912    RAD.
    LENGTH OF LINE OF ACTION=      0.22699     IN.
       PROFILE CONTACT RATIO=      1.36750
          LOAD SHARING RATIO=      0.59280
  AGMA BENDING STRESS,PINION=   2079.14673  P.S.I.
  AGMA BENDING STRESS,  GEAR=   1455.96265  P.S.I.
    AGMA HELICAL FACTOR, CH=       1.45985
```

```
AGMA HELICAL FACTOR, CH=        1.45985
          ----- O U T P U T   D A T A -----
TOOTH GEOMETRY
   PHI (PRESSURE ANGLE
        TRANSVERSE PLANE)    =  22.79590

   CIRCULAR PITCH            =   0.15708
   DIAMETRAL PITCH           =  20.00000
                                PINION      GEAR
   PITCH DIA                    2.00000     1.50000
   BASE CIRCLE DIA              1.84378     1.38284
   DESIGN CONTACT DIA           1.92442     1.60000
   END   CONTACT DIA            2.10000     1.42665
   WEAKEST SECTION DIA          1.89949     1.39892
   ARC TOOTH THK AT
   OPERATING DP                 0.07700     0.07700
   CN                           1.70839     1.32230
   YC                           0.47833     0.44442
   KF                           1.46344     1.42917
   J                            0.41353     0.39343
   BENDING STRESS
                 SC (HPC)      1788.43     1472.43
 BENDING STRESS PINION-AT HPC IS LESS
THAN THE ENDURANCE LIMIT OF 175000. PSI - INFINITE LIFE.
 BENDING STRESS GEAR  -AT HPC IS LESS
THAN THE ENDURANCE LIMIT OF 175000. PSI - INFINITE LIFE.
   BENDING STRESS (COMBINED)
                 SC (HPC)      1804.56     1485.00
```

ORIGINAL PAGE IS
OF POOR QUALITY

BALL AND ROLLER BEARING DISPLACEMENT, LOAD AND LIFE DETERMINATION
NASA CVT STUDY OUTPUT PLANET BEARINGS 11-20-79
HEAD CONDITIONS AT 70.CB HP 30630 RPM
* INPUT DATA FOR SYSTEM NO. 1

BEARING NO.	BEARING TYPE	NUMBER OF BALLS/ROLLS	BALL/ROLL DIA.	PITCH DIA.	RACE CURVATURES OUTER	RACE CURVATURES INNER	CONTACT ANGLE	INTERNAL CLEARANCE	DISTANCE TO ORIGIN
1	ROLLER	6.0000E 00	1.3750E-01	6.8000E-01	0.0	0.0	0.0	3.0000E-04	5.0000E-01
2	ROLLER	8.0000E 00	1.3750E-01	6.8000E-01	0.0	0.0	0.0	3.0000E-04	-5.0000E-01
3	BALL	7.0000E 00	1.0000E-01	1.4200E 00	5.2000E-01	5.2000E-01	1.0000E 01	-2.0000E-04	-2.0000E 00

BEARING NO.	BEARING TYPE	EFFECTIVE ROLL LENGTH	TOTAL ROLL LENGTH	BALL/ROLL DENSITY	MODULUS OF ELASTICITY BALLS/ROLLS	MODULUS OF ELASTICITY RACES	POISSON'S RATIO BALLS/ROLLS	POISSON'S RATIO RACES	FRICTION COEFFICIENT
1	ROLLER	1.3750E-01	1.7720E-01	2.8300E-01	2.9000E 07	2.9000E 07	2.5000E-01	2.5000E-01	0.0
2	ROLLER	1.3750E-01	1.7720E-01	2.8300E-01	2.9000E 07	2.9000E 07	2.5000E-01	2.5000E-01	0.0
3	BALL	0.0	0.0	2.8300E-01	2.9000E 07	2.9000E 07	2.5000E-01	2.5000E-01	7.5000E-02

BEARING NO.	BEARING TYPE	PHASE FACTOR	SHIM THICKNESS OUTER	SHIM THICKNESS INNER	INITIAL DISPLACEMENTS AT BEARING CENTER ALONG X	ALONG Y	ALONG Z	ABOUT Y	ABOUT Z
1	ROLLER	0.0	0.0	0.0	0.0	0.0	0.0	0.0	0.0
2	ROLLER	0.0	0.0	0.0	0.0	0.0	0.0	0.0	0.0
3	BALL	0.0	0.0	0.0	0.0	0.0	0.0	0.0	0.0

BEARING NO.	BEARING TYPE	PRELOAD SPRING RATE	AXIAL PRELOAD	RADIAL SPRING RATES ALONG Y	RADIAL SPRING RATES ALONG Z	FATIGUE CONSTANT OUTER	FATIGUE CONSTANT INNER	VALUE OF LAMBDA OUTER	VALUE OF LAMBDA INNER
1	ROLLER	0.0	0.0	0.0	0.0	4.9500E 04	4.9500E 04	6.1000E-01	6.1000E-01
2	ROLLER	0.0	0.0	0.0	0.0	4.9500E 04	4.9500E 04	6.1000E-01	6.1000E-01
3	BALL	0.0	0.0	1.0000E 00	1.0000E 00	7.1400E 03	7.1400E 03	0.0	0.0

* INPUT DATA FOR LOAD CASE NO. 1, SYSTEM NO. 1

LOAD NO.	EXTERNAL LOADS APPLIED TO SHAFT ALONG X	ALONG Y	ALONG Z	ABOUT Y	ABOUT Z	DISTANCE TO ORIGIN	RPM OF OUTER	RPM OF INNER
1	-6.4700E 01	6.9300E 01	0.0	2.6100E 01	0.0	0.0	0.0	3.0603E 04

OUTER RACES ROTATE WITH RESPECT TO LOAD
INNER RACES FIXED WITH RESPECT TO LOAD
-- THIS LOAD CASE IS EFFECTIVE FOR 100.0000 PERCENT OF TIME
* OUTPUT DATA FOR LOAD CASE NO. 1, SYSTEM NO. 1

BEARING NO.	REACTIONS OF BEARINGS ON SHAFT ALONG X	ALONG Y	ALONG Z	ABOUT Y	ABOUT Z	FRICTION TORQUE	FATIGUE LIFE (90 PERCENT SURVIVAL) OUTER	INNER	BEARING
1	0.0	-3.4759E 01	-2.2575E 01	0.0	0.0	0.0	4.1500E 05	3.2704E 04	3.1123E 04
2	0.0	-3.4444E 01	2.2830E 01	0.0	0.0	0.0	4.1670E 05	3.2794E 04	3.1218E 04
3	6.4689E 01	7.6294E-05	2.6703E-04	-3.8414E 00	-1.2025E-02	1.3158E-01	4.3941E 01	1.6148E 01	1.2503E 01

BEARING NO.	DISPLACEMENTS OF INNER RACE WITH RESPECT TO OUTER ALONG X	ALONG Y	ALONG Z	ABOUT Y	ABOUT Z	DISPLACEMENTS OF FLOATING OUTER RACE ALONG X	ALONG Y	ALONG Z
1	0.0	-1.9725E-04	-1.5602E-04	0.0	0.0	0.0	0.0	0.0
2	0.0	-1.9626E-04	1.5739E-04	0.0	0.0	0.0	0.0	0.0
3	8.3541E-04	2.2060E-07	7.9712E-05	-3.1381E-04	-9.8499E-07	0.0	-1.9530E-04	5.4773E-04

BEARING NO.	PARTIAL NON-LINEAR SPRING RATES OF INDIVIDUAL BEARINGS DFX/DX	DFX/DY	DFX/DZ	DFX/DALY	DFX/DALZ	DFY/DY	DFY/DZ	DFY/DALY	DFY/DALZ
1	0.0	0.0	0.0	0.0	0.0	4.8584E 05	1.6956E 05	0.0	0.0
2	0.0	0.0	0.0	0.0	0.0	4.8574E 05	-1.6956E 05	0.0	0.0

```
   2        0.0         0.0         0.0         0.0         0.0          4.8524E 05 -1.6956E 05  0.0         0.0
   3        1.4385E 05 -5.4332E 01 -1.7331E 04 -1.0915E 04 -3.4211E 01  3.7070E 05  4.2266E 00  4.8828E-01  9.4215E 04
BEARING        - - - - - PARTIAL NON-LINEAR SPRING RATES (CONTINUED) - - - - -
  NO.         DFZ/DZ      DFZ/DALY    DFZ/DALZ    DMY/DALY    DMY/DALZ    DMZ/DALZ
   1        4.3679E 05  0.0         0.0         0.0         0.0         0.0
   2        4.4000E 05  0.0         0.0         0.0         0.0         0.0
   3        3.7231E 05  9.4390E 04  5.0000E-01  3.6719E 04  1.6816E 00  3.6201E 04
                   DISPLACEMENTS OF REFERENCE LINE AT ORIGIN
             ALONG X     ALONG Y     ALONG Z     ABOUT Y     ABOUT Z

            8.3543E-04 -1.9682E-04  4.2076E-07 -3.1351E-04 -8.6900E-07
 - OUTPUT DATA FOR BEARING NO. 1, LOAD CASE NO.  1, SYSTEM NO. 1
ELEMENT     ELEMENT        CONTACT FORCE        OPERATING CONTACT ANGLE   CONTACT AREA LENGTH      CONTACT AREA WIDTH
  NO.       AZIMUTH      OUTER       INNER        OUTER       INNER        OUTER       INNER       OUTER       INNER
   5        1.8000E 02  2.2841E 00  9.8081E-01  0.0         0.0          1.5750E-01  1.5750E-01  6.8856E-04  3.5225E-04
   6        2.2500E 02  3.1843E 01  3.0539E 01  0.0         0.0          1.5750E-01  1.5750E-01  2.5411E-03  1.9656E-03
   7        2.7000E 02  1.4468E 01  1.3165E 01  0.0         0.0          1.5750E-01  1.5750E-01  1.7128E-03  1.2905E-03
 OTHERS                 1.3033E 00  0.0         0.0         0.0          1.5750E-01  0.0         5.1408E-04  0.0
ELEMENT   CENTRIFUGAL  GYROSCOPIC   ORBITAL     ROTATIONAL      ROLLING VELOCITY    CONTROLLING MEAN COMPRESSIVE STRESS
  NO.        FORCE       MOMENT     VELOCITY    VELOCITY      OUTER       INNER        RACE        OUTER       INNER
   5        1.3033E 00  0.0         1.1757E 04 -6.2520E 04 -5.0763E 04  8.1366E 04                2.1309E 04  1.7479E 04
   6        1.3033E 00  0.0         1.1758E 04 -6.2530E 04 -5.0772E 04  8.1375E 04                7.9564E 04  9.8648E 04
   7        1.3034E 00  0.0         1.1758E 04 -6.2524E 04 -5.0767E 04  8.1370E 04                5.3631E 04  6.4768E 04
 OTHERS     1.3033E 00  0.0         1.1758E 04 -6.2522E 04 -5.0765E 04  0.0                       1.6097E 04  0.0
ELEMENT     MAX. ORTHOGONAL SHEAR   MAX. ORTH. SHEAR DEPTH  MAXIMUM SHEAR STRESS    DEPTH TO MAXIMUM SHEAR
  NO.        OUTER       INNER       OUTER       INNER       OUTER       INNER       OUTER       INNER
   5        6.7029E 03  3.6273E 03  1.7014E-04  8.8063E-05  8.1472E 03  6.7592E 03  2.6751E-04  1.3846E-04
   6        2.5326E 04  3.1401E 04  6.3527E-04  4.9139E-04  3.0420E 04  3.7716E 04  9.9883E-04  7.7262E-04
   7        1.7079E 04  2.0616E 04  4.2821E-04  3.2263E-04  2.0505E 04  2.4763E 04  6.7327E-04  5.0727E-04
 OTHERS     5.1236E 03  0.0         1.2852E-04  0.0         6.1541E 03  0.0         2.0207E-04  0.0
 - OUTPUT DATA FOR BEARING NO. 2, LOAD CASE NO.  1, SYSTEM NO. 1
ELEMENT     ELEMENT        CONTACT FORCE        OPERATING CONTACT ANGLE   CONTACT AREA LENGTH      CONTACT AREA WIDTH
  NO.       AZIMUTH      OUTER       INNER        OUTER       INNER        OUTER       INNER       OUTER       INNER
   1        0.0         2.5427E 00  1.2394E 00  0.0         0.0          1.5750E-01  1.5750E-01  7.1805E-04  3.9597E-04
   7        2.7000E 02  1.4956E 01  1.2853E 01  0.0         0.0          1.5750E-01  1.5750E-01  1.6943E-03  1.2752E-03
   8        3.1500E 02  3.1837E 01  3.0534E 01  0.0         0.0          1.5750E-01  1.5750E-01  2.5408E-03  1.9654E-03
 OTHERS                 1.3033E 00  0.0         0.0         0.0          1.5750E-01  0.0         5.1408E-04  0.0
ELEMENT   CENTRIFUGAL  GYROSCOPIC   ORBITAL     ROTATIONAL      ROLLING VELOCITY    CONTROLLING MEAN COMPRESSIVE STRESS
  NO.        FORCE       MOMENT     VELOCITY    VELOCITY      OUTER       INNER        RACE        OUTER       INNER
   1        1.3033E 00  0.0         1.1757E 04 -6.2521E 04 -5.0763E 04  8.1366E 04                2.2483E 04  1.9873E 04
   7        1.3034E 00  0.0         1.1758E 04 -6.2524E 04 -5.0767E 04  8.1370E 04                5.3050E 04  6.3998E 04
   8        1.3035E 00  0.0         1.1758E 04 -6.2530E 04 -5.0772E 04  8.1375E 04                7.9557E 04  9.8639E 04
 OTHERS     1.3033E 00  0.0         1.1758E 04 -6.2522E 04 -5.0765E 04  0.0                       1.6097E 04  0.0
ELEMENT     MAX. ORTHOGONAL SHEAR   MAX. ORTH. SHEAR DEPTH  MAXIMUM SHEAR STRESS    DEPTH TO MAXIMUM SHEAR
  NO.        OUTER       INNER       OUTER       INNER       OUTER       INNER       OUTER       INNER
   1        7.1566E 03  6.1258E 03  1.7951E-04  9.8994E-05  8.5960E 03  7.5981E 03  2.8225E-04  1.5565E-04
```

6	[illegible]	[illegible]	[illegible]	[illegible]	[illegible]	[illegible]	[illegible]	[illegible]
7	1.6886E 04	2.0371E 04	4.2337E-04	3.1879E-04	2.0283E 04	2.4468E 04	6.6598E-04	5.0123E-04
8	2.5324E 04	3.1398E 04	6.3521E-04	4.9135E-04	3.0417E 04	3.7713E 04	9.9874E-04	7.7255E-04
OTHERS	5.1234E 03	0.0	1.2852E-04	0.0	6.1541E 03	0.0	2.0207E-04	0.0

* OUTPUT DATA FOR BEARING NO. 3, LOAD CASE NO. 1, SYSTEM NO. 1

ELEMENT NO.	ELEMENT AZIMUTH	CONTACT FORCE OUTER	CONTACT FORCE INNER	OPERATING CONTACT ANGLE OUTER	OPERATING CONTACT ANGLE INNER	CONTACT AREA LENGTH OUTER	CONTACT AREA LENGTH INNER	CONTACT AREA WIDTH OUTER	CONTACT AREA WIDTH INNER
1	0.0	2.6076E 01	2.5516E 01	1.7315E 01	1.7884E 01	3.4587E-02	3.4691E-02	4.4231E-03	4.0872E-03
2	5.1429E 01	2.5822E 01	2.5246E 01	1.8469E 01	1.9083E 01	3.4467E-02	3.4567E-02	4.4066E-03	4.0738E-03
3	1.0286E 02	2.6012E 01	2.5443E 01	2.1090E 01	2.1783E 01	3.4554E-02	3.4653E-02	4.4150E-03	4.0871E-03
4	1.5429E 02	2.6983E 01	2.6421E 01	2.3204E 01	2.3939E 01	3.4981E-02	3.5089E-02	4.4671E-03	4.1412E-03
5	2.0571E 02	2.6988E 01	2.6426E 01	2.3213E 01	2.3948E 01	3.4985E-02	3.5091E-02	4.4674E-03	4.1415E-03
6	2.5714E 02	2.6017E 01	2.5449E 01	2.1109E 01	2.1803E 01	3.4556E-02	3.4656E-02	4.4153E-03	4.0874E-03
7	3.0857E 02	2.5820E 01	2.5244E 01	1.8485E 01	1.9098E 01	3.4466E-02	3.4566E-02	4.4065E-03	4.0737E-03

ELEMENT NO.	CENTRIFUGAL FORCE	GYROSCOPIC MOMENT	ORBITAL VELOCITY	ROTATIONAL VELOCITY	ROLLING VELOCITY OUTER	ROLLING VELOCITY INNER	CONTROLLING RACE	MEAN COMPRESSIVE STRESS OUTER	MEAN COMPRESSIVE STRESS INNER
1	6.0664E-01	-3.6229E-03	1.4276E 04	-2.1642E 05	-2.0275E 05	2.3187E 05	OUTER	2.1719E 05	2.2913E 05
2	6.0724E-01	-3.8601E-03	1.4284E 04	-2.1645E 05	-2.0285E 05	2.3176E 05	OUTER	2.1647E 05	2.2826E 05
3	6.1073E-01	-4.3951E-03	1.4301E 04	-2.1650E 05	-2.0309E 05	2.3150E 05	OUTER	2.1710E 05	2.2873E 05
4	6.1206E-01	-4.8231E-03	1.4317E 04	-2.1654E 05	-2.0331E 05	2.3126E 05	OUTER	2.1986E 05	2.3151E 05
5	6.1207E-01	-4.8240E-03	1.4317E 04	-2.1654E 05	-2.0331E 05	2.3126E 05	OUTER	2.1987E 05	2.3152E 05
6	6.1075E-01	-4.3990E-03	1.4302E 04	-2.1650E 05	-2.0310E 05	2.3149E 05	OUTER	2.1711E 05	2.2874E 05
7	6.0725E-01	-3.8632E-03	1.4284E 04	-2.1645E 05	-2.0285E 05	2.3176E 05	OUTER	2.1646E 05	2.2826E 05

ELEMENT NO.	BALL CENTER COORDINATES X	BALL CENTER COORDINATES Z	SPINNING VELOCITY	SPINNING TORQUE OUTER	SPINNING TORQUE INNER	GYRO SLIP COEFFICIENT	SV VALUE	PATH HEIGHT/BALL DIA. OUTER	PATH HEIGHT/BALL DIA. INNER
1	2.9582E-04	9.3317E-05	1.1413E 04	1.2999E-02	1.2710E-02	2.7766E-03	2.9688E 05	1.0329E-01	1.0674E-01
2	3.3690E-04	7.5676E-05	1.2177E 04	1.2818E-02	1.2531E-02	2.9898E-03	3.1441E 05	1.0925E-01	1.1302E-01
3	4.3013E-04	4.6194E-05	1.3815E 04	1.2945E-02	1.2661E-02	3.3793E-03	3.5835E 05	1.2456E-01	1.2902E-01
4	5.0559E-04	1.9786E-05	1.5026E 04	1.3593E-02	1.3312E-02	3.5750E-03	3.9944E 05	1.3882E-01	1.4379E-01
5	5.0589E-04	1.9673E-05	1.5031E 04	1.3597E-02	1.3316E-02	3.5756E-03	3.9961E 05	1.3888E-01	1.4385E-01
6	4.3081E-04	4.3937E-05	1.3827E 04	1.2948E-02	1.2664E-02	3.3816E-03	3.5869E 05	1.2468E-01	1.2915E-01
7	3.3744E-04	7.8487E-05	1.2186E 04	1.2817E-02	1.2529E-02	2.9924E-03	3.1465E 05	1.0933E-01	1.1310E-01

ELEMENT NO.	UPPER EDGE OF PATH OUTER	UPPER EDGE OF PATH INNER	LOWER EDGE OF PATH OUTER	LOWER EDGE OF PATH INNER	GOTHIC ARCH CLEARANCE OUTER	GOTHIC ARCH CLEARANCE INNER	SPIN/ROLL RATIO	ROLLING TORQUE OUTER	ROLLING TORQUE INNER
1	3.6739E 01	3.7379E 01	-2.1098E 00	-1.6013E 00	0.0	0.0	4.9223E-02	9.2765E-04	9.1248E-04
2	3.7824E 01	3.8496E 01	-8.8499E-01	-3.3020E-01	0.0	0.0	5.2540E-02	9.1161E-04	8.9641E-04
3	4.0495E 01	4.1247E 01	1.6844E 00	2.3197E 00	0.0	0.0	5.9678E-02	9.2292E-04	9.0792E-04
4	4.2859E 01	4.3657E 01	3.5492E 00	4.2212E 00	0.0	0.0	6.4974E-02	9.8100E-04	9.6646E-04
5	4.2869E 01	4.3667E 01	3.5565E 00	4.2285E 00	0.0	0.0	6.4994E-02	9.8131E-04	9.6677E-04
6	4.0515E 01	4.1268E 01	1.7020E 00	2.3377E 00	0.0	0.0	5.9727E-02	9.2324E-04	9.0826E-04
7	3.7838E 01	[illegible].8511E 01	-8.6929E-01	-3.1392E-01	0.0	0.0	5.2583E-02	9.1149E-04	8.9629E-04

ELEMENT NO.	MAX. ORTHOGONAL SHEAR OUTER	MAX. ORTHOGONAL SHEAR INNER	MAX. ORTH. SHEAR DEPTH OUTER	MAX. ORTH. SHEAR DEPTH INNER	MAXIMUM SHEAR STRESS OUTER	MAXIMUM SHEAR STRESS INNER	DEPTH TO MAXIMUM SHEAR OUTER	DEPTH TO MAXIMUM SHEAR INNER
1	8.7199E 04	8.5628E 04	1.0926E-03	1.0115E-03	-1.0466E 05	-1.1006E 05	1.6812E-03	1.5598E-03
2	8.0850E 04	8.5305E 04	1.0886E-03	1.0081E-03	-1.0432E 05	-1.0964E 05	1.6749E-03	1.5548E-03
3	[illegible]	[illegible]	[illegible]	[illegible]	[illegible]	[illegible]	[illegible]	[illegible]

2	[illegible]	[illegible]	[illegible]	[illegible]	[illegible]	[illegible]	[illegible]	[illegible]
3	8.1082E 04	8.5479E 04	1.0907E-03	1.0114E-03	-1.0461E 05	-1.0985E 05	1.6782E-03	1.5598E-03
4	8.2114E 04	8.6344E 04	1.1035E-03	1.0240E-03	-1.0592E 05	-1.1116E 05	1.6981E-03	1.5802E-03
5	8.2121E 04	8.6522E 04	1.1036E-03	1.0240E-03	-1.0594E 05	-1.1121E 05	1.6982E-03	1.5803E-03
6	8.1091E 04	8.5484E 04	1.0907E-03	1.0115E-03	-1.0461E 05	-1.0984E 05	1.6783E-03	1.5600E-03
7	8.0040E 04	8.5363E 04	1.0885E-03	1.0081E-03	-1.0432E 05	-1.0962E 05	1.6749E-03	1.5547E-03

ELEMENT NO.	VECTOR ATTITUDE
1	1.6190E 01
2	1.7271E 01
3	1.9720E 01
4	2.1711E 01
5	2.1719E 01
6	1.9745E 01
7	1.7296E 01

APPENDIX II

SYMBOLS

SYMBOL	DESCRIPTION
$\propto$	proportional
Δ	measure of change
μ	Traction Coefficient or Micro($1x10^{-6}$)
∞	Infinity
C^{o}	Centigrade
Cs	Cone Speed
CVT	Continously Variable Transmission
EV	Electric Vehicle
F	Force
f	Frequency
F_t	Feet
G	Gate
Hr	Hours
HP	Horsepower
Hz	Herts (Cycles/Seconds)
I/O	Input to Output Buffer Circuit
ϕ	Angle (Degrees)
J	Joules
K	Kilowatts
k	$1x10^{3}$
Lb	Pounds
Kg	Kilograms
M	Meters or Milli ($1x10^{-3}$)

APPENDIX II

SYMBOLS (CONTINUED)

SYMBOL	DESCRIPTION
MPU	Microprocessor Unit
N	Newtons
n	Nano ($1x10^{-9}$)
OTC	Optimized Traction Control
P	Pressure
PCV	Pressure Control Valve
PT	Pressure Transducer
TPC	Traction Pressure Control
Rc	Rockwell Hardness Scale "C"
R_c	Roller/Cone Ratio
ROM	Read Only Memory
RPM or W	Revolutions Per Minute
Rs	Roller Speed
Sp or u	Slip
T	Torque
t	Time
T_f	Traction Force
Si	Speed
V	Velocity or Volts
V_c	Surface Velocity of Cone
V_R	Surface Velocity of Roller
W_n	Normal Load